The Pennsylvania State University

The Graduate School

HYDROTHERMAL VALORIZATION OF FOOD WASTE

A Dissertation in

Chemical Engineering

by

Bita Motavaf

Submitted in Partial Fulfillment
of the Requirements
for the Degree of

Doctor of Philosophy

May 2022

The dissertation of Bita Motavaf was reviewed and approved by the following:

Phillip. E. Savage
Walter L. Robb Family Department Head of Chemical Engineering
Dissertation Advisor
Chair of Committee

Robert. M. Rioux
Friedrich G. Helfferich Professor of Chemical Engineering

Kristen Fichthorn
Merrell Fenske Professor of Chemical Engineering and Professor of Physics

Sarma Pisupati
Professor of Energy and Mineral Engineering
Professor of Chemical Engineering

Seong. H. Kim
Associate Department Head for the McWhirter Graduate Program

ABSTRACT

Hydrothermal liquefaction (HTL) utilizes high temperature water properties and converts wet biomass into an energy-dense crude bio-oil. This technology uses water as the reaction medium, and therefore obviates the need of drying feedstock prior to the process, as is required by other thermochemical processes like pyrolysis. HTL typically occurs at temperatures between 200 and 400 °C and at pressures between 10 and 40 MPa.

Food waste has high moisture content with primary components of proteins, lipids, and carbohydrates. A most common practice is disposing of food waste in landfills which consequently leads to decomposition of organic matter and emission of greenhouse gases. HTL reduces these detrimental effects by utilizing food waste, this readily available resource, and producing valuable products including an energy-dense bio-oil and a nutrient-rich aqueous phase. In this dissertation, the effect of process variables and the use of different catalysts on HTL of food waste are elucidated. Additionally, the recovery of fatty acids from the food waste lipid fraction and nutrients from the protein fraction were studied by conducting low-temperature hydrothermal treatment, and two-step thermochemical treatments, respectively.

This thesis reports the HTL of simulated food waste over a wide range of temperatures, pressures, biomass loadings, and times. The highest biocrude yields were from HTL near the critical temperature. The most severe reaction conditions (600 °C, 35.3 MPa, 30 min) gave biocrude with the largest heating value (36.5 MJ/kg) and transferred up to 50% of the nitrogen and 68% of the phosphorus in the food mixture into the aqueous phase. Energy recovery in the biocrude exceeded 65% under multiple reaction conditions. Saturated fatty acids were the most abundant compounds in the light biocrude fraction under all the reaction conditions. Isothermal HTL gave a higher fraction of heavy compounds than fast HTL. A kinetic model for HTL of

microalgae predicted 2/3 of the experimental biocrude yields from HTL of food waste to within ±5 wt %, and nearly 90% to within ±10 wt %.

This thesis further focuses on screening potential catalysts (i.e. supported metals, bulk metal oxides, and a set of salt, acid, and base additives) for the HTL of food waste to improve biocrude yields and qualities. Supported metals and the additives did not increase biocrude yields, but three of the metal oxides did lead to higher yields, with the following order: SiO_2 > La_2O_3 > CeO_2. The elemental compositions and heating values of the biocrudes were sensitive to the type of potential catalyst used, especially in the presence of high-pressure hydrogen. The higher heating values of the biocrude from HTL were higher with added H_2 and supported metal. Of all the potential catalysts tested, K_3PO_4 produced oil with the greatest HHV. Fatty acids were the major GC-elutable compounds in most of the oils, save that produced with added CaO, where amides and N-containing compounds dominated. Thermogravimetric analysis showed that the distribution of the volatilities of the molecules in the biocrude oils is sensitive to the type of metal oxide used. Aqueous-phase products from HTL with CaO and SiO_2 recovered the most nitrogen and phosphorus, respectively, in the aqueous phase.

This work also investigated hydrothermal carbonization of food waste under different reaction conditions, with the aim of recovering both fatty acids from the hydrochar and nutrients from the aqueous-phase products. HTC of the simulated food waste produced hydrochar that retained up to 78% of the original fatty acids. These retained fatty acids were extracted from the hydrochar using ethanol, a food-grade solvent, and gave a net recovery of fatty acid of ~50%. The HTC process partitioned more than 50 wt% of the phosphorus and around 38 wt% of the nitrogen into the aqueous-phase products.

Finally, sequential carbonization (200 °C, 30 min) and liquefaction steps (300 – 600 °C, 30 min) were also conducted on simulated food waste to produce renewable bio-oil and recover

nitrogen. Thermal and hydrothermal approaches were used for both steps. Pyrolysis at Stage I produced biochars in the greatest yield (57 wt %). The biocrude oil with the greatest heating value (39.4 MJ/kg) was produced from pyrolysis of biochar from HTC at Stage I. Pyrolysis as the second step treatment gave negligible aqueous-phase product yields, so nitrogen recovery with this approach was limited to that recovered in the first step (39% for HTC and 12% for pyrolytic carbonization). Using hydrothermal liquefaction for the second step gave much higher nitrogen recoveries. The highest recovery of N (75%) in the aqueous-phase products from the two stages occurred for the run where HTL (350 °C) was the treatment at Stage II and the biochar was produced hydrothermally from food waste. This N recovery greatly exceeds the recoveries of < 10% reported for single-step HTL of this same simulated food waste mixture. Energy recovery in the biocrude oil that was produced from this two-step process exceeded 50% in several runs, but fell short of the energy recoveries (~ 60%) from single-step HTL of this same simulated food waste mixture. Thus, a two-step valorization process provides an opportunity for much greater N recovery from food waste at the expense of slightly lower energy recoveries.

Taken together, these results provide new insights into the valorization of food waste by producing energy dense crude bio-oil and nutrient rich aqueous phase products.

TABLE OF CONTENTS

LIST OF FIGURES

LIST OF TABLES

ACKNOWLEDGMENT

I would like to acknowledge and give my warmest thanks to my advisor Professor Phillip Savage for his support and guidance throughout my time as a graduate student at Penn State. His dedication, encouragement, and patience to help his students had been mainly responsible for completing my Ph.D. degree. Phil provided me a great amount of freedom on conducting research, while providing valuable feedback, and guidance at every step. I am especially appreciative of his encouragement for pursuing internship opportunity during my graduate career. Phil you are an amazing academic mentor!

I would like to thank my committee members Kristen Fichthorn, Rob Rioux, and Sarma Pisupati for letting my defense to be an enjoyable moment, and for their brilliant comments and suggestions. I am also thankful to Dr. Ephiram Govere, and Dr. John Spargo for their help with running analytical tests.

I would like to further thank all past and present members of the Savage lab, that I have had pleasure of interacting with including James Sheehan, Jimeng Jiang, Akhila Gollakota, Yang Guo, David Hietala, Jianwen Lu, Alejandra Sanchez, Sesha Mahadevan, Xin Ding, Alex Carley, Tim Shokri, Patricia Pereira, Peter Guirguis, and Madeline Vonglis. I would also like to acknowledge the hard work of fantastic undergraduate researchers that I had the pleasure of working with including Sofia Capece, Jad Abou Samra, Robert Dean, Joseph Nicholas, and Tomer Eldor.

I am grateful to the administrative staff of the Department of Chemical Engineering for their assistance, and patience, especially Cathy Krause for her genuine kindness.

I especially am thankful to my parents, my brother and sister for their unconditional support, and love, and their endless patience. Without your encouragement and support I would not have come this far.

Last but not least, I would like to thank my friends from back home who always have kept in touch with me during these years, Bahram Saleh, Nona Mirzamohammadi, Sanaz Rashidzadeh, Azita Karamifar, Elaheh Nabavi, Sahar karimnia, Elaheh Tavakkoli, Sahand Saberi Bosari, Saba Fazeli, and Arvin Tavanaei.

Chapter 1

Introduction

Motivation

Oil is the key source of energy and chemicals for the world. Currently about 12 million tons of oil is being consumed per day, and this amount is projected to increase to 16 million tons per day by 2030.[1] Of this 4 million rising demand, 2.4 millions of it corresponds to transportation. Due to the expansion of transport sector in the world, these values can easily be underestimated and increase even further.[2]

Global warming, and climate change is scientifically agreed as the consequence of fossil fuel combustion and anthropogenic emissions of greenhouse gases (GHG).[3] About three-quarters of carbon dioxide emissions, during the past 20 years, were human made and from burning fossil fuels.

Hence, there is a rising demand for an alternative energy source that can reduce the reliance on oil and supply the world so that GHG emissions target would be met. Currently, several alternatives are being examined to substitute for natural gas, coal and oil. Among those, biofuels, crop-based fuels, such as biodiesel and bioethanol, became known as real alternatives.[4] Biofuels have been gaining popularity, with exponential increase in their consumption, in the last few years.[4] Compared to fossil fuels, biofuels can improve independence and energy security, and contribute to lessen carbon emissions. They are also more advantageous in terms of long term availability and can be replenished easily and quickly.

Food Waste as a Feedstock

Large amounts of bio-wastes are generated by the agricultural and food industries. Food waste is among the most produced bio-wastes. According to the Food and Agricultural Organization of the United Nations, approximately one third of food produced for human consumption, about 1.3 billion tons of food,[5] is wasted globally each year, which leads to an estimated loss of $940 billion.[6]

There are some conventional ways to manage or valorize food waste. For instance, food wastes are traditionally disposed in landfills, which consequently leads to decomposition of organic matter, emission of greenhouse gases and ground water contamination. Another conventional way is to incinerate food waste with other inflammable municipal wastes to generate energy or heat.[7] However, it should be noted that food waste is a potential resource of biomass that can be treated and converted into high-value compounds. Therefore, incineration of food waste is energetically undesired. Food wastes are further valorized by feeding to animals (e.g., fruit and vegetable pulp, distiller's wash and pomace) and composting to provide fertilizers for farmers. However, animal feed is limited due to some regulatory issues and costs of implementing composting methods are considerably high.[8,9] Hence, there is a critical need of new methods to manage food waste and prevent its accumulation. This, along with the significant demand of new renewable resources caused by the society's concern over the exhaustion of fossil fuel reserves, has resulted in a remarkable research avenue to valorize food waste.[10]

Food waste is rich source of proteins, carbohydrates, lipids, and different minerals, which can be potentially employed in production of high-value compounds. There are thermochemical and biological techniques, such as hydrothermal processes, pyrolysis (to produce liquid bio-crude oils), gasification, anaerobic digestion (to produce biogas for heat and electricity production), and fermentation of sugars (to produce alcohol), to utilize food waste for valuable products and

convert it into energy.[11] Each of these routes requires specific operating conditions or feedstock pretreatment. For example, during anaerobic digestion, the contribution of the environmental factors such as temperature, pH etc., to the process efficiency has led to a significant need of process optimization.[12] Fermentation, alternatively, requires hydrolyzing food waste and producing fermentable sugars in advance of the process, which makes it economically unfavorable.[13] Among thermochemical processes, pyrolysis and gasification face some technical challenges with high-moisture content food waste, since they both require dry biomass, generally less than 30 wt % moisture content.[14] Hence, these processes are not well adapted to using wet untreated biomass. In contrast, hydrothermal processes are promising routes to valorize food waste since they can directly use high-moisture food waste and avoid the need of drying feedstock prior to processing.

Properties of sub- and supercritical water

High temperature water (HTW) plays the reaction medium role for hydrothermal processes, owing to its unique properties at high pressures and temperatures (above 200 °C).[15] The properties of water at elevated temperature are very different than the ones for ambient liquid water. These properties are also largely affected by temperature and pressure. For example, the dielectric constant of water reduces with temperature as it increases to the critical point (T=374 °C and P=22.1 MPa) or above. It is about 78.46 at 25 °C and 0.1 MPa, and decreases to 1.51 at 550 °C and 30 MPa.[16] Furthermore, water exhibits a higher diffusion rate and lower viscosity and surface tension at temperatures around the critical temperature.[17] The ion product (K_w) of high temperature liquid water is greater by about three orders of magnitude than that of the ambient water. Consequently, the concentration of H^+ and OH^- ions from self-ionization of HTW is very high, that provides a favorable environment for acid- and base- catalyzed reactions to occur.[18]

Overall, these unique and tunable properties of water at high temperature provide great environments for chemical processes.

Hydrothermal Liquefaction

Owing to its unique properties, high temperature water liquefies biomass into bio-crude oil, a biofuel precursor. This process is known as Hydrothermal Liquefaction (HTL), and it occurs at temperatures between 200 and 400 °C, and pressures between 10 to 40 MPa. At this pressure and temperature range, biomass hydrolyzes, so that biomacromolecules break down and further react to produce products including viscous hydrophobic bio-crude oil.[19] Utilizing HTL to process biomass is also beneficial in terms of energy consumption, as it avoids the need of drying feedstock that is required by other conversion processes like pyrolysis. Moreover, efficient product recovery can be achieved in aqueous phase environment, as biocrude oil tends to partition into an organic fluid phase at ambient temperature.

HTL of wet biomass results in formation of energy-dense bio-crude oil along with nutrient rich aqueous phase, gaseous and solid products. Biocrude oils have higher heating values of 30-35 MJ/kg.[19] Depending on reaction conditions and feedstock composition, biocrude oil yields reportedly vary from 10 to 68 wt %.[20] Aqueous phase products typically contain organic and inorganic nitrogen, phosphorus, and carbon constituents, that are suitable towards being used as fertilizers or growing additional biomass like microalgae that would ultimately reduce cultivation costs.[21,22] The solid residues are composed of ash, chars with high molecular weights, and metals.[23] Lastly, the gas products are mainly composed of carbon dioxide (CO_2), and smaller fractions of methane, ethane, ethylene, and hydrogen.[19] The yield of each product fraction is dependent on process variables like temperature, pressure, time, and biomass loading, as well as the biochemical composition of the feedstock.[24–26]

HTL of Food Waste

Food waste is composed of three main components including carbohydrates, lipids (fats), and proteins in varying ratios. There have been studies investigating HTL of a variety of feedstocks including each of these individual components and their compounds.

Posmanik et al.[27] , Gollakota et al.[28] and Robin et al.[29] conducted HTL on individual components of food waste including lipids, proteins and carbohydrates. They showed that the biochemical composition of the feedstock strongly affects the products yield and quality. Higher yields of bio-crude oil were reported from lipids than protein, which gave higher yields than carbohydrates.[28,30–33] Pavlovic et al.[34] , Daniel et al.[14,35] , Posmanik et al.[27] and Zastrow et al.[36], subjected model food waste compounds of carbohydrates, lipids and proteins to different reaction conditions and investigated bio-crude oil and in some cases other co-products including aqueous phase, gas and solids. Although the literature provides numbers of reports on individual components and model food waste compounds, there are few data available from using real food as feedstock to the reactors. Zastrow et al.[36] employed HTL on a surrogate food waste, developed based on military waste analysis data. They studied the effect of temperature (250, 280, 315 °C) and batch holding time (10, 30, 60 min) on HTL of food waste. They reported the highest bio-crude oil yield of 45 wt % at 315 °C and reaction time of 10 minutes. Maag et al.[37] also conducted HTL on a food waste mixture containing American cheese, canned chicken, instant potatoes, green beans, white rice, apple sauce and butter at temperature of 300 °C with a holding time of one hour. They observed 38 wt % for bio-crude oil yield and HHV of 35.6 MJ/kg. In most cases, liquefaction studies focused on temperature between 200 to 350 °C. The reactors were also filled with determined amount of water so the pressure inside them would be high enough to keep water in the liquid phase. Reported HHV and yield of the bio-crude oil was typically 34-36 MJ/kg and 25-47 wt %, respectively. Furthermore, there have been few published studies that examined the

water-soluble products, solids and gas products that are generated along with bio-crude oil by HTL of food waste.

Moreover, HTL is typically performed with reaction time varying between 3 to 60 min. "Fast" HTL, which is conducted nonisothermally under high heating rates and batch holding times less than 3 min, has not been reported for real food waste. However, there have been published studies of fast HTL on individual components of food waste. Improved HHVs and greater bio-crude oil yields were reported for soy protein, potato starch, casein and sun flower oil compared to "isothermal" HTL, which involves reactions with holding times more than 3 minutes.[28,38]

Due to the high capital costs of conducting HTL at larger scales, researchers have shown extensive interest in improving bio-crude oils quantity and quality by conducting assisted HTL (catalysts, additives) at milder reaction conditions, which also would be more economically favorable for scale-up purposes.[39] There have been studies of assisted HTL on biomass with a positive effect on bio-crude oil yield and quality.

Maag et al.[37] conducted both heterogeneous and homogeneous catalyzed HTL on food waste by using $CeZrO_x$ and Na_2CO_3, respectively. The comparison between catalyzed and uncatalyzed HTL demonstrated an improvement of bio-crude oil yield from 38 wt % to 53 wt %, however with a slight decrease of HHV by using $CeZrO_x$ as a catalyst. Employing 5 wt % Na_2CO_3 resulted in less nitrogen content of oil products and lower HHV of 24.2 MJ/kg, and had modest effect on oil yield.

Heterogeneous catalysts have further been screened for HTL on soy protein.[40] The study showed that employing metal catalysts (Pd, Pt or Ru) supported on porous solids resulted in reduction of heteroatom contents of bio-crude oil, with Ru/C showing the strongest effect. The Ru/C catalyzed reaction led to 16% higher HHV of oil with sulfur content below detection limits. Similarly, Duan et al.[41] conducted HTL on microalga *Nannochloropsis* sp. in the presence of

heterogeneous catalysts. They reported supported Ni as the strongest catalyst for bio-crude oil desulfurization and Pt/C as the catalyst resulting in the highest oil HHV. The inconsistency of results provided by a brief literature review makes the selection of appropriate metal catalysts for improving HTL of food waste complicated. This story is also true for HTL processes conducted using acid and alkali catalysts. Posmanik et al. reported the highest bio-crude oil yield by using phosphoric acid as acidic catalyst and the highest bio-crude oil HHV and no furans using sodium hydroxide as basic catalyst.[42] Hence, a comprehensive study on screening potential catalysts for the HTL of food waste is necessary.

Hydrothermal carbonization (HTC) utilizes food waste for the production of biochars and enhancing their properties as solid fuels.[43–47] HTC also has been employed for the recovery of fatty acids from algal biomass, by producing biochars retaining the lipid fraction and using a food grade solvent (ethanol) to extract the fatty acids.[48] Food wastes can have lipid fractions composed of more than 70% fatty acids. Therefore, a similar process can potentially be effective for food waste valorization.

Another benefit of subjecting of food waste to HTC would be the recovery of nutrients in the aqueous phase, which consequently reduces the level of N in biochars. Combustion of biochar containing N forms NO_x and therefore retaining of this element within the biochar limits its application. Successful results have been reported for the recovery of this element in the aqueous phase products by conducting HTC on organic feedstocks. [47,49–51] However, there is a lack of knowledge in understanding the effect of process variables on nutrient recovery during HTC of food waste.

Another potential method to recover nutrients and reduce the N level in biochars and biocrudes is conducting two-step treatments. This approach is basically coupling low temperature HTC with a subsequent HTL step at higher pressures and temperatures. Using HTL in one step can enhance the yield of the biocrudes, but it also can be detrimental by reducing their quality and

retaining N element within them.[52] Therefore, this two-step approach can also address this challenge by reducing N level in biochars and transferring more N into the aqueous phase products at the first stage, followed by promoting biocrude yields at higher temperatures in the second step.

Overview

A review of literature on hydrothermal valorization of food waste shows there has been no report of investigating the effect of a wide range of HTL process variables for food waste. There are very limited studies on improving the HTL of food waste with the aid of catalysts. There are also insufficient studies on investigating low temperature processes to recover nutrients and fatty acids from food waste. To fill these gaps in the research field, the following group of research studies are designed to elucidate the effect of process variables and catalysts on producing biocrude oils for the HTL of food waste, and to demonstrate the use of thermochemical methods to recover nutrients and fatty acids from food waste components.

Chapter 2 provides an overview of biocrude oil yields and qualities, and nutrients migration into different products for HTL of food waste, under the wide range of reaction conditions. In Chapter 3, we utilized different types of potential catalysts including supported metals, metal oxides, acid, bases, and salts, to improve the biocrude oil qualities and quantities. Chapter 4 focuses on low temperature hydrothermal carbonization with the goal of not only recovering nutrients in the aqueous phase products, but also producing biochars retaining fatty acids from food waste, and further extracting them with the use of ethanol, a food grade solvent. Chapter 5 aims similarly to recover nutrients into the water soluble products, but also focuses on improving biocrude oil yields as well. We employed the two-step thermochemical treatments

including both hydrothermal and pyrolytic processes to accomplish this goal. Chapter 6 contains the results of work in this dissertation and recommendations for future research.

Chapter 2

Effect of Process Variables on Food Waste Valorization Via Hydrothermal Liquefaction

This chapter contains results originally published in *ACS ES&T Engineering* written along with co-author Professor Phillip E. Savage.[53] Hydrothermal liquefaction (HTL) of simulated food waste was conducted over a wide range of temperatures, pressures, biomass loadings, and batch holding times. The effects of operating parameters on the yields of biocrude oil, water-soluble products and solids were investigated. Further, the effects of process variables on the elemental and chemical compositions and thermal stability of biocrudes and the nutrient recoveries in water-soluble products were examined. Finally, a kinetics model for HTL of microalgae was tested for predicting biocrude oil yields from HTL of simulated food waste.

Introduction

About 1.3 billion tons of food (one-third of all food produced for human consumption) is wasted globally every year.[5] Composting, animal feed, and fermentation are current alternatives to landfills.[9] However, due to disease control concerns, use as animal feed has become illegal in some countries.[8] The environmental issues associated with food waste, along with the recognition that it represents a renewable resource, have resulted in research into conversion of food waste into value-added products.[10] Thermochemical processes such as pyrolysis, gasification, and hydrothermal treatment are promising routes for valorizing food waste.[11] For high-moisture feedstocks like food waste, hydrothermal processing is advantageous, since it can accept wet feedstocks directly and avoid the need of drying prior to processing.[24]

Hydrothermal liquefaction (HTL) converts wet biomass at high pressures and temperatures into an energy-dense biocrude oil and a nutrient-rich aqueous phase product. Gaseous and solid products also form, but typically in lesser amounts. During this process, the biomacromolecules hydrolyze and the primary products can further react to produce the viscous hydrophobic biocrude oil.[19] Water plays the role of reaction medium and facilitates the process due to its unique properties at high pressures and temperatures.[15] For example, the dielectric constant of liquid water decreases with temperature as the critical point (T=374 °C and P=22.1 MPa) is approached. Furthermore, water affords faster diffusion rates and lower viscosity and surface tension around the critical temperature. The ion product of hot compressed liquid water is about three orders of magnitude greater than that of ambient liquid water. This greater abundance of H^+ and OH^- ions provides a favorable environment for acid- and base- catalyzed reactions, such as hydrolysis.[18]

The main components in food wastes are carbohydrates, lipids (fats), and proteins, in varying ratios. There have been prior studies investigating HTL of a variety of these individual components and their constituents[14,27,31,34–36,38]. There are far fewer reports, however, of using real food mixtures as the feedstock for HTL[36,37,54,55]. A surrogate food waste, developed from military waste analysis data, was subjected to HTL to study the effects of temperature (250, 280, 315 °C) and batch holding time (10, 30, 60 min).[36] The highest biocrude oil yield of 45 wt% was reported for HTL at 315 °C and 10 min. In another study, HTL (300 °C, 60 min) was conducted on a model food waste mixture containing American cheese, canned chicken, instant potatoes, green beans, white rice, apple sauce and butter.[37] The biocrude yield was 38 wt% with a higher heating value (HHV) of 35.6 MJ/kg. In other studies, food waste from a university campus dining hall and from an urban area were used as feedstocks for HTL at 280 - 380 °C and at 300 °C, respectively.[54,55] Finally, Bayat et al. conducted HTL on food waste, collected from New Mexico University's restaurant, to investigate optimized HTL conditions for biocrude yield and quality.[56]

In all of these previous studies, however, the HTL temperature was always between 250 to 380 °C and reaction time was from 10 to 60 min. Water was typically in the liquid phase in these prior studies. We are aware of no prior reports on HTL of food waste with water in the vapor phase and there is just one prior study with supercritical water.[54]

There have been few published studies that examined the aqueous-phase products generated along with biocrude oil from HTL of food waste or even waste from the food processing industry.[37,54,57,58] These products can be rich in nutrients (N, P) and the composition depends on reaction conditions.[57] These nutrients can be a source of fertilizer for crop or biomass growth, which can ultimately reduce cultivation costs.[21,22]

Fast HTL, which is conducted non-isothermally with high heating rates for short times (e.g., 1 min) provided improved HHVs and greater biocrude oil yields than isothermal HTL for a variety of feedstocks including model biopolymers in food (e.g., soy protein).[28,38] However, there are no published studies on fast HTL of real food mixtures to ascertain its efficacy for process intensification in this application.

Herein we investigate the effect of a wide range of HTL reaction conditions, including fast HTL, for food waste. We examine the effect of temperature (200- 600 °C), batch holding time (1- 33 min), pressure (10.2- 35.7 MPa) and biomass loading (2- 20 wt%) on product yields, biocrude elemental and chemical composition, HHV, thermal stability, and aqueous phase nutrient contents. We examine hydrothermal treatment with water in the vapor, saturated liquid, compressed liquid, and supercritical states.

Materials and Methods

Feedstock and Solvents

A mixture of food items from a local grocery store was made such that it would represent a typical food waste.[36] The mixture was made by blending together canned green beans (23.2 wt%), canned baked beans (32.4 wt%), potato salad (24.2 wt%), canned chicken (10.9 wt%) and shredded parmesan cheese (9.3 wt%). We refer to this mixture as "simulated food waste", as it is not obtained from an actual waste source but it is made of real food items.

The simulated food waste contained 71.3 wt% moisture as prepared. Table **2-1** presents the feedstock composition as determined by a commercial lab. Deionized (DI) water, prepared with Direct-Q3 UV-R EMD Millipore, was used as the hydrothermal medium. Dichloromethane (DCM) (HR-GC grade, EMD Millipore) was used for recovering biocrude oil from the reactors. Nitrogen gas was used (99.999%, Praxair) for evaporating DCM from the biocrude oil samples.

Table **2-1**: Dried feedstock composition.

Feedstock Composition	*wt % Dry Matter*
Protein	27.5
Non-Structural Carbohydrates	36.5
Fiber	14.9
Lipids	15.7
Ash	5.4

Reactors and HTL Procedure

316 stainless-steel batch reactors, constructed from one ½ in. Swagelok port connector and two Swagelok caps, were used to conduct all the experiments. A high nickel alloy might be needed for an HTL reactor at scale, due to potential corrosion issues from salt in food. Each

reactor had an internal volume of approximately 4.1 mL. Prior to using the reactors in experiments, they were loaded with DI water and treated at 500 °C for 60 min to remove any organic material from the as-manufactured components. The treated reactors were then cooled, opened, thoroughly washed with DCM, and dried in the oven.

The conditioned reactors were loaded with the wet food mixture and water such that each contained the desired wt% loading of dry biomass, relative to the total mass in the reactor. For each reaction condition, the water loading was calculated such that the desired pressure (values from 10.2- 35.7 MPa) would be attained when the reactors reach the sand bath set-point temperatures of 200 - 600 °C.

Pressure was not measured, but an estimated value was calculated from thermodynamics, based on the known temperature, amounts of water and air in the reactor, and reactor volume. This calculation gives just an approximate value, as it neglects gas formation during HTL and the portion of the reactor volume occupied by solids (e.g., biomass, residual solids), both of which would vary during the course of the reaction. Even so, the pressure estimate based on considering only water and air serves as a useful proxy that assists in interpreting the experimental results.

The loaded reactors were then sealed and placed in a preheated fluidized sand bath (Techne IFB-51). After the desired batch holding time had elapsed, the reactors were removed from the sand bath. They were quenched in an ice-water bath for 15 minutes, thoroughly dried, and equilibrated at room temperature for two hours.

A proxy reactor identical to those used in the hydrothermal experiments except for an Omega 1/8 in. K-type thermocouple was used to measure the internal reactor temperature during the reaction. The proxy reactor was loaded with DI water and 5 wt% biomass, as were the other reactors. Temperature was recorded automatically every 1 s. Two trials were done at each set-point temperature and the mean values were used as the representative temperature profile for the

reactor. Reactor temperature profiles at 500 °C and 600 °C sand bath set-point temperatures are shown in Figure **A-1**.

Product Recovery

The cooled, equilibrated reactors were opened and the gas products were vented. Then, the contents of each reactor were drawn into a 10 mL plastic syringe. A Whatman grade 1 qualitative 25 mm filter paper was placed into a Sartorious stainless steel 25-mm syringe filter holder, fitted into the plastic syringe. The solids were then filtered out from the liquid products and collected on the filter paper. To ensure all of the contents inside the reactor were recovered, the reactor and the cap were washed three times with 3 mL aliquots of DCM followed by 2 mL aliquots of DI water. Each time, the contents, including DCM and DI water, were drawn into the same plastic syringe and the solids were filtered out through the same filter holder and filter paper.

The filtered water and DCM phases were poured into centrifuge tubes, well mixed with a vortex mixer, and centrifuged at 6000 rcf for 6 min. The DCM phase was withdrawn using Pasteur pipets and added to pre-weighed glass tubes. The glass tubes were placed in Labcono RapidEvap Vertex Evaporator to evaporate DCM by flowing N_2 at 40 °C for 8 hours. The material remaining in the tubes was then weighed to determine the mass of biocrude oil. The filter papers with solid residues and the aqueous phase products were dried in an oven at 60 °C and 40 °C, respectively. Next, the filters and tubes were weighed to measure solids and aqueous phase masses. The mass of each product fraction was divided by the mass of the biomass loaded to the reactors to calculate each product fraction yield. For each reaction condition, the experiments were done in triplicate. Product yields reported here are mean values ± the sample standard deviation. When assessing whether differences between experimental values were statistically

meaningful, we used one-way ANOVA followed by Tukey's test or the Bonferroni test (*$p < 0.05$, **$p < 0.01$ and***$p < 0.001$) using GraphPad Prism 8.0.

Analytical Chemistry

The C, H, N and S contents of the feedstock and biocrudes were measured using a CEInstruments (Thermo Electron Corp) Elemental Analyzer EA 1110 equipped with a thermal conductivity detector (TCD). The oxygen contents were determined by the difference subtracted from 100%. The HHVs of biocrude samples were estimated using the Dulong-Berthelot correlation as given in Equation 1, where each element represents its wt% in the biocrude. The HHV of the feedstock was measured experimentally using ASTM D5865. Equation 2 was used to calculate the energy recoveries in the biocrude.

$$\text{HHV (MJ/kg)} = 0.3414\,C + 1.4445\,(H - ((N+O-1)/8)) + 0.093\,S \quad (1)$$

$$\text{Energy Recovery (\%)} = (\text{HHV of Biocrude} \times \text{Biocrude Yield}) / \text{HHV of Feedstock} \quad (2)$$

Aqueous phase product samples from different runs were analyzed for total carbon and total nitrogen using dry combustion and total phosphorus using EPA 3050B (acid digestion)[59] and EPA 6010 (inductively coupled plasma-atomic emission spectrometry).[60]

Biocrude oil samples were analyzed using gas chromatography mass spectrometry (GC-MS). The samples were dissolved in DCM and 3 μL was injected with a 5:1 split ratio and an injection temperature set to 310 °C, into a Shimadzu GC-MS QP-2010 Ultra equipped with a 0.2 mm inner diameter Agilent HP-5MS nonpolar capillary column (50 m x 0.33 μm). The column temperature was initially set to 40 °C with a hold time of 3 min, followed by a ramp at 5 °C min^{-1} to 300 °C with a 5 min hold time. The mass spectrum of each individual peak was compared against the NIST mass spectral library to tentatively identify the molecular species when there was at least an 85% match factor.

Thermal Gravimetric Analysis (TGA) of biocrude oil samples was done using a thermal analyzer (SDT Q600, TA Instruments, U.S.A.). The analysis was carried out from 25 to 700 °C at the heating rate of 10 °C min^{-1}. Nitrogen (99.99% purity) with the flow rate of 100 mL min^{-1} was used as the carrier gas.

Results

This section first discusses the effects of reaction conditions on product fraction yields and subsequent sections focus on the biocrude elemental and chemical composition, HHV, and thermal stability, and aqueous phase nutrient contents.

Effect of reaction conditions on product fraction yields

Effect of Temperature

HTL was conducted at set-point temperatures of 200, 300, 350, 400, 500, and 600 °C with a simulated food waste loading of 5 wt%. The reactors were loaded with water such that the pressure inside the reactor would reach 35.3 MPa at the set-point temperature. Figure **2-1** shows the product fraction yields from isothermal HTL with 30 min batch holding time and from fast HTL with 1 min batch holding time.

The distinction between fast and isothermal HTL is that fast HTL is accomplished entirely non-isothermally, with rapid heating for a short period of time, and does not reach the sand bath set point temperature. Isothermal HTL, on the other hand, is accomplished for 30 min and the reactor is held at the sand bath set point temperature for > 90% of that time.

The highest oil yields (28- 30 wt%) for isothermal HTL were from treatment at 300 - 400 °C. The biocrude oil yield dropped to 12 and 14 wt% at 500 and 600 °C, respectively. Brown et al.[19] conducted similar isothermal HTL experiments with the microalga *Nannochloropsis* and reported similar results for that feedstock. HTL at 350 °C led to the highest bio-oil yield. Lower temperatures provided insufficient thermal energy to produce much biocrude and higher temperatures promoted gasification reactions that consumed much of the biocrude.

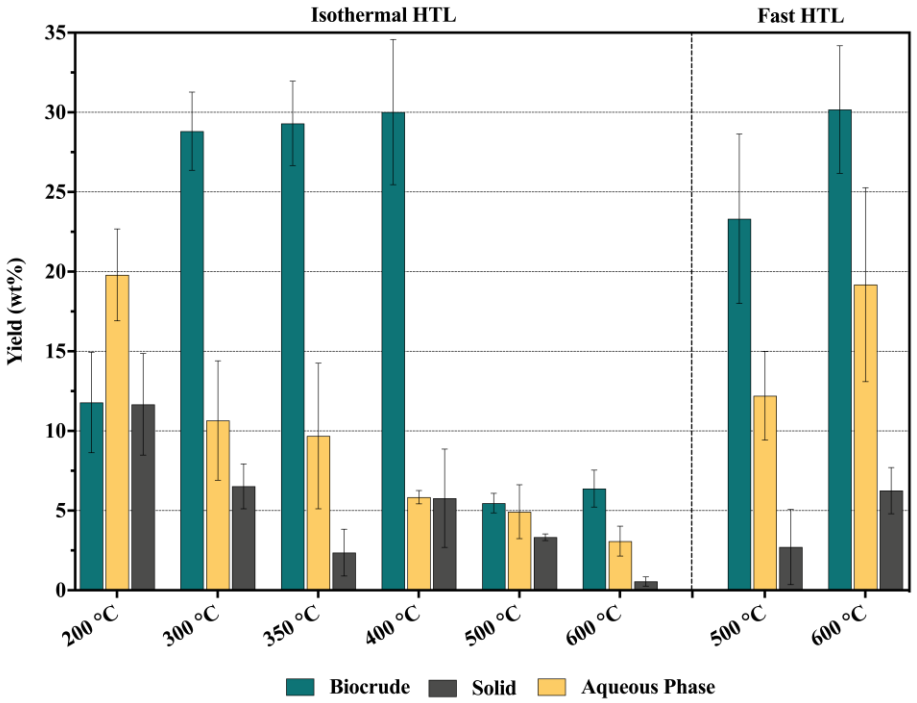

Figure **2-1**: Product fraction yields from HTL of simulated food waste (5 wt% biomass loading). The first six columns represent isothermal HTL for 30 min and the last two columns represent fast HTL for 1 min batch holding time. The water loading was such that the pressure inside the reactor would reach around 35.3 MPa at each set point temperature. Data are represented as mean ± std dev.

The biocrude oil yield from fast HTL of food waste was approximately as high as the highest yields from isothermal HTL. The reactors reach 339 -382 °C prior to being removed from the sand bath and quenched (see Figure **A-1**). These temperatures are in the range where the

maximum biocrude oil yield was achieved for isothermal HTL. This high biocrude oil yield at a short time of just one minute shows the possibility of process intensification via fast HTL.

Isothermal HTL of simulated food waste generated <12 wt% yield of solids, which are insoluble in both DCM and water. This yield decreased with increasing temperature. The yield of water-soluble products from HTL at 200 °C exceeded the biocrude oil yield. These yields decreased with increasing HTL temperature, likely due to decarboxylation, dehydration, and decarbonylation of the initially formed water-soluble molecules.[27]

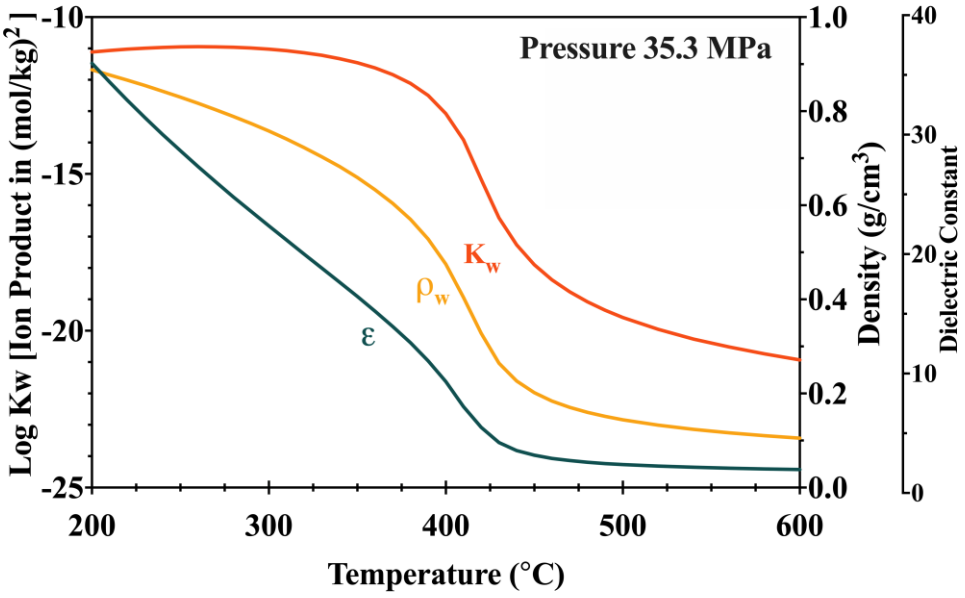

Figure **2-2**: Properties of water as a function of temperature at 35.3 MPa.[16,61]

As noted above, thermal energy itself can play a major role in producing the results in Figure **2-1**. Additionally, the properties of water change significantly over the wide temperature range examined and these changes may also be playing a role.

As shown in Figure **2-2**, the dielectric constant (ε) of water decreases with increasing temperature (and decreasing density) at constant pressure of 35.3 MPa[16]. Water with such a low

dielectric constant behaves more like a polar organic solvent than ambient liquid water.[15] The ion product (K_w) remains approximately unchanged from 200-350 °C but decreases sharply beyond 400 °C (Figure **2-2).** [61] This is also the region where the biocrude yields started to decrease (Figure **2-1)**. As mentioned earlier, the highest biocrude yields were achieved between 300-400°C. In this temperature range, log K_w maintains a high value but both density (ρ_w) and dielectric constant are decreasing. Thus, the experimental biocrude yields are highest when the value of log K_w remains high and the value of the dielectric constant and density have decreased to around 10-20 and 0.5-0.76 (g/cm^3), respectively.

Effect of Pressure and Water Density

To investigate the effect of pressure on the product yields, three sets of experiments were conducted at 350 °C with a batch holding time of 30 min. In each of these sets, only one of the following was kept constant: the biomass wt% loading in the reactor, the water loading (mass), or the biomass loading (mass), along with time and temperature.

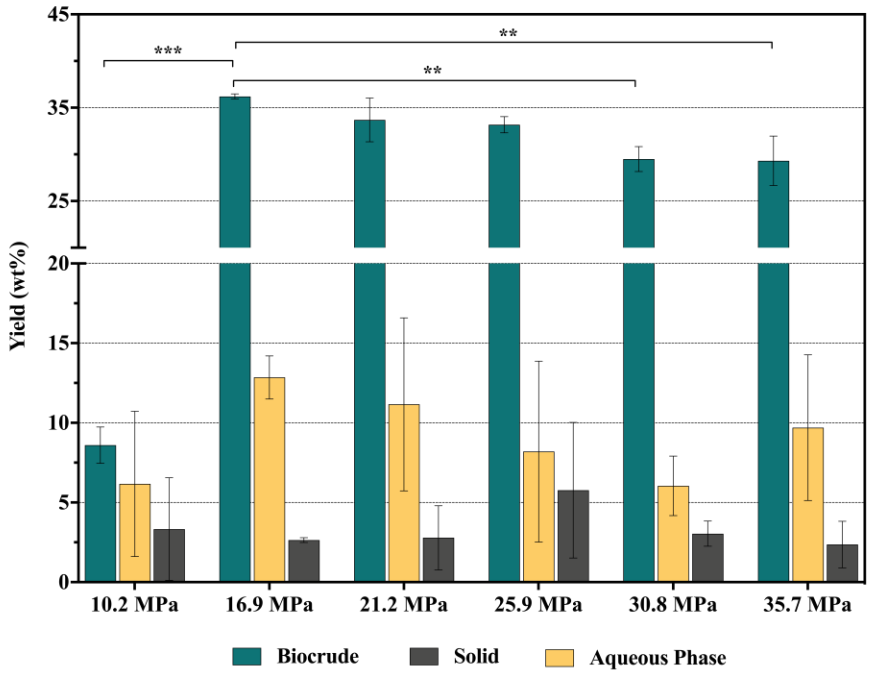

Figure **2-3**: Product fraction yields from hydrothermal treatment of simulated food waste (350 °C, 30 min, 5 wt% biomass loading). The water loading was such that the reactor would be at the desired pressure (x-axis entries) at 350 °C. Yields are represented as mean $\pm$ std dev (**$p < 0.01$, and ***$p < 0.001$, $n > 3$). .

Figure **2-3** compares product fraction yields from hydrothermal treatment runs where the reactors were loaded with different amounts of food waste and water but always with the same ratio (a fixed 5 wt% loading of simulated food waste). The amount of water loaded was such that the pressure inside the reactors, as calculated from thermodynamics, would range from 10.2 to 35.7 MPa at the 350 °C set point. This set of experiments explores hydrothermal treatment with water as a vapor, saturated liquid, and compressed liquid.

There was a significant increase of biocrude oil yield as pressure increased from 10.2 MPa (vapor phase) to 16.9 MPa (close to saturated liquid). The biocrude oil yield then decreased gradually as pressure increased further to 35.7 MPa (compressed liquid).

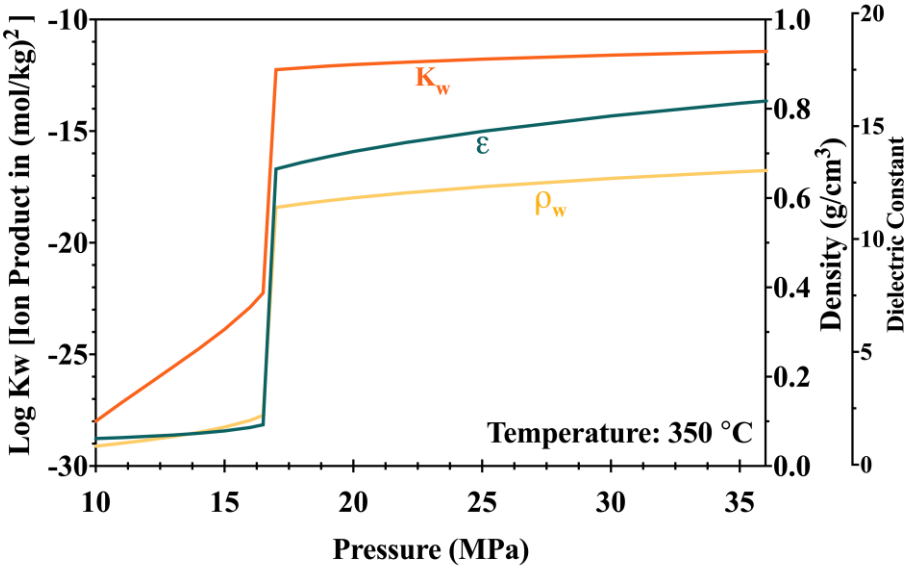

Figure **2-4**: Properties of water as a function of pressure at 350 °C.[16,61]

Figure **2-4** shows the properties of water at 350 °C for pressures from 10 to 36 MPa. The empirical equations proposed by Uematsu and Franck[16] and Marshall and Franck[61] were used to calculate the dielectric constant (ε) and ion product (K_W) of water, respectively. At 16.5 MPa (saturation pressure of water at 350 °C), where the vapor-liquid phase change occurs, there is a corresponding abrupt change in the values of these properties. It should be noted that 16.9 MPa (very close to the saturation pressure) is where the biocrude yield increased from 8.6 wt% at 10.2 MPa, to 36.2 wt% at 16.9 MPa (Figure **2-3**). These observations indicate that hydrothermal treatment does not function as well in the vapor phase as it does in the liquid phase.

As pressure increased further (> 16.9 MPa), Figure **2-4** shows no considerable change of log K_w or density for liquid water. The dielectric constant, however, increases steadily from ~13.3 at 16.9 MPa to ~16.3 at 35.7 MPa. In addition, Figure **2-3** shows a modest decrease in biocrude yields in this compressed liquid phase, which might be related to the changing dielectric constant.

Overall, these results show that hydrothermal treatment in the vapor phase is not as effective as it is in liquid water and that once the pressure is high enough to keep water in the liquid phase, increasing pressure further does not greatly alter the water properties or the biocrude yields.

To generate the results in Figure **2-3**, we loaded reactors with different amounts of biomass, and the mass of water loaded was varied, to keep the 5 wt% loading constant in all experiments. To determine whether the varying biomass amount (mass) or the water loading (mass) was responsible for the observed behavior, two additional sets of experiments were conducted.

All reactors were loaded with the same fixed amount of dried biomass (62 mg). The reactions were conducted at 350 °C for 30 min. The water loading (mass) was varied such that the pressure inside the reactors would reach 13.8 to 35.7 MPa at the reaction temperature. 13.8 MPa was the lowest pressure attainable in this set of experiments as loading lesser quantities of biomass could lead to unacceptably high experimental variability in the mini-batch reactors. This experimental approach led to the biomass wt% loading differing from run to run.

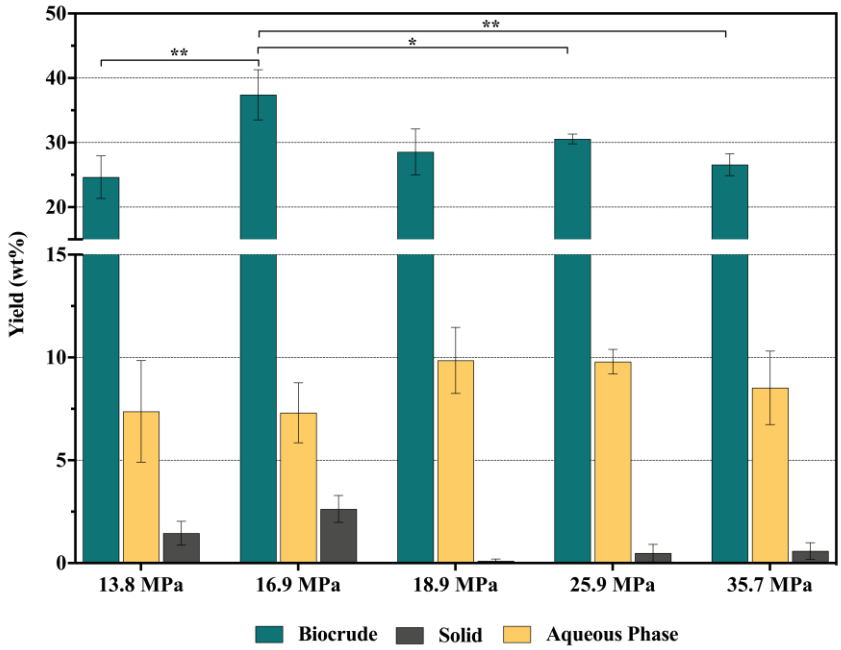

Figure **2-5**: Product fraction yields from hydrothermal treatment of simulated food waste (350 °C, 30 min, fixed mass (62 mg) of simulated food waste loaded). The biomass loadings are 20.0 wt% for 13.8 MPa, 8.69 wt% for 16.9 MPa, 2.57 wt% for 18.9 MPa , 2.42 wt% for 25.9 MPa, and 2.29 wt% for 35.7 MPa. Data are represented as mean $\pm$ std dev (*$p < 0.05$, **$p < 0.01$, $n > 3$).

Figure **2-5** shows there was an increase of biocrude oil yield from 13.8 MPa (water in vapor phase) to 16.9 MPa (water in liquid phase). Then, the biocrude oil yield decreased gradually as the pressure increased. The same behavior was apparent in Figure **2-3**. The biocrude oil yield observed here at 13.8 MPa (vapor phase) is higher than that at 10.2 MPa in Figure **2-3** (also vapor phase). The higher yield here could be due to the higher reactor pressure and water density. Linear interpolation from the biocrude yields at 10.2 MPa and 16.9 MPa in Figure **2-3** gives a value of 23.44 wt% at 13.8 MPa, which is very close to the experimental value of 24.7 wt%. There may be a linear trend for the biocrude yield with pressure at low pressures where water is in the vapor phase.

In this set of experiments, the mass of water loaded into the reactor was kept constant (2.564 g), which led to the same pressure (25.9 MPa) inside the reactors at the 350 °C reaction temperature all runs. The batch holding time was 30 min. The reactors were loaded with varying

amounts of biomass, so the biomass wt% loading varied from run to run. Figure **2-6** presents the results.

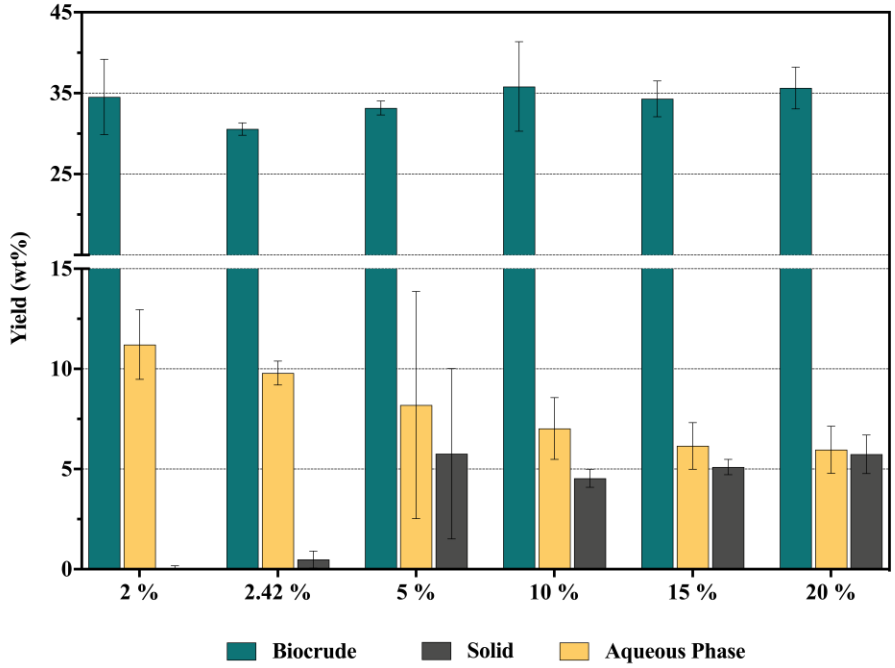

Figure **2-6**: Product fraction yields from HTL of simulated food waste (350 °C, 30 min, fixed mass of water loaded) at different loadings wt% loadings of biomass. The reactor pressure was 25.9 MPa at 350 °C. Data are represented as mean ± std dev.

The biocrude oil yields remained largely unaffected by the reactor biomass loading, as it was varied from 2 wt% to 20 wt%. This behavior points to the mass of water in the reactor, which controls both the water density and water phase present in the reactor, as being a key variable in the production of biocrude during hydrothermal treatment. The aqueous phase product yields in Figure **2-6** decreased from 12% at the lowest loading to 6% at the highest. The reason for this trend is not clear at present. The low solid yields at the two lowest loadings could be due to the difficulty of recovering and measuring these low yields when loading a very small amount of feedstock into the reactors.

Effect of batch holding time

Figure **2-7** compares product fraction yields from HTL of simulated food waste at different batch holding times at 300 °C. The biomass loading was 5 wt% and water loading was such that the pressure inside the reactor would reach 13 MPa, at 300 °C.

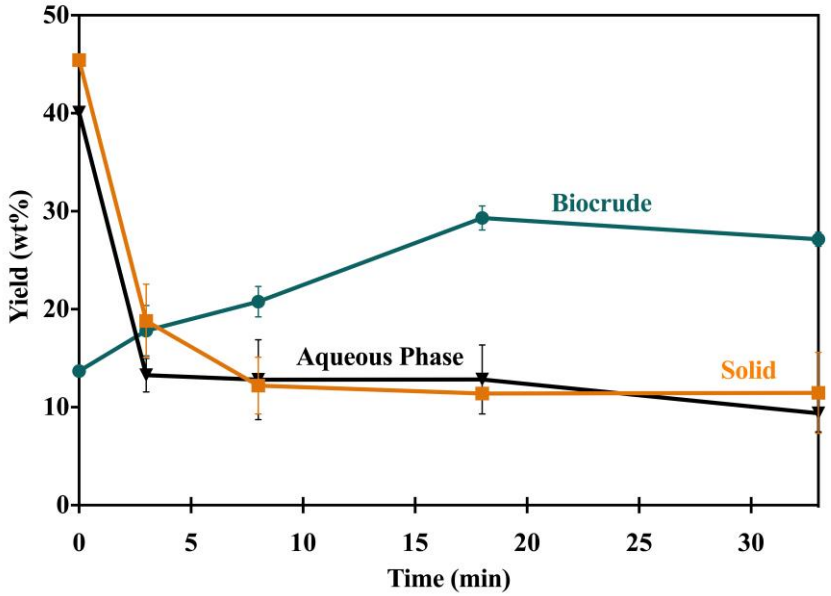

Figure **2-7**: Product fraction yields from HTL of simulated food waste (300 °C, 13 MPa, 5 wt% biomass loading). Data are represented as mean ± std dev.

The first data point in Figure **2-7** (t = 0) represents a control experiment wherein the reactor was at room temperature and never placed in the sand bath. The reactor contents were then subjected to the same product recovery protocol used in the HTL experiments. Thus, this experiment shows the proportions of different product fractions in the simulated waste before any HTL occurs. Note that the yields of solids, biocrude, and aqueous-phase products sum to nearly 100% for this run at t=0. This outcome is consistent with the methods used herein to recover these product fractions being reliable and accurate. HTL converts the biomass solids and water-soluble material in the simulated food waste within a few minutes. After 8 min, the solids yield

was time invariant, and it most likely represented the ash component in the biomass. HTL increased the biocrude oil yield to 29.3 wt% as the batch holding time increased to 18 minutes. The trends in Figure **2-7** are consistent with prior reports on HTL of food waste. [36,54]

Effect of reaction conditions on biocrude composition and properties

Elemental Composition

The elemental compositions of simulated food waste and biocrude from hydrothermal treatment under all the experimental conditions are given in Table **2-2**. The carbon content of the biocrude always exceeded that of the feedstock. The hydrogen content of the biocrude did as well, save for one experiment at 35.7 MPa. The carbon content increased with temperature for isothermal HTL runs at 35.3 MPa, 5 wt% loading, and 30 min batch holding time. As the HTL temperature increased from 200 to 600 °C, the carbon content in the biocrude increased from 68.7% to 77.4%, consistent with greater loss of heteroatom-containing functional groups at more severe reaction conditions. The hydrogen content however did not show any specific trend with temperature. Similar to this behavior, Brown et al.[19] reported an increase in carbon content from 74.6 wt% to 81.2 wt% with increasing temperature from 200 to 500 °C for isothermal HTL of *Nannochloropsis*. They also reported the hydrogen content remained unaffected as temperature increased except that it dropped from 10 wt% to 7.1 wt% at 500 °C. This behavior is in accord with the present results (Table **2-2**). The biocrude carbon contents in Table **2-2** show no systematic changes with pressure, batch holding time, or reactor loading.

Table **2-2**: Elemental Composition (wt%) of simulated food waste and biocrude from hydrothermal treatment under different reaction conditions. Oxygen is calculated by difference.

			C	H	N	S	O
Simulated Food Waste			47.8	5.11	4.78	0.23	41.6
Biocrudes		**Set-Point Temperature (°C)**					
5 wt% biomass loading 35.3 MPa Variable water & biomass amounts	30 min	200	68.7	7.73	0.66	-	-
		300	72.9	7.82	4.30	0.59	14.4
		350	73.2	7.50	4.57	0.15	14.6
		400	73.6	7.95	4.75	0.14	13.6
		500	77.4	6.89	6.25	0.28	9.17
		600	77.4	8.11	2.09	0.68	11.7
	1 min	500	71.3	6.71	2.97	0.24	18.7
		600	74.4	7.64	3.94	0.23	13.9
		Pressure (MPa)					
5 wt% biomass loading Variable water & biomass amounts 350 °C, 30 min		10.2	74.1	7.76	1.96	0.22	16.0
		16.9	73.4	6.67	4.58	0.14	15.2
		21.2	70.5	6.83	4.27	0.51	17.9
		25.9	71.7	6.54	4.17	0.37	17.3
		30.8	70.7	6.82	4.14	0.21	18.2
		35.7	73.2	7.50	4.57	0.15	14.6
62 mg biomass Variable water amount Variable wt% biomass loading 350 °C, 30 min		13.8	70.1	6.06	3.95	1.08	18.8
		16.9	70.7	6.83	4.30	0.15	18.0
		18.9	66.7	6.78	3.30	0.00	23.2
		25.9	71.0	7.34	3.93	0.25	17.5
		35.7	68.9	3.95	3.71	1.59	21.9
2.564 g water Variable biomass amount Variable wt% biomass loading 350 °C, 30 min, 25.9 MPa		**Biomass Loading (wt%)**					
		2	72.8	6.29	4.25	0.23	16.4
		2.42	71.7	6.54	4.17	0.37	17.3
		5	73.1	6.71	4.71	0.13	15.4
		10	71.1	7.05	4.34	0.37	17.1
		15	73.5	7.31	4.70	0.00	14.5
		20	73.6	7.42	4.76	0.22	14.1
		Batch Holding Time (min)					
5 wt% biomass loading 300 °C, 13 MPa Variable water & biomass amounts		3	73.1	6.92	1.46	0.12	18.4
		8	73.0	6.34	1.79	0.14	18.8
		18	71.9	6.06	4.30	0.33	17.5
		33	72.5	6.73	4.60	0.52	15.6

Both fast and isothermal HTL produced biocrude oil that had much lower oxygen content than did the feedstock. The oxygen content decreased steadily with HTL temperature except at 600 °C with 30 min batch holding time. It also exhibited the same trend with increasing batch

holding time. A decrease in oxygen content in biocrude as reaction severity increases has been noted in prior HTL studies.[19,26,62,63] Lower heteroatom content is desired since it corresponds to an increase in the heating value of biocrude. At different pressures where biomass loading was kept constant at 5 wt%, the oxygen content was as low as 16.0 and 15.2 wt% at 10.2 and 16.9 MPa, respectively, but it increased to ~18 wt% at higher pressures of 21.2, 25.9 and 30.8 MPa. Otherwise, the oxygen content did not show any specific trends with changing process variables.

The biocrude contained both nitrogen and sulfur, as these elements were present in the simulated food waste. In some runs, these elements were in lower amounts in the biocrude than in the biomass and in other runs they were higher. There were no clear trends. Table **2-2** shows higher nitrogen content in the biocrude from HTL at the more severe reaction conditions. This observation is consistent with nitrogen-containing compounds (e.g., amino acids) originally in the aqueous phase reacting more readily amongst themselves (dimerization) and with sugars (Maillard reaction) to form hydrophobic molecules that partition into the biocrude, as the reaction conditions become more severe. This results in the transfer of nitrogen atoms from the aqueous to the organic phase. Luo et al. made a similar observation for the HTL of soy protein, where nitrogen content of the biocrude increased as the batch holding time increased from 10 to 20 minutes.[33]

The HHV of the simulated food waste was measured via bomb calorimetry to be 22.3 MJ/kg, based on its dry weight. The HHVs for biocrude were estimated from elemental composition data and are depicted in Figure **2-8.** The HHVs for the various biocrudes were all ~ 35 MJ/kg, which is comparable to those from HTL of food waste in prior studies.[37,36] Energy recovery in the biocrude exceeded 65% at 16.9 MPa (Figure **2-8c)** and at a loading of 20 wt% Figure **2-8e**. Also, Figure **2-8e** shows an increase in energy recovery as reactor loading increased from 2.4 to 20 wt%.

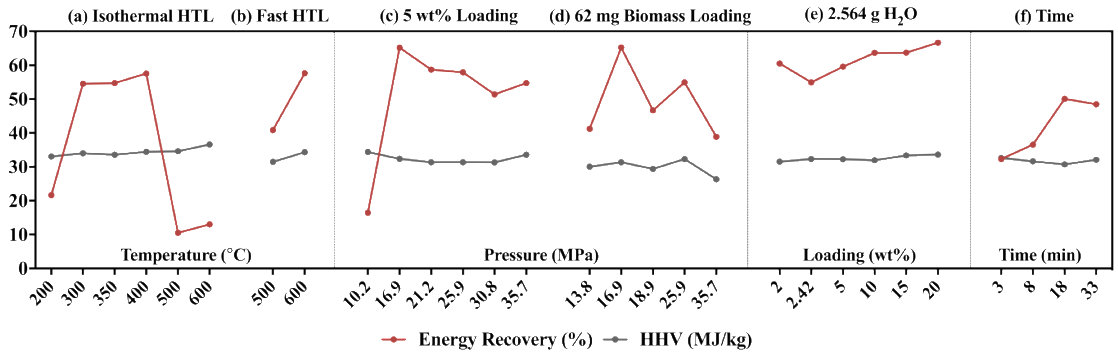

Figure **2-8**: Higher Heating Values (HHVs), and energy recoveries of biocrudes from hydrothermal treatment of simulated food waste under different reaction conditions. a) Isothermal HTL, 35.3 MPa, 5 wt% biomass loading, 30 min, b) Fast HTL, 5 wt% biomass loading, 1 min, c) Constant 5 wt% biomass loading, 350 °C, 30 min, d) Constant 62 mg mass loading of biomass, 350 °C, 30 min, e) Constant water mass loading of 2.564 g, 350 °C, 30 min, 25.9 MPa, f) Effect of batch holding time, 300 °C, 13 MPa, 5 wt% biomass loading.

Thermal Stability

The thermal stability of several of the biocrudes was determined using TGA. The biocrude samples where heated from room temperature to 700 °C under nitrogen. Figure **2-9** summarizes the weight loss during TGA of biocrudes, within temperature ranges that correspond with boiling point fractions for different petroleum fractions.[64] The TGA curves are given in Figure **A-2.**

The biocrudes from isothermal HTL were largely composed of products that evaporated in the boiling range of diesel fuel. Bayat et al.[56] also reported a large fraction of biocrude oil from HTL food waste was in the diesel and lubricating oil range. Fast HTL, on the other hand, resulted in biocrudes with a much higher fraction of heavy compounds in the heavy gas oil range. Comparison of the first three columns in Figure **2-9** shows that the TGA profile for the bio oil was not much affected by the HTL temperature. The sixth column represents results from TGA of biocrude from HTL at 350 °C, 16.9 MPa with 5 wt% loading and 30 min batch holding time.

Comparing that data with the second column, which had the same HTL conditions except the pressure was 35.7 MPa, shows a reduction of diesel-range compounds and an increase of light compounds (gasoline range) accompanied the reduction in HTL pressure. The last two columns show that increasing the batch holding time increased the fraction of mid-range compounds.

Figure **2-9** shows the residual mass from the biocrudes produced by fast HTL was just 2 wt%, which is much lower than the ~16 wt% residue for the biocrudes from isothermal HTL. The longer reaction times in isothermal HTL led to greater conversion of biocrude molecules into larger and heavier compounds. A similar outcome was reported for biocrudes from fast and isothermal HTL of chitin[65] and five other different polysaccharides[62]. Chen et al.[55] also reported ~15% residuals from TGA of biocrude produced by isothermal HTL of real food mixture at 320 °C.

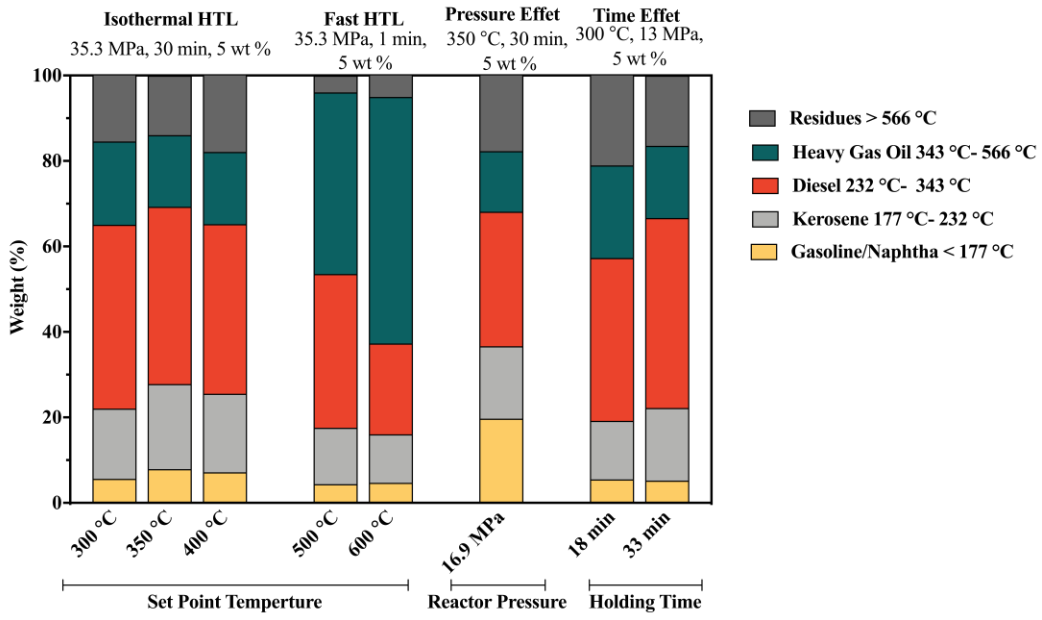

Figure **2-9**: Cumulative weight loss (%) from biocrudes from HTL of simulated food waste, as determined by TGA, with temperature ranges that correspond with boiling point fractions for different petroleum products.

About 35 wt% of the biocrude oil from isothermal HTL remained at 350 °C. This amount corresponds to the existence of heavy components in the biocrudes. It is similar to the amount remaining at 350 °C from TGA of biocrude from isothermal HTL of Chlorella pyrenoidosa algae (~ 34 wt%), but higher than that from HTL of sewage sludge (~ 22 wt%).[66,67]

Molecular Composition

The TGA results illustrate how the composition of the biocrude can be affected by reaction conditions, but it does not give any molecular details. Figure **2-9**, shows that about 55 wt% of biocrudes from isothermal HTL and 40 wt% of biocrudes from fast HTL were lost after heating to 300 °C, which means this fraction of the oil would be amenable to GC-MS analysis. We tentatively identified compounds in the biocrude oil produced under both isothermal and fast HTL by matching (at least an 85% match factor) mass spectra for GC peaks with mass spectra of known compounds stored in the NIST library. Each of the compounds had at least 0.1% relative peak area. These components account for more than 75% of the total area of the chromatogram.

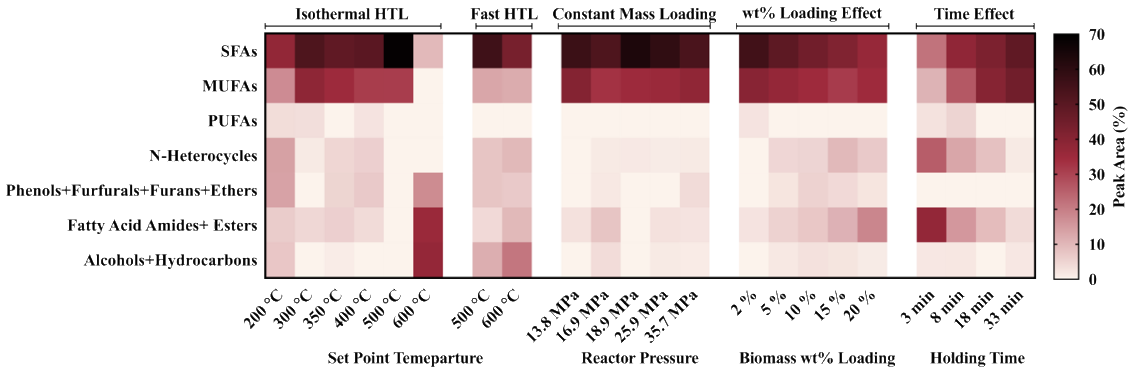

Figure **2-10**: Heat map for peak area percentage of compound classes in biocrude oils from hydrothermal treatment of simulated food waste. Experimental sets include isothermal HTL (35.3 MPa, 5 wt%, 30 min), fast HTL (5 wt%, 1 min), constant food mixture mass loading with varying water loading (350 °C, 30 min), constant water mass loading (350 °C, 25.9 MPa, 30 min), and the effect of batch holding time (300 °C, 13 MPa, 5 wt%).

Biocrude from hydrothermal treatment of the simulated food waste contained a combination of saturated fatty acids (SFA), mono-unsaturated fatty acids (MUFAs) and poly-unsaturated fatty acids (PUFA), along with nitrogen heterocycles, phenols, furfurals, furans, ethers, fatty acid amides, esters, alcohols, and hydrocarbons. Figure **2-10** shows a heat map for the total peak area percentage of the different compound classes for the biocrudes from different hydrothermal treatment conditions. Under all reaction conditions, SFAs (stearic acid, myristic acid) and MUFAs (oleic acid, palmitoleic acid) were the compound classes with the largest peak areas. Stearic, myristic, and oleic acid are all abundant in parmesan cheese, one of the components of the simulated food waste used in this work. The abundance of SFAs and MUFAs is consistent with similar analyses of biocrude from hydrothermal treatment of a different food mixture[54].

Carbohydrates, lipids, and proteins are the main components of food. During HTL, proteins produce pyrroles, indoles, and other nitrogen heterocycles.[35,68] Proteins decompose initially into peptides and amino acids, which then undergo deamination, dehydration, and decarboxylation depending on their structures.[33] Carbohydrates hydrolyze under subcritical conditions and then these primary products form phenolic compounds and ketones by dehydration and condensation.[24,69] The chief hydrothermal reaction for triglycerides is hydrolysis to generate glycerol, mono- and di-glycerides, and fatty acids.[70,25] Hydrothermal treatment of the simulated food waste produced compounds in addition to those expected from proteins, lipids, and carbohydrates, individually. For example, fatty acid amides were observed in the total ion chromatogram. These may form via condensation reactions between amino acids from proteins and fatty acids from lipids, and their presence demonstrates the interactions between different biomolecules.

Reaction conditions appear to affect the abundance of different compounds in the biocrude oil. SFAs and MUFAs were most strongly affected by reaction conditions. For isothermal HTL with 5 wt% loading, 30 min batch holding time, and 35.3 MPa pressure, SFAs increased with temperature from 200 °C to 500 °C, while the rest of the compounds decreased. Higher biomass wt % loading in the reactor resulted in lower relative amounts of SFAs, and had little effect on MUFAs and PUFAs. However, the abundance of the rest of the compounds increased with the increase of biomass wt % loading. SFAs and MUFAs increased with the increase of batch holding time from 3 minutes to 33 minutes. Different reactor pressures with the same mass loading of feedstock did not have much effect on the relative abundance of different compounds. For fast HTL, the relative abundance of SFAs and MUFAs were lower at the higher set-point temperature, and the rest of the compounds became more abundant.

Taken collectively, the results in Figure **2-10** show that the contribution from each of the reactions in the overall network for hydrothermal treatment of food waste can be enhanced or diminished by different reaction conditions. Although the reaction mechanisms are not fully clear for the HTL of food waste, this product slate variability points to the possibility of engineering the biocrude composition, to an extent, by controlling the reaction conditions.

Effect of reaction conditions on aqueous-phase nutrient contents

The post-HTL recovery of nitrogen and phosphorus from the food waste is important for sustainability as these elements are used in fertilizers to grow food. Figure **2-11** shows the percent of the biomass N, C, and P that was recovered in the aqueous-phase products and in the biocrude.

The nitrogen and phosphorus recoveries reported herein for the aqueous phase and biocrude are the first accounts of nutrient recovery from HTL of real food over a wide range of temperatures.

Nitrogen recovery in the aqueous phase was 23% from HTL at 200 °C and it gradually decreased as the HTL temperature approached 400 °C (Figure **2-11a)**. Meanwhile, the N recovery in the biocrude showed the opposite trend. These trends indicate that N-containing compounds initially partition into the aqueous phase (e.g., amino acids) but reactions occurring at greater reaction severities (e.g., Maillard reaction, amino acid dimerization) render these compounds less hydrophilic and more likely to partition into the biocrude phase. As the temperature increased further to 600 °C, the N recovery in the aqueous phase increased to 50% and that in the biocrude dropped to nearly zero. This high amount of N in the aqueous phase could be from decomposition at 500 and 600 °C of N-containing molecules that would have been lost as volatiles during product workup from HTL at lower temperatures. In addition, decomposition of N-containing molecules in the biocrude at high temperatures also appears to contribute.

Figure **2-11b** shows the carbon recovery in the biocrude always exceeded that in the aqueous phase for HTL at 400 °C and below. Carbon recovery in the aqueous phase remained low but gradually increased with HTL temperature. At the highest temperatures, biocrude yields were low, so the C recovery in biocrude was low as well.

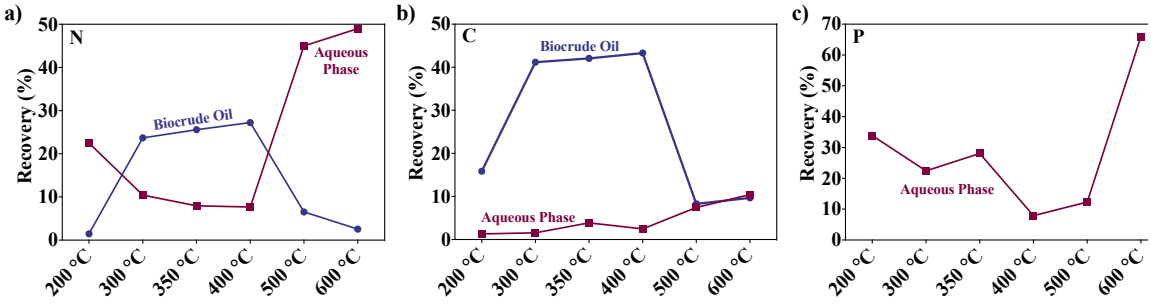

Figure **2-11**: Recovery (%) of a) nitrogen, b) carbon, c) phosphorus atoms from simulated food waste in the biocrude and aqueous-phase products from isothermal HTL (35.3 MPa, 5 wt% biomass loading, 30 min).

The phosphorus recovery in the aqueous phase was similar to the N recovery in that it first decreased with increasing HTL temperature and then increased sharply at the most severe HTL conditions. Retention of phosphorus in the aqueous phase is favored at either low temperature (200 °C) or at high temperature (600 °C). The retention of phosphorus at mild reaction conditions was shown before for the HTL of *Nannochloropsis sp.*[26], where more than 80% of the initial phosphorus partitioned into the aqueous phase, primarily as phosphate, after HTL at 250 °C. Additionally, Ekpo et al.[71] reported that the post-HTL aqueous phase contains both organic and inorganic phosphorus. They also reported that phosphorus was mainly in the form of phosphate at the more severe HTL conditions. It also has been shown that organic P breaks down to form phosphate as the reaction conditions become more severe.[72] Therefore, the 68% P recovery in the aqueous phase from HTL at 600 °C is most likely to be in the form of phosphate.

Predictions from a Kinetic Model for HTL of algae

Sheehan et al. developed an empirical kinetic model for the HTL of microalgae that predicted biocrude yields based on the protein, lipid, and polysaccharide content of the algae, along with the HTL time and temperature.[73] Their model parameters were determined by fitting the model to experimental product fraction yields from algal HTL studies at different temperatures (250-400 °C) and times (10-90 min), with biomass loadings around 15 wt%.[74,75] Their model could predict 70 published algal biocrude yields from HTL within this parameter space to within $\pm$ 5 wt%, which is similar to the typical experimental uncertainty.

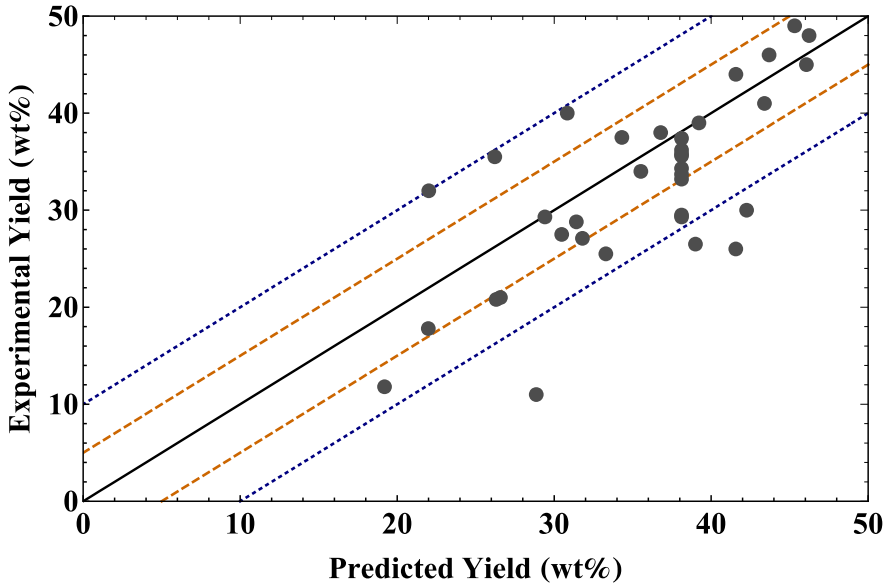

Figure **2-12**: Predicted and experimental yields (dry basis) of biocrude oil from HTL of different real food mixtures (Details are in Table **A-1**). The black, orange and blue lines represent 0, 5, and 10 wt% deviation, respectively.

We further tested the predictive capability of their model by predicting the yields of biocrude from HTL of the simulated food waste reported in this work along with some literature results[36,37,54]. Structural and non-structural carbohydrates were lumped together as polysaccharides for their model input. The ordinary differential equations, which arose from the proposed reaction network, were solved using Mathematica 12. Table **A-1** presents the details and the parity plot in Figure **2-12** provides a visual comparison.

Of 35 data points in Figure **2-12**, their model predicted 22 to within $\pm$ 5 wt% of the experimental yields and 31 to within $\pm$ 10 wt%. The reaction conditions for these 35 data points are in the same range of reaction conditions used to determine the Arrhenius parameters in their model. This test shows that their HTL kinetics model, though developed for microalgae, can give useful predictions of biocrude yields for food-based feedstocks as well. It also supports the hypothesis that HTL outcomes can be modeled by using biochemical composition of the feedstock as key input data.

Figure **2-12** shows the predicted biocrude yields exceed the experimental values (data points below the solid diagonal) about three times as frequently as the converse. We speculate that this outcome is due to the model not being parameterized for the accurate prediction of yields from HTL of polysaccharide-rich biomass. All of the food wastes in Figure **2-12** had polysaccharide content exceeding 40 wt% and most were over 50 wt%. The model parameters, on the other hand, came from consideration of data for HTL of algal biomass with, at most, 32 wt% polysaccharides.

Conclusions

This study reports the effect of process variables on HTL of a real food mixture over the broadest range of conditions yet explored with a single feedstock. In addition, we elucidated the influence of pressure, a process variable largely neglected in previous studies and explored fast HTL.

The yields (~ 30 wt%) and HHV (~ 35 MJ/kg) of bio-oil from HTL of this simulated food waste are comparable to those achieved from HTL of microalgae. Reaction conditions that favor high biocrude yields are temperatures near the critical point (374 °C) and pressures high enough to maintain water as a liquid or a dense (> 0.4 g/cm^3) supercritical phase. HTL at 350 °C in the vapor phase is not nearly as effective as it is in the liquid phase at the same temperature. Once the reactor pressure is high enough to keep water in the liquid phase, further pressure increases have little effect on the water properties and the biocrude yields.

Fast HTL can convert the food mixture into biocrude oil yields of 25-30 wt% within a batch holding time of just 1 min. Fast HTL is successful for valorizing food components just as it was for valorizing microalgae, sewage sludge, and other wet biomass resources.

HTL of the simulated food waste afforded energy recovery in the biocrude of up to 65%. Half or more of the biomass N and P, potential nutrients, partitioned into the aqueous phase after HTL and could potentially be recovered for use in fertilizer. The HTL conditions (30 min at 500, 600 °C) that led to these high nutrient recoveries, however, led to low biocrude yields and low energy recoveries. Additional research and modeling is needed to determine the conditions that give the optimal balance of energy recovery and nutrient recovery.

About half of the mass of the biocrudes from HTL of the food mixture comprised compounds that evaporated at 300 °C or below, and saturated and unsaturated fatty acids were major components in this lighter fraction. About 60% of the mass of the biocrudes from isothermal HTL evaporated in the temperature range corresponding to the boiling range of diesel fuels, kerosene, and gasoline. For fast HTL, this percentage dropped to 40-50%.

A kinetics model for predicting biocrude yields from algae HTL was able to predict biocrude yields from HTL of food waste to within ± 5 wt% for two-thirds of the cases examined and to within ± 10 wt% for nearly 90% of the cases. This level of agreement supports the hypothesis that biocrude yields from HTL can be predicted from knowledge of the HTL time and temperature and the biochemical composition of the wet biomass feedstock. The predictive ability of the current kinetics model might be broadened by using data from HTL of polysaccharide-rich feedstocks to regress new values for its kinetics parameters.

Chapter 3

Screening Potential Catalysts for the Hydrothermal Liquefaction of Food Waste

Results from the following chapter were previously published in *ACS Energy & Fuels* and co-authored by Sofia H. Capece, and Professor Phillip E. Savage.[76] This work studies the effect of supported metals, bulk metal oxides, and a set of salt, acid and base additives on HTL of simulated food waste. The yields, elemental compositions, heating values, thermal stabilities, and molecular compositions of the biocrudes produced from assisted HTL of simulated food waste are reported. The nutrient recoveries in aqueous phase products from HTL with metal oxides are also elucidated.

Introduction

Rather than being relegated to landfills, where it decomposes and forms greenhouse gases, food "waste" can be viewed as a wet biomass resource (15 million dry tons annually in US alone[77]). Different portions could be used as a feedstock for different renewable fuels. Fats and oils can be converted to biodiesel, sugars in polysaccharides can be converted to bioethanol, and whole biomass can be converted to crude bio-oil by pyrolysis or hydrothermal liquefaction (HTL).

HTL is an effective process for producing bio-oil from wet biomass and it requires no energy-intensive drying process[78]. The products from HTL are an energy-dense, crude bio-oil and aqueous, gas, and solid phase product fractions. Nutrients (N, P) to produce more food can potentially be recovered from the solids or aqueous phase. The hot, compressed water serves as

reaction medium, reactant, and catalyst precursor by generating H^+ and OH^- in situ, which can catalyze hydrolysis reactions that break down the biomacromolecules such as proteins and polysaccharides[15]. HTL is typically conducted between 250 - 400 ℃, and it results in a bio-oil of lower oxygen content and greater heating value than bio-oil from fast pyrolysis[79].

If catalysts can be identified for HTL of food waste, they could increase reaction rates, improve selectivities to desired products, and generate bio-oil of higher quality. Catalytic HTL has received much attention for feedstocks such as microalgae and model components of biomass. [40,80–82] These studies showed that metal nanoparticles supported on different porous materials (e.g., activated carbon, Al_2O_3), [41,83–85] metal oxides, [86–89] , and various salts, bases, and acids [25,36,97,98,70,90–96,42] can sometimes improve biocrude yields and properties from HTL. Much less work has been done on catalytic HTL of an actual food mixture.

The limited literature in this area shows that red mud and clay increased the biocrude yield and HHV and doubled the energy recovery compared to HTL of the same food waste without use of these materials[99]. Nickel supported on metal oxides also led to an increase in energy recovery and biocrude yields from HTL of food waste.[100] A CeZr oxide was also an effective catalyst.[37] Employing 5 wt % Na_2CO_3 resulted in less nitrogen in the oil products for the HTL of surrogate military food waste.[36] In two other studies on HTL of food waste, carbonates were used but only for pre-treatment, as a part of two-step liquefaction, and they enhanced the biocrude yields and qualities.[101,102] Adding NaOH to the HTL of food waste also increased the HHV of the biocrude oil about 9 %.[42]

Though there are some prior reports on catalytic HTL of food waste, we are aware of no comprehensive study that examined a broad set of different classes of potential catalysts for HTL of the same food waste feedstock. Such a study would provide valuable comparisons of the efficacy of different materials under identical HTL conditions. To fill this gap in the literature, we report herein on the influences of different salts, bases, and acid (K_2CO_3, Na_2CO_3, KH_2PO_4,

K_2HPO_4, K_3PO_4, NaOH, KOH, HCOOH), different supported metals (Ni/C, Pt/C, Ru/C, Pd/C, activated carbon, Ni/SiO_2-Al_2O_3, Pt/Al_2O_3, Ru/Al_2O_3) and different bulk metal oxides (CaO, Al_2O_3, CeO_2, Ca_2O_3, SiO_2) on the biocrude oil yield and quality for the HTL of a simulated food waste at 350 °C. We also report on the nitrogen and phosphorus recoveries in the aqueous phase products, as sustainability considerations dictate recovering and reusing these elements to make fertilizer and grow more food.

Experimental Section

Materials

A simulated food waste was made from a mixture of food items as discussed in previous work.[53] The mixture was 27.5% protein, 36.5 % non-structural carbohydrates, 14.9% fiber, and 15.7% lipids, by mass. Its elemental composition was 47.8% carbon, 5.11% hydrogen, 4.78% nitrogen, 0.47 % phosphorus, 0.23% sulfur, and 41.6% oxygen, by mass. This mixture had been stored in a freezer for 13 months prior to its use in the present experiments. All but four of the potential catalysts were purchased from Sigma-Aldrich. Ni/C was purchased from Riogen, Inc. Pt/Al_2O_3 and Pd/Al_2O_3 were obtained from Strem Chemicals. K_2CO_3 was obtained from JT Baker Chemicals. All of the supported metals were nominally 5 wt% metal, per the suppliers. Ni/SiO_2-Al_2O_3 was 65 wt% Ni. All the potential catalysts were used as received. Deionized (DI) water, prepared with Direct-Q3 UV-R EMD Millipore, was used as the hydrothermal medium. Dichloromethane (DCM, HR-GC grade), used for recovering biocrude oil from the reactors, was obtained from Millipore Sigma. Nitrogen (99.999%), used for evaporating DCM from the biocrude oil samples, was obtained from Praxair. Helium and hydrogen were also obtained from Praxair.

Stainless steel (316) batch mini-reactors were used for this study. They had a volume of 4.1 mL and were made from one ½ in. Swagelok port connector and two Swagelok caps. For the experiments with pressurized hydrogen, a cap on one end of the reactor was replaced by a Swagelok reducing union (½ in to 1/8 in.) and fitted with a 6 in. length of 1/8 in. O.D. tubing with a wall thickness of 0.028 in, connected to a HiP high-pressure valve.

Procedure

Prior to using the new reactors in an experiment, any organic material from the as-manufactured components was removed by loading the reactors with DI water and holding them at 500 °C for 60 min. In this way, the fresh reactor walls were seasoned by exposure to hot, compressed water. Next, the reactors were cooled to room temperature, thoroughly rinsed with DI water and DCM, and dried in an oven. The reactors connected to valves were leak-tested at room temperature with high pressure H_2, using soap solution, prior to use.

In a typical experiment, 0.82 g of wet food mixture (containing 0.59 g water) was loaded into the reactor, followed by 1.8 mL of DI water, to give a 10 wt% biomass loading in the reactor. Next, 0.118 g of the potential catalyst, representing a 50 wt % loading with respect to the dry food mixture, was added into the reactor. In some experiments, the reactors were charged with H_2 to 3500 kPa at room temperature, and the valve was then securely closed. After the reactors were loaded with all components, they were sealed and submerged in a pre-heated Techne Fluidized Sand Bath (Techne IFB-51) at 350 °C. After 40 minutes had elapsed, the reactors were removed from the sand bath and submerged in cold water to quench the reaction. The reactors were then placed on a bench top for 1 hour to allow the reactor contents to equilibrate.

The reactors were next opened, any gases within were released, and solids and liquids were extracted from within. 3 mL of DCM, to dissolve organic products, and 3 mL of DI water, to dissolve water-soluble products, were added in sequence to the reactors. The reactor contents were transferred to a centrifuge tube after being passed through pre-weighed glass fiber syringe filters to trap any solids. This process was repeated until the DI water and DCM from the reactor were clear, indicating that no product remained in the reactors.

The liquid layers in the centrifuge tubes were then centrifuged at 6000 rcf for 6 minutes. The phases were separated from each other using Pasteur pipets, and transferred into separate pre-weighed glass test tubes. The biocrude oil was obtained by evaporating the dichloromethane under a stream of nitrogen at 40 °C for 8 hours using a Labconco RapidEvap Vertex Evaporator. The tubes with aqueous-phase products and the glass-fiber syringe filters were dried in an oven, at 40 °C and 60 °C, respectively. This was done until the tube and filter masses changed by less than 0.5 mg.

The dried tubes and filters were then weighed to find the mass of each product phase by subtracting the mass of the empty tubes and new filters. For the experiments with supported metals and metal oxides, the mass of the potential catalyst was subtracted from the mass of solids recovered, to determine the mass of solid products from HTL of the simulated food waste. The yield of each product fraction was obtained by dividing the mass of each product fraction by the mass of food (dry basis) loaded into the reactor. The values herein are the mean values ± the sample standard deviation, determined from at least three independent trials.

Bio-crude Oil Analysis

A Shimadzu gas chromatograph mass spectrometer (GC-MS) equipped with a 0.2 mm inner diameter Agilent HP-5MS nonpolar capillary column (50 m x 0.33 μm) was used to analyze

biocrude oil samples that were re-dissolved in DCM. Details have been reported previously[53]. The NIST mass spectral library was used to tentatively identify molecular species, with a similarity index > 85% being required for a tentative identification.

An Elemental Analyzer EA 1110 (CEInstruments (Thermo Electron Corp)) equipped with a thermal conductivity detector (TCD) was used to measure the C, H, N, and S contents of the biocrudes. The difference between this sum and 100 % was taken as the oxygen content. We used the Dulong-Berthelot correlation, Equation 1**,** to estimate the HHVs of biocrude samples from their elemental wt% composition.

$$HHV\ (MJ/kg) = 0.3414\ C + 1.4445\ (H-(N+O-1)/8)+ 0.093\ S \quad (1)$$

The energy (heating value) in the biomass recovered in the biocrude samples was then calculated using Equation 2.

$$\text{Energy Recovery (\%)} = (\text{HHV of Biocrude} \times \text{Biocrude Yield})/\ \text{HHV of Feedstock} \quad (2)$$

A thermal analyzer (SDT Q600, TA Instruments, U.S.A.) was used to perform Thermogravimetric Analysis (TGA) of select biocrude oil samples. The analysis was carried out in flowing N_2 (99.99% purity, 100 mL min^{-1}) at a sample heating rate of 10 °C min^{-1} from 25 to 700 °C.

Aqueous Phase Analysis

We used EPA method 6010 (inductively coupled plasma-atomic emission spectrometry)[60] and EPA 3050B (acid digestion)[59] to analyze selected aqueous-phase product samples for total phosphorus. We used EPA 350.1 (specific ion electrode)[103] to determine the ammonium-N content of the same samples. Lastly, the total carbon and total nitrogen in the same samples were determined using dry combustion analysis (Dumas method).

Results and Discussion

This section provides information about the biocrude, aqueous-phase, and solid products formed during HTL in the presence and absence of the different potential catalysts. We first discuss the effect of the different supported metals on the biocrude yields from HTL with the presence and absence of H_2. Then we discuss the elemental and chemical composition of the biocrudes. Next, we focus on HTL of the simulated food waste with different salts, bases, and acid and their effect on biocrude quality and yields. The final section focuses on the biocrudes produced in the presence of added metal oxides. We also discuss the recovery of nutrients (N, P) from the aqueous phase produced from HTL with added metal oxide.

Supported Metals

Effect of Supported Metals on Biocrude Oil Yields.

Figure **3-1** shows the effect of the different materials on the biocrude oil and aqueous phase products yields from HTL of simulated food waste, both in the presence and absence of added H_2 (3500 kPa). The oil yields vary from a low of 8.64 wt% from HTL with Ru/C and H_2 to a high of 41.6 wt% from HTL with Pt/Al_2O_3 in the absence of H_2. The biocrude yield previously reported for the HTL of this simulated food waste at 350 °C, 30 min, and 10 wt% biomass loading,[53] is not statistically different from the 40.8 wt% yield reported for the run with no supported metals in this study.

None of the supported metals increased biocrude yields to a statistically significant extent, whether or not H_2 was added. The carbon-supported Pt, Ru, and Pd resulted in lower biocrude yields than did their Al_2O_3-supported counterparts. In addition, the oil yields from HTL

with Pt/C, Ru/C, and Pd/C were all about same as the oil yield from activated charcoal (no metal). The lower oil yields obtained with some of the materials could be due to the carbon support adsorbing molecules that would otherwise appear in the biocrude or to the material promoting reactions that led to oil-phase molecules becoming gases or volatiles or aqueous-phase products.

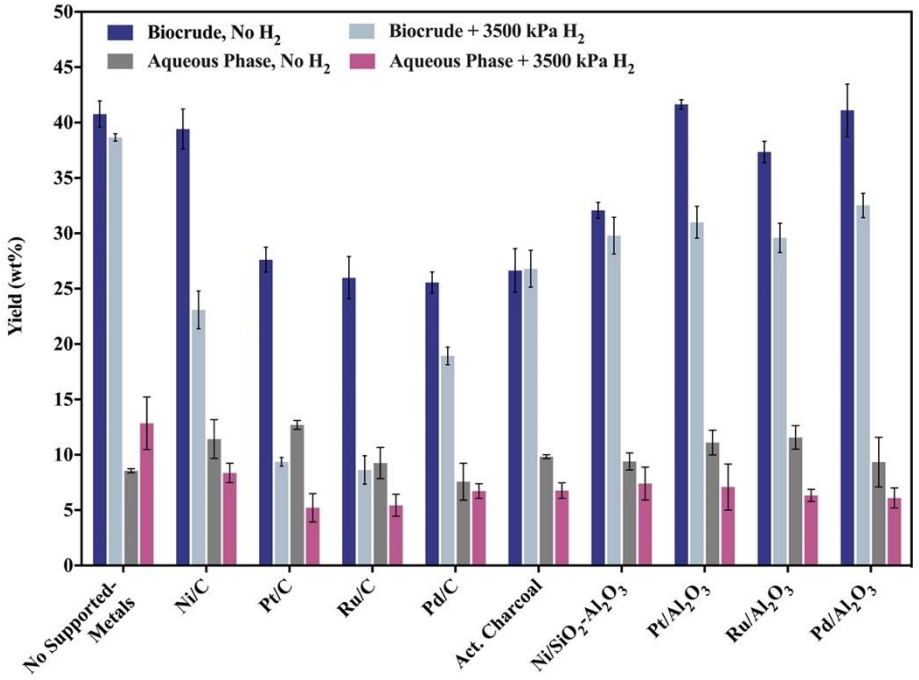

Figure **3-1**: Yields of crude bio-oil and aqueous-phase products from HTL of simulated food waste in the absence and presence of supported metals and 3500 kPa H_2 (350 °C, 40 min, 10 wt % biomass loading, 1:2 supported metal to biomass loading).

The addition of supported metals to the HTL of different types of feedstock has shown both positive and negative effects on the biocrude yields in prior work.[40,41,85,104,105] For instance, when Ru/C was used for the HTL of *Nannochloropsis sp*. at 350 °C, the biocrude yield increased by 15 wt%.[41] But when it was used for the HTL of sewage sludge at 300 °C, the biocrude yield was reduced by 7 wt%.[105] Potential factors for these opposing effects could be the different feedstock compositions, supported metal loadings, or reaction conditions (time and temperature) that were

used for these studies. Prior work showed that temperature and metal loadings can be important factors in determining the extent to which supported metals improve the biocrude yields from HTL.[105,106]

The metals having little effect on the biocrude oil yields could be due, in part, to the HTL conditions selected for this study. We chose conditions that gave the highest oil yields in prior work[53]. It is possible that HTL at these conditions is already generating the highest oil yield physically possible, so there could be little opportunity for a potential catalyst to increase the biocrude yields further. Another potential factor could be metal poisoning (e.g., by sulfur[107]). Additional experiments would be needed to test these hypotheses.

Lastly, aqueous-phase product yields were always in the range of 5 -13 wt%. Supported metals had little effect on the yield of aqueous phase products when no H_2 was present. The aqueous phase yield increased by 4.3 wt%, however, when H_2 was introduced to the HTL run with no supported metals and resulted in the highest value of 12.9 wt% among all the runs. The addition of H_2 to all the other runs with any of the supported metals or with activated charcoal reduced the aqueous-phase product yields. This reduction with added H_2 has been reported previously for catalytic HTL of food waste.[37,99] These reduced yields of aqueous-phase products in the presence of the supported metals and H_2 could be due to catalytic removal of O and N atoms from some of the molecules in the aqueous phase. These metals can catalyze hydrodenitrogenation (HDN) and hydrodeoxygenation (HDO) reactions,[108] which would remove functional groups from molecules and make them more hydrophobic and less likely to partition into the aqueous phase after HTL.

Effect of Supported Metals on Biocrude Oil Elemental Composition.

Although the addition of supported metals failed to increase biocrude yields, we desired to determine whether they could improve the biocrude quality. Tables **3-1 and 3-2** give the elemental composition and estimated heating values of the biocrudes from HTL of simulated food waste with supported metals, both in the presence and absence of H_2. Pt on both supports and Pd/C were the only materials that produced biocrude with a heating value exceeding that of the control experiment both with and without added H_2. This increase was due primarily to these bio-oils having a higher H wt%. Of these three materials, Pt/Al_2O_3 is the only one to also give high biocrude yields, so the run with this material and no added H_2 was the only one in Tables **3-1** and **3-2** to give an energy recovery in the biocrude (72.2%) that exceeded the 67.3% recovery available without a potential catalyst added. Even in this case, the difference in energy recoveries lacked statistical significance.

The sulfur content was eliminated in the biocrudes produced from HTL with supported metals, except for Pt/C, in the presence of H_2. Elimination of S was also the outcome for HTL with Ni/C and Ru/Al_2O_3 when no H_2 was present. Nickel, whether supported by carbon or alumina, has also provided the greatest sulfur removal in prior work.[41,80]

Conducting assisted HTL with no H_2 always produced biocrude oils with lower nitrogen content than the run with no supported metals and no H_2. Of all these runs in Table **3-1**, HTL with Pt/C had the greatest effect and reduced nitrogen to 3.90 wt %. When H_2 was used in the control experiment, Table **3-2** shows a biocrude oil with 4.28 wt % nitrogen content was generated. HTL with Ru/C (and H_2) had the greatest performance by lowering the nitrogen content to 3.57 wt%. Prior work showed that Ru/C was also more effective than other supported metals for reducing the biocrude N content from HTL of soy protein.[40]

Table **3-1**: Elemental composition and heating values of biocrudes from HTL of simulated food waste with supported metals (No added H_2). (350 °C, 40 min, 10 wt % biomass loading, 1:2 mass ratio of supported metal to biomass)

	C (wt %)	H (wt %)	N (wt %)	S (wt %)	O (wt %)	O/C	H/C	HHV (MJ/kg)	Energy Recovery (%)
Blank	73.3	5.66	5.11	0.28	15.6	0.16	0.93	29.7	67.3±1.35
Act. Carbon	69.6	5.68	4.38	0.39	19.9	0.21	0.98	27.8	41.2±1.37
Pd/C	73.8	7.12	4.01	0.07	15.0	0.15	1.16	32.2	45.8±3.76
Pt/C	72.2	6.58	3.90	0.09	17.2	0.18	1.09	30.5	46.9±1.33
Ru/C	72.8	6.19	4.88	0.20	15.9	0.16	1.02	30.2	43.7±3.46
Ni/C	69.4	5.74	4.80	0.00	20.0	0.22	0.99	27.7	60.7±2.40
Ru/Al_2O_3	73.4	5.79	5.03	0.00	15.8	0.16	0.95	29.8	62.0±1.59
Ni/SiO_2- Al_2O_3	71.1	5.81	4.43	0.05	18.6	0.20	0.98	28.7	51.2±1.12
Pt/Al_2O_3	72.0	6.92	4.90	0.84	15.4	0.16	1.15	31.2	72.2±0.74
Pd/Al_2O_3	68.8	5.77	4.58	3.03	17.8	0.19	1.01	28.2	64.6±3.69

The H/C ratios for the biocrudes from HTL under H_2 pressure (Table **3-2**) always exceeded the H/C ratio from the corresponding biocrude from HTL without added H_2 (Table **3-1**). This outcome suggests that H atoms from the gas-phase H_2 were incorporated into the biocrude during HTL. The H/C ratio of the oil produced from HTL with supported metals always exceeded that ratio for the control experiment. This outcome suggests that there might be some common mechanism for carbon rejection from and/or hydrogen addition to the oil in the presence of all of the added materials. Determining whether this mechanism is connected to the greater surface area and enhanced surface reactions or some other feature requires additional research.

Table **3-2**: Elemental composition and heating values of biocrudes from HTL of simulated food waste with supported metals (3500 kPa H_2). (350 °C, 40 min, 10 wt % biomass loading, 1:2 mass ratio of supported metal to biomass)

	C (wt %)	H (wt %)	N (wt %)	S (wt %)	O (wt %)	O/C	H/C	HHV (MJ/kg)	Energy Recovery (%)
Blank	73.4	5.89	4.28	0.29	16.2	0.17	0.96	30.1	64.7±0.56
Act. Carbon	71.8	7.79	3.83	1.18	15.4	0.16	1.30	32.6	48.6±3.03
Pd/C	69.7	7.74	4.00	0.00	18.5	0.20	1.33	31.1	32.7±1.36
Pt/C	74.9	7.51	4.43	0.80	12.2	0.12	1.20	33.7	17.6±0.73
Ru/C	59.8	6.66	3.57	0.00	29.9	0.38	1.34	24.2	11.6±1.74
Ni/C	72.0	8.57	4.81	0.00	14.7	0.15	1.43	33.6	43.2±3.18
Ru/Al_2O_3	71.8	7.14	4.68	0.00	16.4	0.17	1.19	31.2	51.4±2.50
Ni/SiO_2- Al_2O_3	64.8	6.62	3.99	0.00	24.6	0.28	1.23	26.7	44.3±2.47
Pt/Al_2O_3	71.9	7.04	4.92	0.00	16.1	0.17	1.17	31.1	53.6±2.49
Pd/Al_2O_3	66.3	7.31	5.98	0.00	20.4	0.23	1.32	28.6	51.7±1.75

Effect of Supported Metals on Biocrude Oil Molecular Composition

The biocrude oils from HTL with and without supported metals were analyzed at the molecular level using GC-MS. Compounds sufficiently volatile to elute from the GC column were tentatively identified by matching (at least 85% similarity index) their mass spectra with spectra stored in the NIST library. This analysis was done for compounds with at least 0.1 % relative peak area. The identified compounds were placed into one of 11 different groups**.** When a compound could fit into more than one group, we followed the following priority order: fatty acids (FA) > esters > amides > phenols > nitriles > aldehydes > amines > ketones > alcohols > ethers.

Table **3-3**: Relative peak area % for different classes of compounds tentatively identified in the biocrude oils produced from HTL runs with and without supported metals and H_2. (350 °C, 40 min, 10 wt % biomass loading, 1:2 mass ratio of supported metal to biomass)

	Alcohol	**Aldehyde**	**Amide**	**Amine**	**Ester**	**Ether**	**FA**	**HC**	**Ketone**	**Nitrile**	**Phenol**
Blank	3.82	1.44	9.48	8.93	2.11	0.00	55.5	3.24	13.4	0.64	1.46
Blank +H_2	7.39	0.00	14.8	1.26	0.94	0.00	70.4	1.93	3.24	0.00	0.00
Ni/C	9.45	4.39	18.0	9.35	3.08	0.14	28.5	13.7	9.63	2.75	1.02
Ni/C+H_2	0.38	0.00	15.7	3.75	1.71	0.00	71.7	2.92	0.26	0.59	2.93
Pt/C	3.35	0.27	8.79	5.22	1.11	0.00	64.0	6.59	3.84	1.31	5.55
Pt/C+H_2	2.78	0.00	5.05	0.85	5.26	0.10	58.4	22.6	0.00	0.86	4.18
Ru/C	9.63	0.23	6.46	7.32	13.8	9.80	19.4	20.2	6.76	0.00	6.32
Ru/C+H_2	0.70	0.57	2.51	0.31	3.47	0.00	41.1	31.2	1.73	0.15	18.2
Pd/C	3.31	0.30	14.1	4.81	3.02	0.13	55.1	11.2	4.55	0.73	2.84
Pd/C+H_2	0.23	0.00	12.0	0.90	1.67	0.00	72.0	12.8	0.24	0.24	0.00
AC	7.13	0.61	16.6	9.71	7.83	0.49	33.4	5.07	8.94	1.46	8.81
AC+H_2	1.67	0.00	8.37	2.43	3.17	0.00	68.0	8.00	0.66	1.26	6.54
Ni/SiO_2-Al_2O_3	3.52	0.59	11.4	5.94	3.44	0.00	57.4	3.90	6.82	0.69	6.28
Ni/SiO_2-Al_2O_3+H_2	4.50	0.00	16.4	4.34	1.49	0.00	61.0	8.40	1.36	0.47	1.99
Pt/Al_2O_3	6.92	0.71	7.25	3.57	0.97	0.27	71.0	1.20	5.54	0.48	2.06
Pt/Al_2O_3+H_2	1.52	0.88	15.8	1.86	2.12	0.00	71.9	1.77	3.01	0.00	1.23
Ru/Al_2O_3	8.75	0.47	9.63	9.04	7.31	0.00	42.5	8.32	10.0	0.54	3.47
Ru/Al_2O_3+H_2	3.92	0.35	6.86	2.64	5.72	1.02	61.9	12.4	4.64	0.25	0.31
Pd/Al_2O_3	8.87	1.77	16.5	15.0	15.1	4.23	14.3	5.95	11.5	1.13	5.68
Pd/Al_2O_3+H_2	1.85	0.00	17.4	2.73	1.53	0.15	69.4	3.23	2.00	0.61	1.11

FA: Fatty Acids, HC: Hydrocarbons, AC: Activated Carbon

Table **3-3** shows the relative peak area % for each of the compound classes. We use this metric as a proxy for relative abundance. This approximate metric shows that the volatile portion of the biocrude oils from all the runs contains fatty acids (FA) in high abundance (14 – 72 area%). All of the supported metals but Pt/C gave a larger proportion of fatty acids from HTL in the presence of H_2 than in its absence. The biocrude oils from HTL in H_2 with Pt/Al_2O_3, Ni/C, Pd/C, and no supported metal all had fatty acid areas of 70% or greater. Fatty acids can arise from hydrolysis of the triglycerides in the simulated food waste. Depending on the type of lipids, hydrolysis can be accelerated or slowed in the presence of supported metals and H_2.[109]

The use of heterogenous catalysts for deoxygenation of fatty acids has been documented in a number of studies.[70,109–112] The types of lipids and fatty acids determine the impact of the catalysts on the extent of deoxygenation. For example, Pt-based catalysts increased the rate of deoxygenation for oleic acid in the presence of H_2,[109] while Pt/C, Pd/C, and MoO_2/CNTs showed promise for enhancing deoxygenation of palmitic acid without H_2.[110,112] In another study, Ru/C converted fatty acids to a range of hydrocarbons when no H_2 was present.[111] The results in Table **3-3** are consistent with some deoxygenation of fatty acids taking place. The high abundance of hydrocarbons and low abundance of fatty acids in the oil from HTL with Ru/C (no H_2) is a prominent example.

The use of Ru/C, both with and without H_2, shifted the groups of organic compounds in the oil from being primarily fatty acids and amides to being primarily hydrocarbons and phenolic compounds. These results are consistent with results from a study on HTL with Ru/C of soy protein concentrate.[40] It also should be noted that the presence of H_2 led to a larger relative contribution from hydrocarbons, which was accompanied by lesser contributions from alcohols and esters.

The biocrude oil from HTL with no supported metal (no H_2) had a relatively high abundance of ketones (~13 %). All of the supported metals decreased the area % of this class of compounds in the bio-oil, and the addition of H_2 reduced it even further. Previous HTL studies with rice straw[106] and *Dunaliella tertiolecta*[85] also showed that the use of supported metals (Ni/CeO_2, Pt/CNT) resulted in a lower abundance of ketones in the biocrude oils.

Overall, the use of supported metals with and without hydrogen did not show improvement in biocrude yields or energy recoveries. Therefore, we did no further analyses on the HTL products from these experiments and instead examined a different group of potential catalysts.

Additives

Effect of Additives on Product Yields.

Figure **3-2** shows the effect of different salt, base, or acid additives on the yields of biocrude oil, aqueous-phase products, and solids from HTL of simulated food waste. None of the additives increased the biocrude yields with statistical significance. The solid yield was highest, ~9 wt%, when K_2CO_3 was used, and it was lowest for the run with no additives. The aqueous phase yield was highest (45 wt %) for the run with NaOH.

Added Na_2CO_3 and K_2CO_3 gave similar biocrude yields of 33 wt %. Added Na_2CO_3 gave a greater yield of aqueous-phase products and added K_2CO_3 gave a greater yield of solids. Interestingly, the total of these two product fractions are about 27 wt% in both runs. The addition of Na_2CO_3 and K_2CO_3 to the HTL of food waste[37] and starch, amylose, amylopectin, chitin and pectin[91] increasing the yields of aqueous-phase products has also been noted previously. A study on HTL of kitchen waste with added Na_2CO_3 showed that the biocrude yield depends strongly on the additive loading and reaction temperature.[97] This suggests the possibility of obtaining higher biocrude yields with the use of carbonates in this study by using different reaction temperatures and/or different additive loadings.

The addition of potassium phosphates produced biocrude oil yields in the following order: KH_2PO_4 > K_2HPO4 > K_3PO_4. The aqueous-phase yields followed the opposite order. Solids yields were about the same for all three potassium phosphates. Ding et al. observed the same trend for HTL of soy protein and triglyceride, and the opposite trend for HTL of potato starch and a carbohydrate-rich mixture mimicking sweet potato waste.[90] The effects of the phosphates depend on

the composition of the feedstock, and the present simulated food waste apparently had sufficient protein and lipids for the positive effect of KH_2PO_4 on these groups to be dominant. The effect of added KH_2PO_4 could be due to its creating an acidic solution. The high biocrude yield in Figure **3-2** with added formic acid is consistent with this hypothesis. We recognize, however, that the composition of feedstock can play a significant role in determining the effectiveness of formic acid during HTL.[25] Additionally, formic acid breaks down during HTL and forms CO_2 and H_2.[25] The results in Figure **3-1** showed that the addition of H_2 to HTL during the control experiment with no supported metals increased the yield of aqueous-phase products. Thus, the increase in the yield of aqueous-phase products with the added formic acid might be due to the effect of the H_2 that formed during HTL.

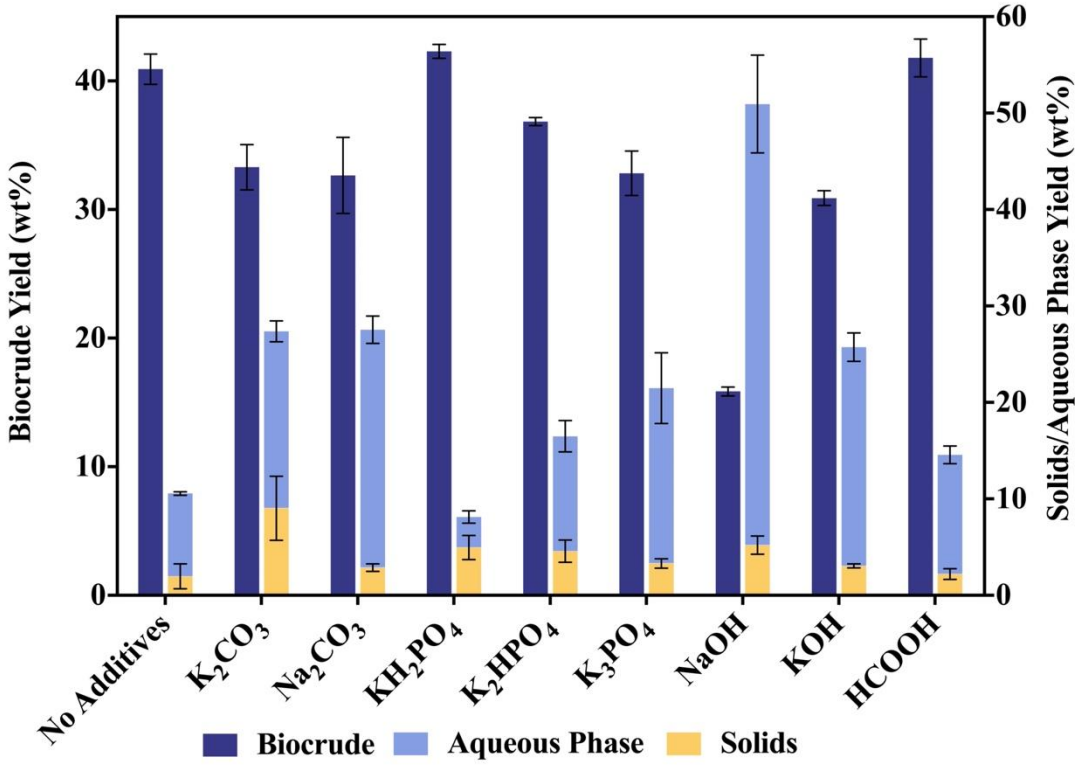

Figure **3-2**: Product fraction yields from HTL of simulated food waste with additives (350 °C, 40 min, 10 wt % biomass loading, 1:2 additive to biomass loading).

The use of KOH and NaOH resulted in biocrude yields of 31 wt% and 16 wt%, respectively. The aqueous-phase yield was at its highest, about 46 wt %, for the run with NaOH. The addition of NaOH to the HTL of food waste and black currant pomace at 300 °C for 60 min also consistently reduced the biocrude yields.[35,42] The lower biocrude yields with added K_2HPO4 and K_3PO_4 are also consistent with basic conditions inhibiting biocrude yields for HTL of this simulated food waste.

Effect of Additives on Biocrude Oil Elemental Composition.

Figure **3-3** illustrates the elemental composition of biocrudes from HTL of simulated food waste with added salts, bases, and acid. None of the additives made any meaningful change in the amount of carbon in the biocrudes, which remained around 71 wt %. The hydrogen content in the oil was about 10 wt % for HTL with all of the additives, which was about twice that from the control experiment and higher than any of the runs with the added supported metals. The nitrogen content of the oils from HTL with additives was always lower than the 5 wt % value for the control experiment. The sulfur content was often below the detection limit.

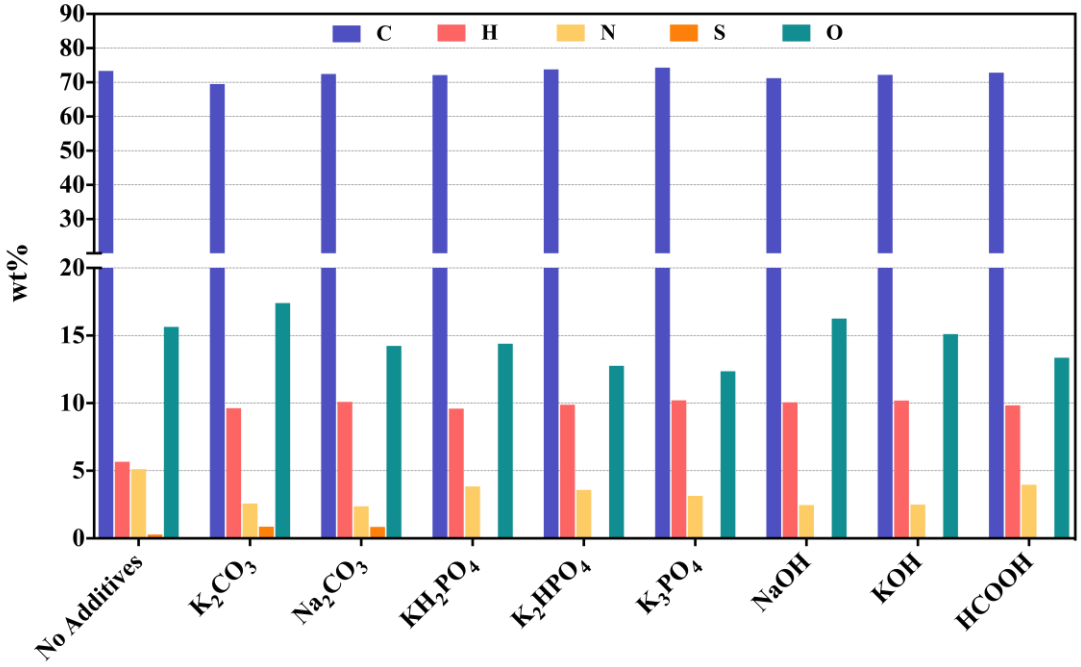

Figure **3-3**: Elemental composition of biocrudes from HTL of simulated food waste with additives. (3 °C, 40 min, 10 wt % biomass loading, 1:2 mass ratio of additives to biomass)

The elemental composition of the oils from HTL with added K_2CO_3 and Na_2CO_3 were nearly the same, except for the oxygen content, which was 3 wt% lower for Na_2CO_3. The oxygen content of the oil from the run with K_2CO_3 was not only higher than the run with Na_2CO_3 but also higher than the control run with no additives. HTL of chitin and pectin at 350 °C with added K_2CO_3 also gave biocrudes with higher oxygen content than did HTL without the additive.[91] However, HTL with added K_2CO_3 of cellulose, starch, amylose, and amylopectin (350 °C), and of barley straw (300 °C) gave biocrudes with lower oxygen content than the run with no salt added.[91,113] Taken collectively, these outcomes suggest that the feedstock composition is as important as the type of additive in determining the elemental composition of biocrude oil from HTL. Another factor could be the additive loading. For example, Maag et al. [37], reported a higher oxygen content for the oil from HTL of food waste with Na_2CO_3 than from HTL with no additives. They also reported no

change in the hydrogen content. This difference could possibly be due to their using a 5 wt% additive loading whereas we used 50 wt%.

The biocrudes from HTL with potassium phosphates had no detectable sulfur. The amount of oxygen was lowest for the biocrude from HTL with K_3PO_4, which also had the highest carbon and hydrogen and lowest nitrogen contents of all the potassium phosphates. Both NaOH and KOH gave biocrudes with similar elemental compositions. The results from HTL with added formic acid show that the acidic environment could reduce the oxygen and nitrogen content of the oil, an outcome also reported for HTL of *Chlorella* with added formic acid at 350 °C.[25]

Figure **3-4** shows the HHVs of the biocrude oils from HTL with the additives as well as the energy recoveries in the biocrudes. For all of the runs with additives, the HHV values were at least 15% higher than that from the control experiment. The run with K_3PO_4 gave the highest value of 37.5 MJ/kg. The energy recovery in the biocrude exceeded 83% for HTL with added formic acid or KH_2PO_4 and this increase above the control experiment outcome was statistically significant with $p < 0.001$.

Overall, the additives tested were beneficial for reducing the oxygen and nitrogen content of the oils and increasing their hydrogen content. These effects led to HHV values greater than the control experiment with no additives. Formic acid and KH_2PO_4 had the added benefits of also increasing the energy recovery.

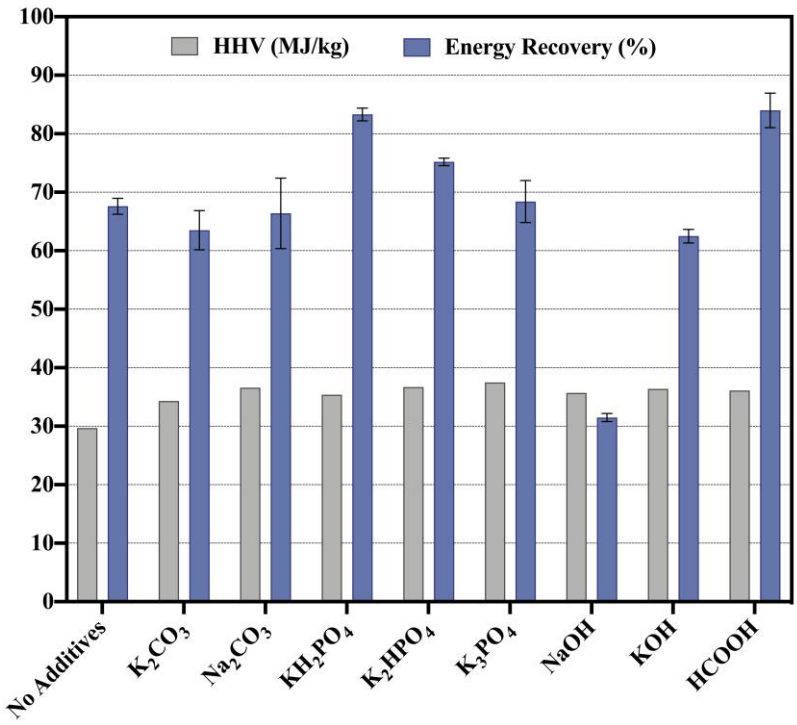

Figure **3-4**: Higher heating values (HHV) of biocrudes and energy recoveries from HTL of simulated food waste with additives. (350 °C, 40 min, 10 wt % biomass loading, 1:2 mass ratio of additive to biomass)

Effect of Additives on Biocrude Oil Molecular Composition.

The molecular components in the lighter fraction of the biocrudes from HTL with additives were identified by GC-MS and categorized into different groups. Figure **3-5** gives the changes in abundance (area %) for each group brought about by each additive. For reference, the first row in Table **3-3** (no supported metals) gives the abundance of each group in the biocrude from HTL with no additives. Table **3-3** did not list furans, as none were detected in those runs. Likewise, the "other nitrogenous compounds" category was omitted in Table **3-3**. This category includes compounds such as pyridine and indole derivatives, which were not detected in those experiments. Some groups present in small amounts are grouped together.

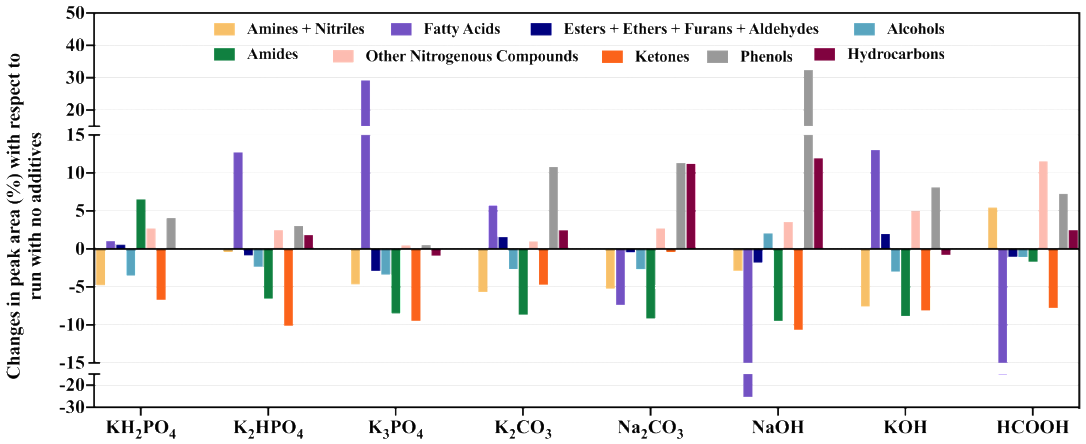

Figure **3-5**: Changes in abundance of different classes of compounds (area % from total ion chromatogram) in the biocrude oils after HTL of simulated food waste with additives (350 °C, 40 min, 10 wt % biomass loading, 1:2 mass ratio of additives to biomass), with respect to HTL with no additive.

The addition of phosphates led to changes in the product distribution that exceeded 5 area % for ketones (always lower) fatty acids (lower with KH_2PO_4 but otherwise higher), and amides (higher with KH_2PO_4 but otherwise lower). The lower pH accompanying addition of KH_2PO_4 may have facilitated reactions of fatty acids with NH_3 to produce more amides.

The addition of the carbonates to the HTL of simulated food waste increased the area % for phenols more than 10 area % and Na_2CO_3 had a similar impact on the area % for hydrocarbons. In another study, the addition of Na_2CO_3 also increased the formation of hydrocarbons for the HTL of *Spirulina* at 350 °C.[93] We hypothesize that adding Na_2CO_3 enhances the decarboxylation of acids as well as dehydration and isomerization reactions. Like the basic phosphates, the carbonates also reduced the area % of ketones and amides.

The addition of hydroxides led to changes like those observed with other basic additives. The area % for phenols increased and that for ketones and amides decreased. The larger area % for phenols with the addition of NaOH is consistent with a prior study.[42] The area % for fatty acids

decreased more than 20 area % with added NaOH but increased more than 10 area % with added KOH.

Lastly, when HCOOH was added, fatty acids remained the major compounds in the oil, but their abundance was 15 area % lower than that of the oil from the control experiment with no additives. This oil with added HCOOH also contained 11.6 % nitrogenous compounds, much higher than all of the other oils. In another study for the HTL of food waste, the addition of acid similarly reduced the fatty acids proportion in the biocrude oil, but in contrast to our work, it reduced the amount of nitrogenous compounds to zero. [42] This difference could be due to the different compositions of feedstock used or also the different type of acid used for the study. Ross et al. previously showed that feedstock compositions should be considered as effective factors determining the oil molecular composition when additives are used in the HTL process.[93]

Note, that the area % for ethers, esters, aldehydes, and nitriles was low in all the oils. A prior study on HTL of food waste with additives made a similar observation.[42]

Ultimately, none of the additives examined improved the biocrude yield beyond what the control run provided. Therefore, we did not run additional analyses on the products from these experiments.

Metal Oxides

Effect of Metal Oxides on Product Yields.

The product fraction yields from HTL of simulated food waste with five different metal oxides are given in Figure **3-6**. The biocrude yields range from 32 wt % (CaO) to 49 wt % (SiO_2). The latter value represents a 20% increase over that obtained in the control experiment with no

metal oxide and this increase is statistically significant at $p < 0.001$. Previous studies have also shown higher biocrude yields from HTL with metal oxides (e.g., La_2O_3 and rice husk[87], CeO_2 and food waste.[37,100]) La_2O_3 has basic sites on its surface, which can increase hydrolysis rates and produce more biocrude.[87] CeO_2 is known for its stability in hydrothermal environments and can promote oxidation reactions.[114] CeO_2 and La_2O_3 gave higher biocrude yields in this work as well.

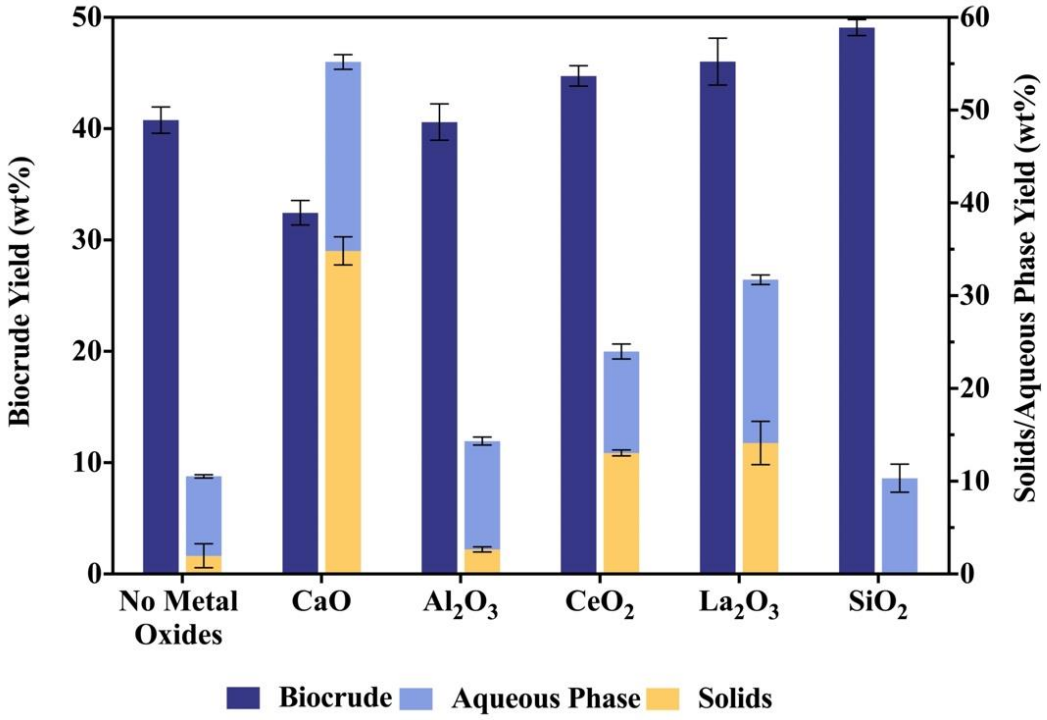

Figure **3-6**: Product fraction yields from metal-oxide assisted HTL of simulated food waste (350 °C, 40 min, 10 wt % biomass loading, 1:2 metal oxide to biomass loading).

Added CaO showed a negative effect on biocrude yield. There is a literature report, however, that it increased the production of biocrude oil from HTL of *Nannochloropsis gaditana* at 320 °C for 10 min.[89] This difference could be due to the different composition of feedstock used. CaO promoted the formation of solids from HTL of the simulated food waste. CaO being the metal

oxide that gave the highest solid products yields was also observed previously for the HTL of food waste.[99]

Previous studies[88,89] showed that biocrude yields from HTL correlate with the electronegativity of the metal oxides. Figure **3-7** shows how the relative yields (yields from the run with added metal oxide divided by yields from the control experiment) of biocrude oil and aqueous-phase products change with the electronegativity of the metal oxides. The electronegativity values were calcualted using the equation in Yim et al.[88] The greatest yield of biocrude oil was from HTL with added silica, which has the highest electronegativty. CaO, on the other hand, gave the lowest yield.

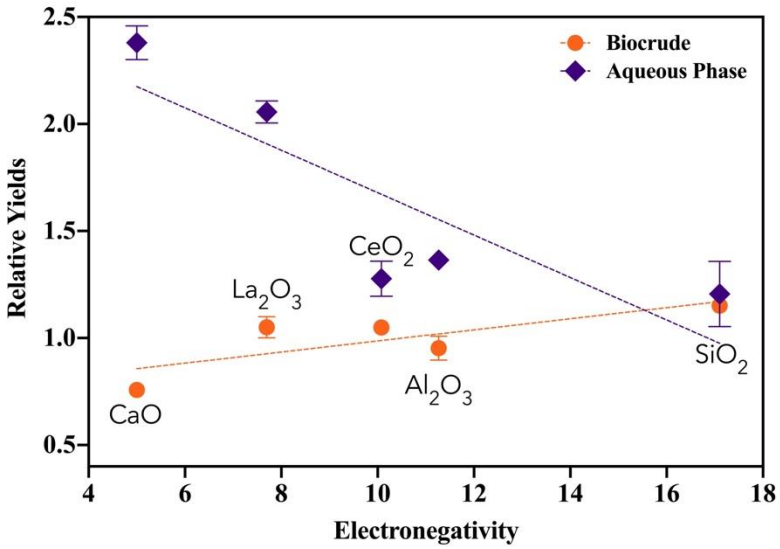

Figure **3-7**: Effect of electronegativity of metal oxides on relative yields (yields from HTL with metal oxide divided by that from the control experiment) of biocrude oil and aqueous-phase products from HTL of simulated food waste. (350 °C, 40 min, 10 wt % biomass loading, 1:2 metal oxide to biomass loading).

The relative yields of aqueous-phase products always exceeded unity. The lower the electronegativity of the metal oxide, the more aqueous-phase products they generated. Thus, CaO produced the greatest yield of water-soluble products, about 20 wt %. This was also true for HTL of

microalgae with CaO at 320 °C.[89] This environment promotes the formation of water-soluble carbon, which would be undesired as it seems to come at the expense of having more carbon (and heating value) in the oil phase.

Effect of Metal Oxides on Biocrude Oil Elemental Compositions.

Figure **3-8** shows the elemental composition of biocrudes from HTL with added metal oxides. The carbon content was always about 70 wt% regardless of whether a metal oxide had been present. Likewise, the N content was always between 4.0 and 5.1 wt%. All of the metal oxides increased the hydrogen content in the oils (by about 50 – 90%) beyond the 5.7 wt% mark obtained in the control experiment. The oxygen content was at its lowest (11.1 wt%) when alumina was present during HTL, but otherwise, it was always around 15 wt%.

CaO, Al_2O_3, and SiO_2 were previously evaluated for the HTL food waste.[99] The metal oxides showed little effect on the H and N content of the biocrudes. They had different impacts on the carbon content, which decreased about 10% and 2% with the use of SiO_2 and Al_2O_3, respectively, and increased about 3% with use of CaO. The composition of their food mixture was different than the simulated food waste used in the present work. The prior study also conducted HTL at a lower temperature (300 °C) and with a lower mass ratio of metal oxide to food mixture (1:20). Any of these factors could contribute to the different effects observed for metal oxides.

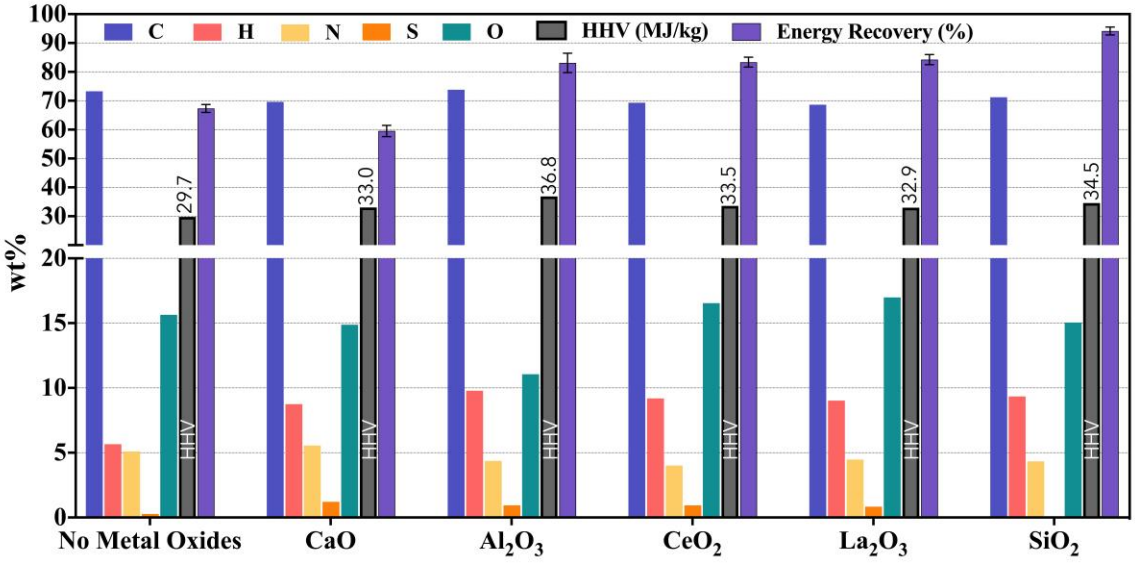

Figure **3-8**: Elemental composition and HHVs of biocrudes from HTL of simulated food waste with metal oxides (350 °C, 40 min, 10 wt % biomass loading, 1:2 mass ratio of metal oxide to biomass).

Figure **3-8** shows that the HHVs of the biocrude oils were at least 11% higher for the runs with metal oxides than the control run. HTL with alumina produced the oil with largest HHV of 36.8 MJ/kg. This value is about 24% higher than that of the oil obtained from the control experiment.

The impact of the metal oxides on energy recovery in the biocrude is also shown in Figure **3-8**. HTL with added SiO_2 provided the highest energy recovery of 94%. Al_2O_3, La_2O_3, and CeO_2 also gave high energy recoveries of around 83%. For each of these four metal oxides, the increases in energy recovery were statistically significant ($p < 0.001$). These present energy recoveries are much higher than the energy recoveries (19% to 39 %) previously reported for the HTL of food waste with added metal oxides (SiO_2, Al_2O_3, Fe_2O_3, CaO, $CeZrO_x$, CeO_2, and ZrO_2). [37,99,100] These differences are likely due to the feedstocks having different elemental and biochemical compositions.

Overall, the addition of metal oxides to the HTL of food waste showed promising results in increasing both the biocrude yields and energy recoveries. Therefore, we examined some of the characteristics of the products in more detail.

C, N and P Recoveries in Biocrude Oil and Aqueous Phase Products from HTL with Metal Oxides.

Nitrogen and phosphorus are present in food waste and other biomass. These elements are important constituents in fertilizer, and knowing how much of each element resides in the different product phases after HTL can facilitate recovery and reuse. One desires HTL to distribute more of the N to the aqueous phase, where it can be recovered and reused, rather than to the biocrude, where the N would need to be removed via hydrotreating to produce a suitable liquid fuel. Figure **3-9** provides this information for HTL of the simulated food waste with metal oxides. The recovery of nitrogen in the aqueous phase after HTL was highest (23 %) with added CaO, and about 10% higher than that from HTL with no metal oxide. This value falls short of a nitrogen recovery of 40% in the aqueous phase that was reported for HTL of a food mixture at 360 °C.[54] Previous studies showed that the temperature and the biochemical composition of the food waste feedstock can influence the nitrogen recovery in the aqueous-phase products from HTL.[53,54,115] These factors could be responsible for the previous study recording higher N recovery in the aqueous-phase products. Figure **3-9** shows the recovery of N as ammonium in the aqueous phase was always < 5%, though it was enhanced with the use of metal oxides. The highest ammonium recovery occurred from HTL with added La_2O_3. Nitrogen recovery in the biocrude always exceeded that in the aqueous phase.

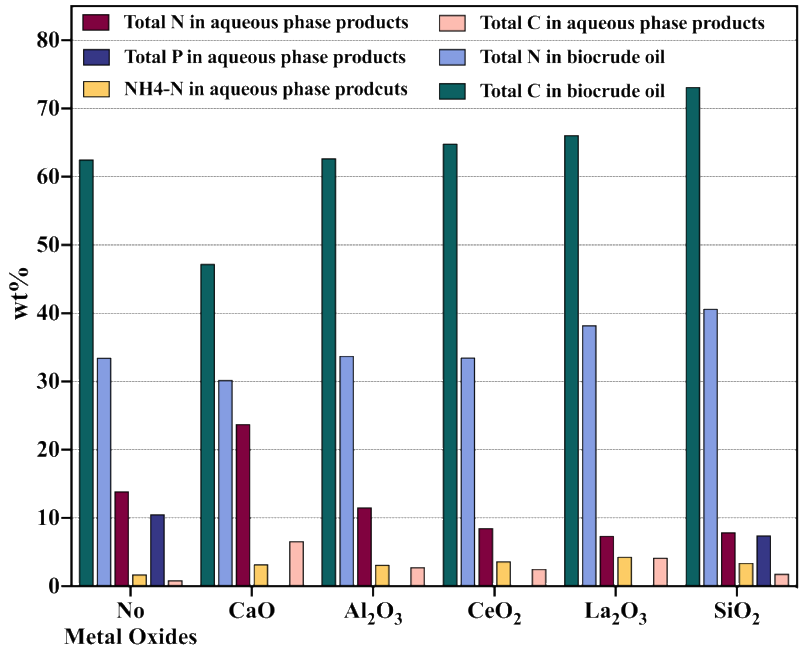

Figure **3-9**: Recovery (%) of carbon, nitrogen and phosphorus in the oil and aqueous phases from metal-oxide assisted HTL of simulated food waste (350 °C, 40 min, 10 wt% biomass loading, 1:2 mass ratio of metal oxide to biomass).

The phosphorus recovery in the aqueous phase was just above 10% for the control experiment, about 7% with added SiO_2, and essentially zero with all of the other metal oxides. A previous study on HTL of microalgae (350 °C) showed that around 20 to 30 % of the initial P in the feedstock transferred to the aqueous phase in the form of phosphates.[93] We expect the majority of the P content in the aqueous phase from HTL of the simulated food waste is also in the form of phosphate. Only a small portion of the biomass phosphorus appeared in the aqueous phase. We expect most of the phosphorus to reside in the solids, as was the case in prior HTL experiments.[54,116]

The carbon recovery in the biocrude oil was 63% for the control experiment, 73% with added SiO_2, about 64% with added Al_2O_3, CeO_2, and La_2O_3, and at its lowest (~ 47%) with added CaO. Meanwhile, total C in the aqueous phase was always low and at its highest amount with added CaO. The data in Figure **3-9** for HTL with SiO_2 show that the biocrude and aqueous-phase products account for 75% of the carbon in the biomass. No solids were recovered so the remaining carbon

must have been in the gas phase. Estimating the gas yield by difference, using the data in Figure **3-6,** gives 40.6 wt%. If we make the reasonable assumption that the gas is predominantly CO_2, we calculate a carbon recovery of 23% in the gas phase. Thus, the carbon balance would be 98% for this HTL run with added SiO_2.

Thermal Stability of the Biocrude Oils from HTL with Metal Oxides.

The biocrude oils formed during HTL of biomass contain many different molecular species with a wide distribution of boiling points. The volatilities of these molecules determine, in part, how they can be used as liquid fuels. Thermogravimetric Analysis (TGA) provides information about the volatilities of the molecules in a mixture by recording the weight loss from a sample in an inert environment while it is heated.

Figure **3-10** shows the relative weight loss within different temperature ranges representing boiling point cuts in petroleum products.[64] For all of the biocrudes, the largest fraction of molecules volatilized in the 232 to 343 °C range, which corresponds to the boiling range of components in diesel fuel. The biocrude oil from the run with added CaO contained the largest amount of material that volatilized in the heavy gas oil region.

Though it produced more biocrude in the heavy gas oil range, HTL of the simulated food waste with CaO produced less residue (about 5 wt%) than did the other runs (about 15 wt%). This suggests that the presence of CaO may have inhibited condensation reactions that produce these heaviest compounds. CaO may be beneficial during HTL of food waste, as it reduced the amount of less valuable residue.

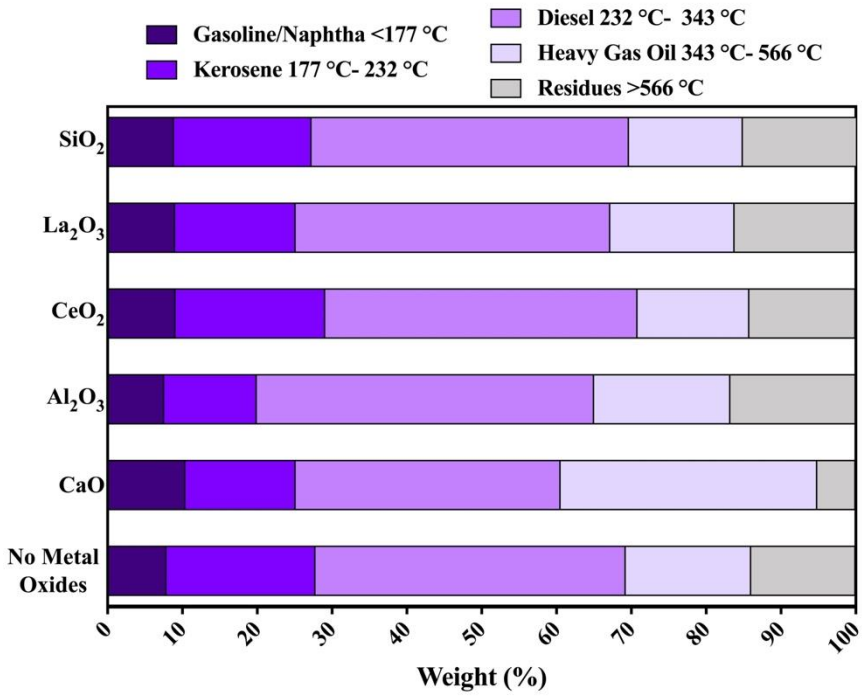

Figure **3-10**: Cumulative weight loss (%) from biocrude oils from HTL of simulated food waste with metal oxides (350 °C, 40 min, 10 wt % biomass loading, 1:2 mass ratio of metal oxide to biomass), within temperature ranges representing boiling point fractions for petroleum products.

Effect of Metal Oxides on Biocrude Oil Molecular Composition.

Figure **3-11** shows the total ion chromatograms for each of the biocrude oils from HTL with metal oxides. The peaks with more than 1% relative peak area are labelled, and Table **3-4** lists the name of the compound tentatively identified for each peak. These compounds include substituted phenols, nitrogen heterocycles (e.g., pyrrole derivatives), fatty acids, amides, and hydrocarbons.

All of the chromatograms are similar except for that corresponding to the oil from HTL with added CaO. In this case, there is a greater abundance of nitrogen heterocycles, a near absence of fatty acids, which are the most prominent peaks in the other chromatograms, and a greater abundance of amides. Figure **3-8** shows that this biocrude also had the highest nitrogen content,

which could be attributed, at least in part, to the greater abundance of nitrogen heterocycles and amides evident in Figure **3-11**. The addition of CaO to the HTL of microalgae similarly decreased the abundance of fatty acids by 35 %, but it also reduced the abundance of amides.[89] Therefore, using CaO during HTL appears to open new chemical reaction pathways that generate a different molecular composition for the biocrude oil.

Overall, the addition of metal oxides to the HTL of food waste showed promising results in increasing both the biocrude yields and energy recoveries. One could envision solid metal oxides being used at scale as heterogenous catalysts in fixed-bed or fluidized bed reactors.

Table **3-4**: Compounds tentatively identified in biocrude oils from metal-oxides assisted HTL of simulated food waste.

No.	Compound	No.	Compound
1	p-Cresol	**14**	Tetradecanamide
2	1-Ethyl-2-pyrrolidinone	**15**	n-Hexadecanoic acid
3	2-Pyrrolidinone, 1-propyl-	**16**	Dodecanamide
4	p-Menth-4-en-3-one	**17**	Oleic Acid
5	2-Pyrrolidinone, 1-butyl-	**18**	Octadecanoic acid
6	n-Decanoic acid	**19**	Hexadecanamide
7	Indole, 3-methyl-	**20**	Octadecanamide
8	2,4,6-Trimethylbenzonitrile	**21**	Myristamide, N-isobutyl-
9	Dodecanoic acid	**22**	Myristamide, N-methyl-
10	1-Nonadecene	**23**	Oleic Acid Amide
11	Tetradecanoic acid	**24**	Octadecanamide, N-butyl-
12	Hexadecanenitrile	**25**	Hexadecanoic acid, pyrrolidide
13	Palmitoleic acid		

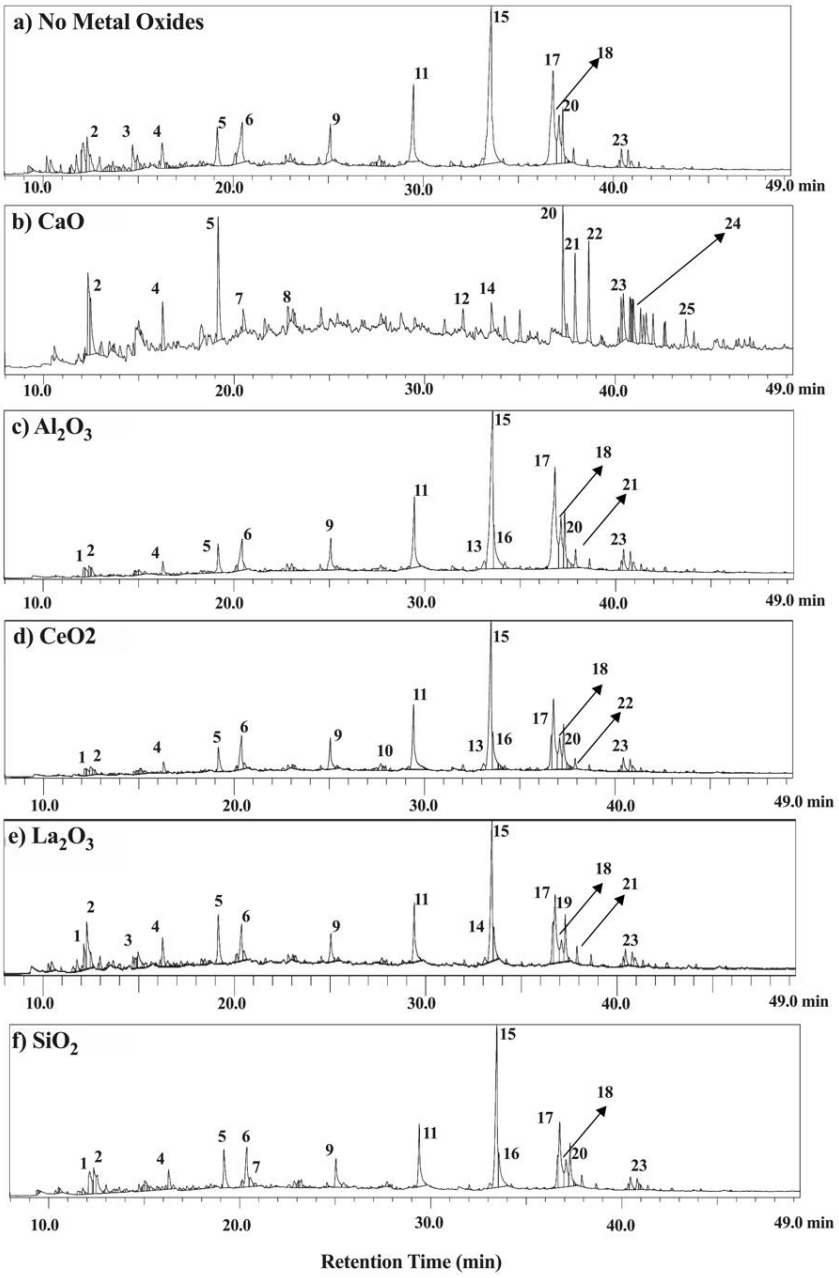

Figure **3-11**: Total ion chromatogram of the biocrudes from HTL of simulated food waste with added metal oxide (350 °C, 40 min, 10 wt % biomass loading, 1:2 mass ratio of metal oxide to biomass), (a) No metal oxide, (b) CaO, (c) Al_2O_3, (d) CeO_2, (e) La_2O_3, and (f) SiO_2.

Conclusions

The use of supported metals increased the HHV of the biocrudes, when it was accompanied by 3500 kPa of H_2. These materials did not increase the biocrude yields, however, so the energy recoveries never exceeded that from the control experiment in a way that was statistically significant.

The use of salts, bases, and acid affected the HHV values more than did supported metals, and all the obtained values were at least 4.6 MJ/kg higher than that of the biocrude oil from the control experiment. Added formic acid and KH_2PO_4 produced about same amount of biocrude as did the control and led to energy recoveries in the biocrude exceeding 83%. Like the control experiment, HTL with supported metals or salts, bases, and acid gave oils that were mostly composed of fatty acids.

The use of metal oxides during HTL provided the most promising results. Silica enhanced the biocrude yield by about 9 wt%, and the energy recovery in the biocrude exceeded 90% with added SiO_2. La_2O_3 and CeO_2 also had positive effects on biocrude yield. Save for CaO, the bio-oils from all HTL runs with metal oxides had less nitrogen and than that from the control. All of the metal oxides produced biocrude oils with HHV values that exceeded that from the control experiment. The thermal stabilities and molecular distribution of the oils were influenced by the metal oxide used. CaO produced an oil with the smallest fraction of residual material.

This work was the first to report the nitrogen and phosphorus recoveries in the aqueous-phase products from HTL of food waste with metal oxides. The most nitrogen was recovered when CaO was present during HTL. The most phosphorus was recovered in the control experiment, with no added metal oxide.

Among the three groups of catalysts tested, only metal oxides enhanced both biocrude yields and energy recoveries. Therefore, metal oxides could be potential catalysts for the HTL of food waste. One could envision solid metal oxides being used at scale as heterogeneous catalysts in, for example, fixed-bed reactors.

Chapter 4

Hydrothermal Carbonization of Simulated Food Waste for Recovery of Fatty Acids and Nutrients

This chapter contains results originally published in *Bioresource Technology* and co-authored by Robert A Dean, Joseph Nicholas, and Professor Phillip E. Savage.[117] This chapter focuses on HTC of simulated food waste, with the aim of recovering both fatty acids from the biochars and nutrients from the aqueous-soluble products.

Introduction

The concept of waste valorization has gained much attention over the past decade, with the goal of using waste for production of energy, fuels, materials, and other valuable products. An additional benefit would be reduction of greenhouse gas emissions, air pollution, and other environmental issues associated with waste materials. [118] For example, food waste, a significant fraction of municipal solid waste, is responsible for one sixth of the methane emissions from landfills in the U.S. [119] This large amount of discarded food (about 1.3 billion tons/yr globally) [5], however, is a potential source of nitrogen and phosphorus, which could be used for fertilizer production, [49] and lipids, which could be converted into fatty acid methyl esters (FAMEs) and biodiesel fuel [120–123].

The high moisture content of food waste renders most of the common thermal treatments like incineration and pyrolysis less suitable to recover energy or value-added products. Hydrothermal carbonization (HTC), on the other hand, avoids the need to dry the feedstock and produces a carbonized solid (termed biochar or hydrochar) and a nutrient-rich aqueous phase.

[43,45,124–128] This process is performed in hot liquid water around 200 °C (milder reaction conditions than those used in pyrolysis), which helps reduce energy inputs and costs, and the biochar that is formed can be recovered via simple filtration. [129]

There are several prior studies of HTC for food waste, and these had the goal of producing and enhancing the properties of biochars as solid fuels. [43–47,130–132] In a parallel branch of research, there have been studies on recovering the oils and fatty acids in food waste through Soxhlet extraction, and then converting them to biodiesel. [120,133] In the present research, we merge these two branches and explore use of HTC on food waste for the recovery of fatty acids. The lipid fraction from food waste typically contains more than 70% fatty acids [134], which have value for liquid biofuels and other applications, such as a food contact surface sanitizer [135] and lipid anchors in bio membranes. [136]

Lu et al. demonstrated the recovery of fatty acids from algal biomass by using HTC to produce biochar, which retained the lipid fraction, followed by the use of a food grade and renewable solvent (ethanol) to extract the fatty acids. [48] We hypothesize that the same process would be effective for valorizing food waste. In this study, we use HTC at 180, 190, 200, 210, and 220 °C, and at 15 and 30 min batch holding times, to produce hydrochar. These reaction conditions should be mild enough to avoid the decomposition of fatty acids during the carbonization process.

Understanding the migration of elements like N and P from the biomass to the aqueous phase is also important for the HTC of food waste. Nitrogen retained within the biochar would form NO_x upon its combustion as a fuel whereas its migration to the aqueous phase could facilitate its recovery and use in producing fertilizers. Previous work on HTC of organic feedstocks has shown great success in recovering nitrogen and phosphorus in the aqueous-phase products. [47,49,50,115,128,137] However, knowledge of the effect of process variables on nutrient recovery during HTC of food waste is still incomplete and these are among the main factors that

govern the fate of N and P during HTC.[51] For example, the fate of nitrogen has been studied for the HTC of food waste at 180 to 275 °C for 60 min.[115], [49] but there is scant data on nutrient recovery for shorter batch holding times. The foregoing considerations combine to motivate the present study, wherein we conduct HTC on food waste at different temperatures and shorter times and recover and quantify fatty acids, quantify the yields of aqueous-phase products, and track the nutrient migration from food waste into the HTC product fractions.

Materials and Methods

Materials

The simulated food waste was prepared by mixing food items from a grocery store as outlined in our previous work. [53] The mixture consisted of 51.4 wt% carbohydrates, 15.7 wt% lipids, and 27.5 wt% proteins. Prior to the use of this mixture in the present study, it had been kept at -4 °C for 18 months. Deionized (DI) water was produced in-house. Tricosanoic methyl ester, used as an internal standard, and acetyl chloride, used as an acid catalyst, were procured from Sigma-Aldrich. Anhydrous ethanol, used for lipids extraction, was purchased from VWR International. Methanol, used for fatty acids transesterification, and n-heptane, were purchased from Millipore Sigma. A food industry FAME mix standard (37 components) was procured from RESTEK. Helium and nitrogen (99.999%) were obtained from Praxair. Batch reactors (316 stainless steel) with internal volume of 4.1 mL were fashioned from a nominal ½ in. Swagelok port connector and two caps.

HTC Process

We loaded 1.24 g of wet simulated food waste (i.e., 0.356 g dried food mixture plus 0.884 g water) and an additional 2.65 g of DI water into each reactor. Then, we sealed the reactors and immersed them in a preheated, isothermal, Techne-fluidized sand bath for the desired amount of time. Next, we removed them from the sand bath and quenched them in an ice-water bath to cool. We examined ten different reaction conditions with carbonization temperatures varying from 180 to 220 °C, and batch holding times being either 15 or 30 min. These low temperatures were selected to avoid the deterioration of unsaturated fatty acids during the process. Prior work showed that it takes less than three minutes for each reactor to reach sand bath set point temperatures below 350 °C. [28,38]

After the reactors had cooled, we recovered the products within using DI water. The products were transferred into 50-mL centrifuge tubes and centrifuged for 6 min at 6000 rcf. The two layers within the tubes (biochar and aqueous-phase products) were then separated using Pasteur pipets, as the aqueous phase was transferred into pre-weighed glass tubes. Next, the glass tubes with the aqueous phase and the centrifuge tubes with biochar layer were placed in an oven at 40 °C and 65 °C, respectively. They were kept in the oven until their masses changed by less than 0.5 mg. The yields of the biochar and aqueous-phase products were calculated as the mass of each material remaining in the tubes after complete drying divided by the mass of dried food mixture initially loaded into the reactor. Each run was performed in triplicate, and the values reported herein are mean values. The standard deviation is also given for each reaction condition as an estimation of uncertainties from run-to-run.

Lipid Extraction

To extract the lipid fraction from the dried biochar, 0.1 g of dried biochar was vigorously stirred with 3 mL ethanol in a glass tube with Teflon-lined screw caps, at 60 °C for 1 hr. To maintain this temperature, a water bath was used and the temperature was manually controlled using a hot plate and a thermometer. A magnetic stirrer was used to constantly agitate the mixture at 1200 rpm. Next, the slurry was centrifuged for 5 min at 3000 rcf. The ethanol phase was then recovered, and the biochar was subjected to another round of extraction just as discussed above. The ethanol phase from the second round was then combined with the ethanol phase collected earlier and transferred into a new pre-weighed glass tube. The tube containing the ethanol phase was then placed into a RapidVap Vertex Evaporator to remove ethanol by flowing N_2 at 40 °C. The mass of material remaining in the tube was then used to calculate the yield of ethanol extract, which we expect to be primarily lipids.

Fatty Acid Quantification

To quantify the fatty acid constituents in the lipids in the food mixture feedstock, the biochar, and the ethanol extract, we used catalytic transesterification to convert them into the corresponding FAMEs. In a typical run, 2 mL of methanol containing 5 % acetyl chloride (acid catalyst) was mixed with 50 mg of the analyte in a glass tube with Teflon-lined screwcap, and vigorously stirred (using a magnetic stir bar at 1200 rpm) at 100 °C for 90 min. Then the glass tube was allowed to cool down to the room temperature and 1 mL of water was added to it. An-heptane solution (3 mL) containing 150 mg/L tricosanoic methyl ester (as an internal standard) was added to the glass tube to extract the FAMEs. The contents of the glass tube were then transferred to a centrifuge tube, vortexed for 1 min, and then centrifuged at 4000 rcf for 6 min.

Lastly, we transferred about 1.5 mL of the upper heptane-FAME layer into GC vials to quantify the fatty acids in the samples. We use a Shimadzu gas chromatograph - mass spectrometer (GC-MS) equipped with a 0.2 mm i.d. Agilent HP-5MS nonpolar capillary column (50 m x 0.33 μm). In each GC run, a 3 μL sample was injected with a 15:1 split ratio. The injection port temperature was 280 °C. The column temperature was initially held at 40 °C for 3 min, and then ramped at 7 °C min^{-1} to 260 °C with 20 min hold time. The carrier gas was helium at a constant flow rate of 0.5 mL min^{-1}. The standard FAME mix was also run using the same method. By matching the retention times for peaks in both the FAME mix and the HTC samples, we could identify specific compounds in the sample. The identified peaks were then quantified by direct peak area comparisons between the samples and the FAME standard mixture, knowing the concentration of each peak in the standard sample. Lastly, the presence of the internal standard helped assure the accuracy of quantification. This was done by calculating the theoretical response factor based on the area of internal standard and its known concentration in each sample.[138]

Product Analysis

The carbon, hydrogen, nitrogen, and sulfur contents of the biochar were quantified using an Elemental Analyzer EA 1110 (CEInstruments (Thermo Electron Corp)) equipped with a thermal conductivity detector (TCD). The oxygen content was calculated by difference. The Dulong-Berthelot correlation, as shown below, was used to estimate the higher heating values (HHVs) of biochar samples using their elemental composition.

$$HHV\ (MJ/kg) = 0.3414\ C + 1.4445\ (H-(N+O-1)/8) + 0.093\ S$$

The total phosphorus in the aqueous-phase samples was measured by using EPA method 6010 (inductively coupled plasma-atomic emission spectrometry)[60] and EPA 3050B (acid

digestion)[59]. Lastly, we used dry combustion (Dumas method) to quantify the total carbon and nitrogen in the same samples.

Results and Discussion

This section first discusses HTC of simulated food waste by providing the yields and the elemental compositions of biochar, the yields of aqueous-phase products, and the carbon and nutrient recoveries in both product fractions. Next, it gives the fatty acids profile in the simulated food waste and fatty acids retention in the biochars. The section then concludes by providing the yields of material extracted from biochar using ethanol as a solvent and reporting the fatty acids recoveries from both the biochars and the simulated food waste.

HTC of Simulated Food Waste

HTC of the simulated food waste produced black, coal-like biochar along with the aqueous-phase products. Figure **4-1** shows the yields of biochar produced from HTC of simulated food waste at different reaction conditions was typically around 45 wt%, though lower yields were obtained at 190 °C. HTC converting about half of the food waste into biochar is consistent with Tradler et al. reporting biochar yields of 49 and 55 wt % from HTC (200 °C, 6 h) of two different food mixtures, with the carbohydrate-rich food waste giving the higher yield. [47] Comparing the yields reported in that study with the ones acquired in the present work suggests that at temperatures around 200 °C, increasing carbonization time has little effect on the amount of biochar produced. However, in another study, higher temperatures (220 to 260 °C) have been investigated, and increasing temperature and time within that range reduced the biochar yields. [46]

This indicates high temperatures and long batch holding times are less favorable for the production of biochar from HTC of food waste.

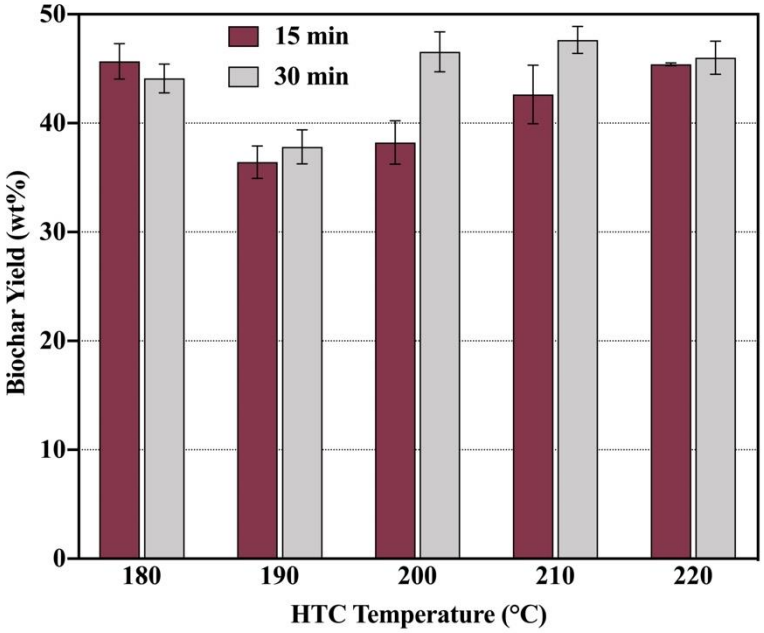

Figure **4-1**: Biochar yields from HTC of simulated food waste (9.1 wt % biomass loading).

Table **4-1** gives the elemental compositions of the biochars from HTC of simulated food waste under different reaction conditions. For a given carbonization time, increasing temperature generally resulted in a higher carbon content in the biochar. The hydrogen content did not show any specific trend with the reaction conditions, but the biochar was always enriched in H relative to the simulated food waste feedstock. The same was true for the sulfur content, which was always around 1 wt % in the biochar. Meanwhile, the nitrogen and oxygen contents were affected by the severity of the HTC conditions. The biochar produced at 180 °C was enriched in N relative to the food waste, and the nitrogen content in the biochar was essentially halved by increasing the HTC severity to 30 min at 210 or 220 °C. The oxygen content was also at its lowest at the most severe conditions (220 °C, 30 min). The biochar produced under these conditions had only half the O content of the original food waste. Overall, the results show that more severe reaction

conditions produce biochar with more carbon and less nitrogen and oxygen, which is consistent with prior studies. [43,127]

Table **4-1**: Elemental composition of biochar produced from HTC of simulated food waste under different reaction conditions.

Material	**C (wt%)**	**H (wt%)**	**N (wt%)**	**S (wt%)**	**O (wt%)**	**HHV (MJ/kg)**
Simulated Food Waste	47.8	5.11	4.78	0.23	41.6	15.5
Biochar from 180 °C, 15 min	53.3	7.82	9.85	1.32	27.7	23.0
Biochar from 180 °C, 30 min	54.8	7.60	9.79	1.01	26.9	23.3
Biochar from 190 °C, 15 min	54.0	7.65	9.57	1.19	27.6	23.1
Biochar from 190 °C, 30 min	59.0	8.62	5.93	1.12	25.3	27.2
Biochar from 200 °C, 15 min	50.6	7.09	6.08	1.00	35.2	20.3
Biochar from 200 °C, 30 min	58.3	7.61	6.25	1.12	26.8	25.2
Biochar from 210 °C, 15 min	58.3	8.10	6.58	0.94	26.1	26.0
Biochar from 210 °C, 30 min	57.9	7.31	4.39	1.11	29.3	24.5
Biochar from 220 °C, 15 min	62.9	7.95	5.80	0.83	22.6	28.1
Biochar from 220 °C, 30 min	64.4	7.92	5.05	1.10	21.5	28.9

Table **4-1** also provides the estimated heating values of the biochar from HTC of simulated food waste. The HHV values exceed that of the food waste feedstock, range from 20 to 29 MJ/kg, and generally increase with the severity of the HTC conditions. These outcomes are all consistent with a prior study on HTC of a fruit and vegetable food waste with HHV of 18.3 MJ/kg. The biochars produced at 175 °C (30 min), 200 °C (15 min), 200 °C (30 min), 225 °C (30 min), and 250 °C (30 min) had reported HHV contents of 21.6, 23.3, 24.7, 24.8, and 26.7 MJ/kg,

respectively. [43] The similarities in these results for two different food waste feedstocks suggest that hydrochar HHV values from HTC will range from 20 – 30 MJ/kg, with the higher values corresponding to use of more severe reaction conditions.

The Van Krevelen diagram in Figure **4-2** illustrates the H/C and O/C atomic ratios in the biochars and in the simulated food waste feedstock. [139] This type of diagram aids in understanding the dominant reaction pathways under different conditions. [140] HTC of the simulated food waste produced biochar with a reduced O/C ratio and higher H/C ratio. This outcome is in agreement with results from Saqib et al. [45] The reduction in O/C and increase in H/C ratios observed from HTC at 180 and 190 °C is consistent with the occurrence of decarboxylation pathways during these initial stages of the carbonization process and is consistent with previous work. [141] Comparing the hydrochars produced at 180 or 190 °C with those produced at 220 °C shows that the more severe conditions promote reactions consistent with dehydration pathways during HTC of simulated food waste.

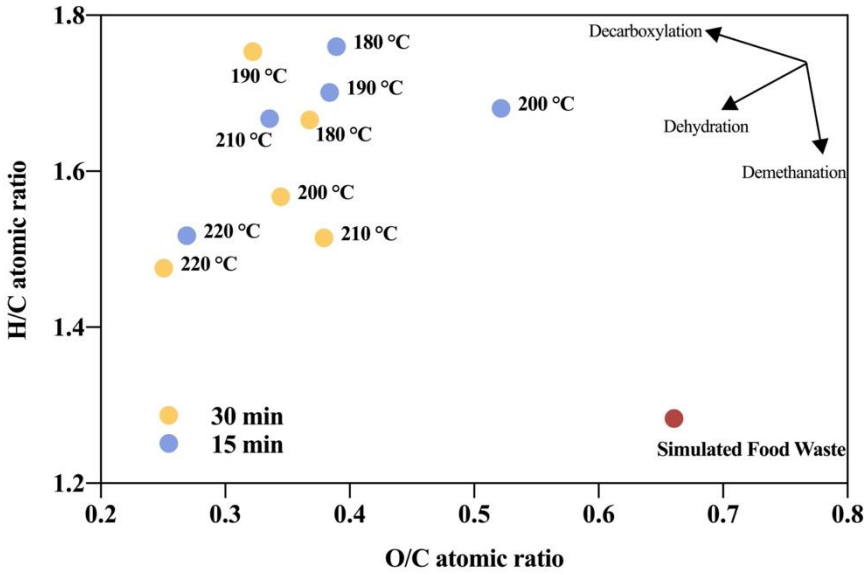

Figure **4-2**: Van Krevelen diagram for biochar from HTC of simulated food waste at varying reaction conditions.

Figure **4-3** provides the yields of the aqueous-phase products. To our knowledge, this is the first report of aqueous-phase product yields from the HTC of food waste. For both carbonization times, the aqueous-phase yield was at its highest value (~ 63 wt %) at 190 °C and at its lowest value (~ 15 wt%) at 220 °C. The carbonization time had little effect on aqueous-phase yields at 180 - 200 °C, but beyond this point, longer times and higher temperature reduced yields. This reduction could be due to the gasification of aqueous-phase molecules formed at lower temperatures. A noticeable gas release upon opening the reactors from the 220 °C HTC experiments is consistent with this hypothesis.

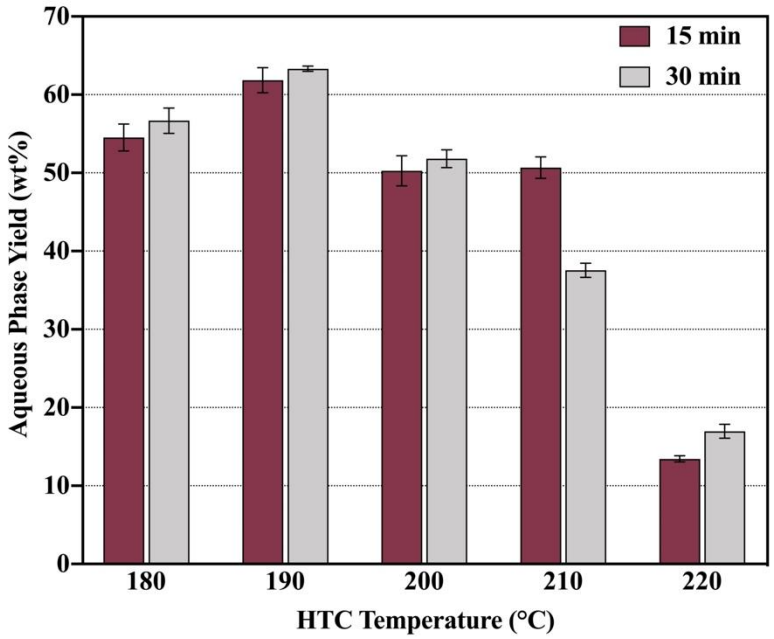

Figure **4-3**: Yields of aqueous-phase products from HTC of simulated food waste (9.1 wt % biomass loading).

Examining Figures **4-1** and **4-3** together show that the hydrochar and aqueous-phase products from HTC at 180 and 190 °C accounted for essentially all of the initial mass of the food waste loaded into the reactor. The mass balances ranged from 98 ± 3 to 101 ± 2 %. This outcome

confirms that the methods used for product recovery were adequate for recovering essentially all of the solids and water-soluble material after HTC. The average mass balance dropped to about 88 and 85% from the carbonization runs at 200 °C (15 min) and 210 °C (30 min), respectively, likely due to the formation of gaseous products. The mass balance was about 60% from HTC at 220 °C, suggesting additional gas formation.

Food waste generally contains nitrogen and phosphorus. These two elements are primary components of fertilizer, therefore understanding how much of each element partitions into the aqueous phase and biochar would facilitate recovering and recycling these nutrients. The preferred outcome from HTC is to recover more N in the aqueous phase and less in the biochar. The data in Table **4-1** for biochar and the results from aqueous phase analysis were used to calculate the recovery of N and C in both biochar and aqueous-phase products, along with the recovery of P in the latter. Figure **4-4** shows the results. For 15 min carbonization times, N recovery in the aqueous phase first increased with the temperature to 34.1 % at 210 °C, and then it decreased with further increase of temperature. The same was observed for runs at 30 min, except that the highest N recovery (38.6%) was obtained at 200 °C. Save for HTC at 210 °C, the 30 min carbonization time transferred more N into the aqueous phase than did 15 min carbonization. Among all of the reaction conditions examined, HTC at 200 °C for 30 min led to the greatest recovery of N in the aqueous phase. Meanwhile, 180 °C was the most unfavorable HTC temperature as ~ 83 % of the N was transferred to the biochar and only 6 to 14 % to the aqueous phase. Wang et al. also studied the fate of nitrogen during HTC of food waste at 180 to 260 °C with 60 min batch holding time. [115] In their study, 180 °C was also unfavorable as it led to the recovery of highest amount of N (~52 %) in biochar. But, that HTC temperature also gave the highest amount of N (~35 %) in the aqueous-phase products. These differences could be due to the different carbonization time (60 min) and different feedstock used.

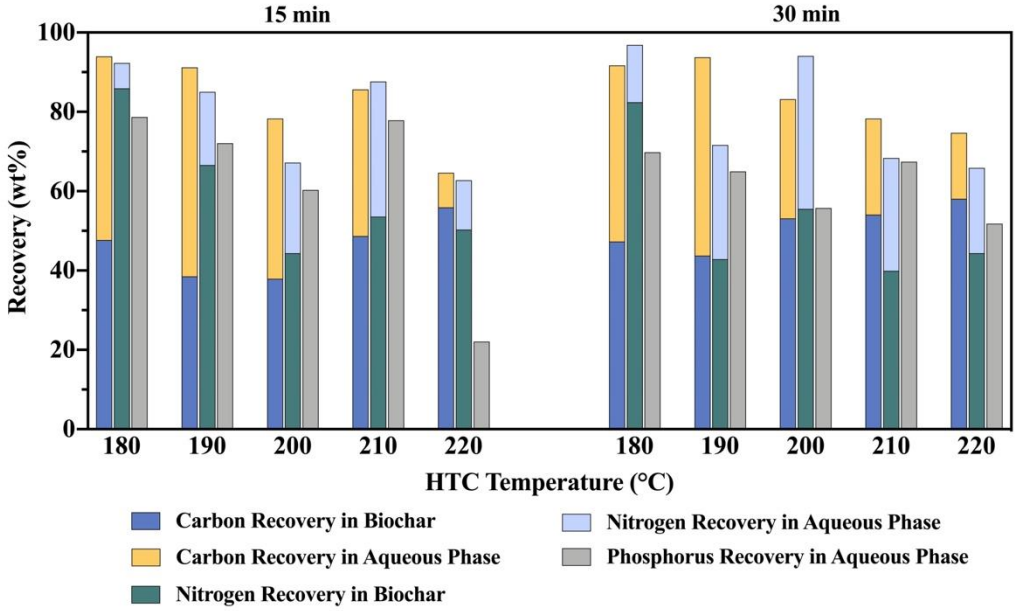

Figure **4-4**: Recovery (%) of carbon, nitrogen, and phosphorus in the biochar and aqueous phase from HTC of simulated food waste (9.1 wt % biomass loading).

Figure **4-4** shows that except for HTC at 220 °C and 15 min, all of the reaction conditions transferred more than 50 % of the initial phosphorus content of the food waste into the aqueous phase. This outcome implies that aqueous-phase products from HTC of food waste can be a potential source of compounds containing phosphorus. Huang et al. reported that molecules containing P generally transform into water-soluble orthophosphates during HTC.[142] These species are the result of breaking down molecules like pyrophosphates, polyphosphates, and phosphate diesters via hydrolysis reactions.[51] In addition to the HTC process variables, the presence of metals like Ca, Mg, and Cu and the phosphorus content of the biomass can influence the fate of this element during HTC.[143]

Figure **4-4** also provides a carbon balance for the products. Consistent with the overall mass balance discussed above, HTC at 180 and 190 °C led to carbon balances exceeding 90%. The

carbon balance was around 70% for HTC at 220 °C. The amount of carbon transferred into the aqueous phase generally decreased as the HTC temperature increased. It dropped to ~ 10 – 15% for HTC at 220 °C. This trend was just the opposite for the biochar, and HTC at the high temperature of 220 °C transferred more than 55 % of carbon into the biochar. According to the literature, the carbon content of the aqueous phase is mainly in organic compounds such as furfural, organic acids, aldehydes, etc. [141,144,145]

Fatty Acids in Food Waste and Biochar.

We used GC-MS and a standard FAME mixture to determine the fatty acid masses and profile in the simulated food waste. This feedstock was richest in saturated fatty acids (80.7 wt% of the total) with capric (C10:0), palmitic (C16:0), myristic (C14:0), lauric (C12:0), stearic (C18:0), and caprylic acids (C8:0) being the most abundant at 24.6, 23.2, 14.4, 7.7, 5.2, and 4.5 wt%, respectively. All other saturated fatty acids were present at 0.7 wt% or less. The most abundant unsaturated fatty acids were oleic acid (C18:1[cis-9]) at 11.5 wt% and elaidic acid (C18:1[trans-9]) at 5.7 wt%. A C14 and a C16 monounsaturated fatty acid (MUFA) were also present at about 1 wt% and a C17 MUFA was present at less than 0.1 wt%. We use the omega nomenclature system for fatty acids. [146] The first number in parentheses is the total number of carbon atoms in the molecule. The second number is the number of double bonds in the molecule, and the item in brackets gives the location of the double bond. Palmitic acid is widely used to produce biodiesel or green diesel. Capric acid has applications in medical, nutritional and dietetic uses. [147,148] Therefore, simulated food waste can potentially be a source of fatty acids that could be used in varying industries and applications.

The total fatty acid content of the simulated food waste was 14.1 wt % on a dry weight basis. Recall the lipid content of the simulated food waste is 15.7 wt%, so most of the lipid fraction consists of triglycerides. About 81 % of the fatty acids were saturated and the rest were monounsaturated. Polyunsaturated fatty acids, or PUFAs, (two or more double bonds) are more susceptible to oxidation and oligomerization, which makes them more difficult to recover after HTC. [48] We detected no PUFAs in the simulated food waste, so HTC could be a good method to recover the fatty acids present in the food waste. To verify the GC method was giving reasonable results, we estimated the fatty acid content in the food waste used the published fatty acid compositions for each component of the simulated food waste and data provided by Cundiff et al. [134]. This estimated value is ~ 13%, which is close to the experimental value of 14.1 wt %.

We next determined the mass of each fatty acid in the biochars produced from HTC of the simulated food waste under different reaction conditions. Table **4-2** gives the fraction of each fatty acid in the food waste that was retained in the biochar. This fraction can be thought of as an efficiency for fatty acid retention in the carbonization step. Overall, the higher HTC temperatures led to greater retention (about 70 %) of total fatty acids in the biochar. For each individual fatty acid, HTC at 220 °C was the most favorable condition for retaining fatty acids in the biochar. For example, only 36 % of the caprylic acid (C8:0) was in biochar formed at 190 °C and 15 min, but this amount increased to 99% for carbonization at 210 °C. Apart from the effect of process variables, the differences in fatty acids retention can also be attributed to the lipid loss during the transfer of reactor contents for product recovery.

Among all of the fatty acids, more than 95 % of C8:0, C11:0, C15:0, C17:0, and C18:-1[trans-9], were recovered in the biochar from HTC at 210 °C and 30 min. This condition also retained the highest total amount (78 %) of fatty acids in the biochar. This outcome confirms that

HTC is suitable for concentrating fatty acids in the biochar, which is easy to separate for water and then dry for further processing or applications.

Table **4-2**: Fraction of fatty acid in simulated food waste retained in the biochar from HTC at different reaction conditions.

Fatty Acid	180 °C		190 °C		200 °C		210 °C		220 °C	
	15 min	30 min	15 min	30 min	15 min	30 min	15 min	30 min	15 min	30 min
C8:0	0.75	0.81	0.36	0.75	0.50	0.96	0.99	0.99	0.98	0.98
C10:0	0.55	0.61	0.36	0.55	0.43	0.64	0.68	0.73	0.74	0.77
C11:0	0.70	0.98	0.35	0.70	0.78	0.97	0.99	0.99	0.99	0.98
C12:0	0.56	0.60	0.33	0.56	0.44	0.64	0.70	0.79	0.76	0.77
C13:0	0.58	0.48	0.36	0.58	0.39	0.69	0.67	0.67	0.78	0.68
C14:0	0.51	0.54	0.37	0.51	0.44	0.58	0.60	0.72	0.64	0.63
C14:1[cis-9]	0.58	0.58	0.34	0.58	0.49	0.62	0.65	0.87	0.78	0.77
C15:0	0.67	0.69	0.43	0.67	0.59	0.69	0.77	0.95	0.82	0.81
C16:0	0.56	0.54	0.40	0.56	0.47	0.60	0.58	0.73	0.63	0.63
C16:1[cis-9]	0.66	0.56	0.39	0.66	0.53	0.67	0.64	0.91	0.73	0.74
C17:0	0.70	0.57	0.39	0.70	0.49	0.64	0.67	0.95	0.76	0.75
C17:1[cis-10]	0.72	0.55	0.38	0.72	0.57	0.60	0.65	0.92	0.71	0.75
C18:0	0.60	0.51	0.45	0.60	0.50	0.57	0.53	0.77	0.62	0.62
C18:-1[trans-9]	0.74	0.51	0.46	0.74	0.61	0.71	0.71	0.97	0.76	0.80
C18:1[cis-9]	0.73	0.52	0.45	0.73	0.59	0.68	0.66	0.90	0.71	0.74
total	0.58	0.58	0.38	0.58	0.47	0.64	0.65	0.78	0.71	0.71

Extraction of Lipids from Biochar.

We used ethanol to extract the lipids from the biochar. It is a food-grade solvent and is available from renewable resources. [48] The fatty acids detected in the feedstock have value in different industries and applications, and the use of an environmentally friendly solvent like ethanol reduces potential limitations for the subsequent use of these fatty acids in any industry. Figure **4-5** displays the extract yields from biochars produced at each reaction condition. The yields are calculated with respect to the mass of simulated food waste (dry basis) loaded into the reactors initially. Recall the lipid content in the simulated food waste feedstock is 15.7 wt%. The highest extract yield (16.1 wt %) is essentially the same as this initial lipid content. It was obtained from biochar produced at 220 °C and 15 min. Similarly, Lu et al. reported the highest yields were extracted from biochar produced from HTC of microalgae at this same condition. [48] Additionally, Figure **4-5** shows that the extract yield was generally higher from the biochar produced at the longer carbonization time for a given temperature.

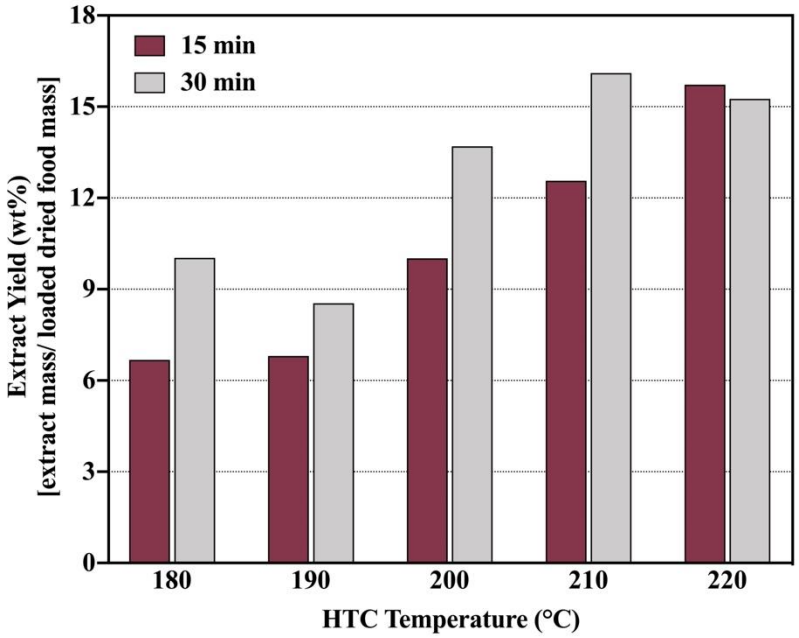

Figure **4-5**: Yields of material extracted from hydrochar after HTC of simulated food waste (9.1 wt % biomass loading).

As discussed above, fatty acids are of interest in different industries. Hence, we determined the amount of each fatty acid in the material extracted from biochar using ethanol, and its recovery in the lipids with respect to their abundance in the biochar. Table **4-3** summarizes the results. The fractions in Table **4-3** can be thought of as an efficiency for fatty acid recovery in the extraction step. The highest recovery of total fatty acids (75 %) was achieved for the biochar produced at 200 °C and 15 min. This HTC condition is not necessarily the best for recovery of each fatty acid, however. For example, only 64 % of C11:0 could be recovered from the biochar produced at this condition, while biochar from most of the other HTC conditions provided more than 90 % recovery. Therefore, depending on the specific fatty acid of interest, the desired HTC reaction condition may vary. Additional experimental work that explores the conditions and solvent(s) used for extraction may lead to more of each fatty acid being recovered from the hydrochar.

Table **4-3**: Fraction of each fatty acid extracted from the biochar produced from HTC of simulated food waste under different reaction conditions.

	180 °C		190 °C		200 °C		210 °C		220 °C	
Fatty Acid	15 min	30 min	15 min	30 min	15 min	30 min	15 min	30 min	15 min	30 min
C8:0	0.48	0.38	0.96	0.48	0.98	0.41	0.89	0.65	0.97	0.59
C10:0	0.53	0.53	0.81	0.53	0.85	0.48	0.60	0.56	0.70	0.57
C11:0	0.98	0.95	0.97	0.98	0.64	0.68	0.91	0.62	0.99	0.99
C12:0	0.51	0.63	0.91	0.51	0.98	0.39	0.76	0.68	0.94	0.77
C13:0	0.56	0.79	0.92	0.56	0.98	0.34	0.71	0.66	0.88	0.90
C14:0	0.46	0.59	0.66	0.46	0.69	0.38	0.58	0.45	0.65	0.63
C14:1[cis-9]	0.48	0.65	0.82	0.48	0.80	0.34	0.70	0.52	0.90	0.72
C15:0	0.44	0.62	0.72	0.44	0.69	0.15	0.67	0.41	0.61	0.70
C16:0	0.44	0.59	0.61	0.44	0.65	0.42	0.61	0.40	0.52	0.61
C16:1[cis-9]	0.44	0.68	0.70	0.44	0.73	0.39	0.69	0.42	0.68	0.68
C17:0	0.41	0.68	0.65	0.41	0.75	0.42	0.79	0.33	0.46	0.63
C17:1[cis-10]	0.38	0.66	0.67	0.38	0.63	0.39	0.61	0.33	0.52	0.63
C18:0	0.40	0.62	0.55	0.40	0.57	0.53	0.69	0.36	0.48	0.59
C18:-1[trans-9]	0.42	0.74	0.63	0.42	0.64	0.46	0.73	0.39	0.52	0.54
C18:1[cis-9]	0.42	0.73	0.62	0.42	0.61	0.48	0.68	0.40	0.54	0.56
total	0.47	0.58	0.72	0.47	0.75	0.43	0.66	0.50	0.69	0.62

Table **4-4** provides the overall fatty acid recoveries from the simulated food waste using this two-step method of HTC followed by extraction with ethanol. These fractions can be thought of as an overall efficiency for the entire two-step process. Total fatty acid recoveries range from 27

– 49%. Recovery from hydrochar produced at 220 ºC gave the best results and the recovery varies from one fatty acid to the next. For example, more than 95 % of C8:0 and C11:0 fatty acids can be recovered from this biochar as can about 70 % of C12:0, C13:0, and C14:1 [cis-9]. The fatty acids have uses in different industries. For example, lauric acid (C12:0) is used in soaps and cosmetics and it is also active against gram-positive bacteria and is used commercially in many different products as an antimicrobial agent. [149] These results demonstrate that HTC pretreatment could be potentially implemented to recover fatty acids from food waste, which could be beneficial for medical, cosmetics, food, fuel, and pharmaceutical purposes.

Table **4-4**: Fraction of each fatty acid in simulated food waste recovered after extraction of hydrochar produced at different HTC conditions.

	180 °C		190 °C		200 °C		210 °C		220 °C	
Fatty Acid	15 min	30 min	15 min	30 min	15 min	30 min	15 min	30 min	15 min	30 min
C8:0	0.36	0.31	0.34	0.36	0.50	0.39	0.89	0.65	0.95	0.58
C10:0	0.29	0.32	0.29	0.29	0.36	0.31	0.41	0.41	0.52	0.44
C11:0	0.68	0.93	0.34	0.68	0.50	0.66	0.91	0.61	0.98	0.97
C12:0	0.28	0.38	0.30	0.28	0.43	0.25	0.53	0.54	0.71	0.60
C13:0	0.32	0.38	0.33	0.32	0.38	0.24	0.48	0.44	0.69	0.61
C14:0	0.24	0.32	0.25	0.24	0.31	0.22	0.35	0.32	0.42	0.40
C14:1[cis-9]	0.28	0.38	0.28	0.28	0.39	0.21	0.46	0.45	0.70	0.55
C15:0	0.30	0.42	0.31	0.30	0.40	0.10	0.51	0.38	0.50	0.57
C16:0	0.25	0.32	0.24	0.25	0.30	0.26	0.35	0.30	0.33	0.38
C16:1[cis-9]	0.29	0.38	0.28	0.29	0.39	0.26	0.44	0.38	0.49	0.50
C17:0	0.29	0.39	0.25	0.29	0.37	0.27	0.53	0.32	0.35	0.48
C17:1[cis-10]	0.27	0.36	0.25	0.27	0.36	0.24	0.39	0.30	0.37	0.47
C18:0	0.24	0.31	0.25	0.24	0.29	0.30	0.37	0.28	0.30	0.37
C18:-1[trans-9]	0.31	0.38	0.29	0.31	0.39	0.33	0.52	0.38	0.39	0.43
C18:1[cis-9]	0.31	0.38	0.28	0.31	0.36	0.33	0.45	0.36	0.38	0.41
total	0.27	0.34	0.27	0.27	0.35	0.28	0.43	0.39	0.49	0.45

Conclusions.

This work demonstrated that HTC of food waste can generate a hydrochar that retains ~ 70% of the fatty acids, which was then extracted with ethanol and resulted in overall fatty acid recovery of 49%. HTC also affords a route to recovering N and P as products in the aqueous phase.

HTC at the milder conditions examined gave higher aqueous-phase product yields and phosphorus recoveries (> 70%) , but lower fatty acid and carbon recoveries in the biochar. Additional experimental work along with a technoeconomic analysis would be required to determine optimal operating conditions.

Chapter 5

Recovery of Energy and Nitrogen via Two-Stage Valorization of Food Waste

Introduction

The global generation of food waste is 1.3 billion tons/yr.[150] Rather than discarding and landfilling this material, as is commonly done, converting it into fuel or fuel precursors would valorize this "waste" biomass. Thermochemical processes like hydrothermal liquefaction (HTL), hydrothermal carbonization (HTC), and pyrolysis have shown promise for this food waste conversion.[36,47,76,124,125,131,151–153] Generally, biocrude oils and biochar contain more nitrogen and oxygen than do petroleum crude oils or coal. Using food waste as the feedstock intensifies this issue as a significant amount of feedstock nitrogen (from the protein fraction of food waste) can be transferred into the biocrude oils. [52] This outcome results in undesirable properties of the biocrude oils, like reduced heating value and high viscosity, and potential catalyst poisoning during conventional refinery operations.[154,155] Even without these issues, application of a high-N biocrude for fuel will be limited due to the NO_x emissions accompanying combustion.[156] Additionally, environmental sustainability considerations argue for recovery of the biomass N as part of the valorization process so it can be re-used as fertilizer. Partitioning the biomass N into a non-fuel product fraction that could be recovered and recycled would reduce demand for NH_3 synthesis, which is an energy-intensive process with high carbon emissions.

A vision for food waste valorization would be to identify processing conditions or novel processes that produce directly biocrude with a low N content and a separate product stream with most of the biomass N. Our previous study on HTL of simulated food waste showed that higher temperatures give both more biocrude oil and also a higher level of N (derived from food waste

proteins) in the oil.[53] Conventional single-step HTL does not appear to have a path to low-N biocrude, high yields of biocrude, and high recovery of N in a separate product stream.

Several studies have demonstrated that HTC of food waste or microalgae partitions N into aqueous-phase products and generates a N-rich recycle stream.[48,117,157–160] These results suggest that HTC may profitably be employed as a pretreatment step prior to HTL. The literature provides several accounts of two-step hydrothermal processes that remove nitrogen from feedstock at a low temperature and then liquefy that material to bio-oil at a higher temperature.[52,157,161–165] A sequential hydrothermal extraction where HTL was conducted at 160 °C as the first step and at 300 °C as the second step reduced the nitrogen present in the *Chlorella sorokiniana* biocrude oil from 1.14 % to 0.78 %.[166] Yeast was subjected to a similar sequential HTL process, and the biocrude nitrogen level decreased from 1.13 % (one step HTL) to 0.51 %.[167]

Conceptually similar two-step treatments have been explored for pyrolysis, with the goal of producing biocrude oils with better qualities and in higher quantities.[168–170] For example, Hammer et al. developed a two-step pyrolysis process for pinewood that produced bio-oils enriched in aromatics relative to those from the conventional one-step treatment.[170] In another study, Zhang et al. used two-step pyrolysis on soy bean stalk to obtain biocrudes with a greater content of hydrocarbons and lower content of oxygen and nitrogen.[171]

There are also a few prior two-step studies that used different types of treatments at each step.[172–175] In these studies, hydrothermal pretreatment was performed to reduce the N content in the feedstock, and then the treated biomass was subjected to pyrolysis as the second step. For example, Du et al. reported that biocrude oil produced from pyrolysis of hydrothermally pretreated *Nannochloropsis* contained fewer nitrogenous compounds than when the algae was used as the feedstock with no pretreatment.[173]

The outcomes of the above-mentioned studies motivate the present work, in which we explore both pyrolysis and HTC of food waste as pretreatment steps to produce carbonized solids.

The biochar solids are then subjected to a second-step treatment to generate biocrude oil. We quantify and evaluate all of the product fractions, investigate different second-step process temperatures, and explore four different combinations of two-step treatments of food waste. To the best of our knowledge, this is the first report of two-step treatment of food waste using both pyrolytic and hydrothermal treatments.

Materials and methods

Materials

The simulated food waste was made by mixing food items as discussed previously.[53] The mixture was 51.4 wt% carbohydrates, 15.7 wt% lipids, and 27.5 wt% proteins, and it had been stored at -4 °C in a freezer for about 23 months prior to its use in this study. Deionized (DI) water, produced in house, was used as the hydrothermal media. It was also used to recover water-soluble products after each treatment. Dichloromethane (DCM, HR-GC grade), purchased from Millipore Sigma, was used to recover biocrude oil after the second treatment. Nitrogen (99.999%), used for evaporating the DCM from biocrude oils and water from aqueous-phase products, and helium were both provided by Praxair. 316 stainless steel mini-batch reactors, with internal 4.1 ml volume, were assembled in the lab using one ½ in. Swagelok port connector and two Swagelok caps.

Processing Methodology

Figure **5-1** outlines the two-stage process used in this study. The first stage, either HTC or pyrolysis, provided biochars that served as the feed to the second stage, which produced

biocrude oils by either HTL or pyrolysis. Both stages generated aqueous-phase products. At each stage, both hydrothermal and pyrolytic treatments were studied and compared.

For the first stage pyrolytic treatment, we dried the original simulated food waste in an oven at 50 °C for as long as needed for the mass of the food mixture to change by less than 0.5 mg. Then, we loaded 0.356 g dried material into each reactor. For the first stage HTC experiments, we loaded 1.24 g of the original food mixture (i.e., 0.356 g dried food mixture plus 0.884 g water) and an additional 2.65 g DI water into each reactor. We next sealed the reactors and placed them in a preheated fluidized sand bath at 200 °C for 30 minutes. We then removed the reactors from the sand bath and cooled them to room temperature using an ice-water bath. Each run was performed in triplicate.

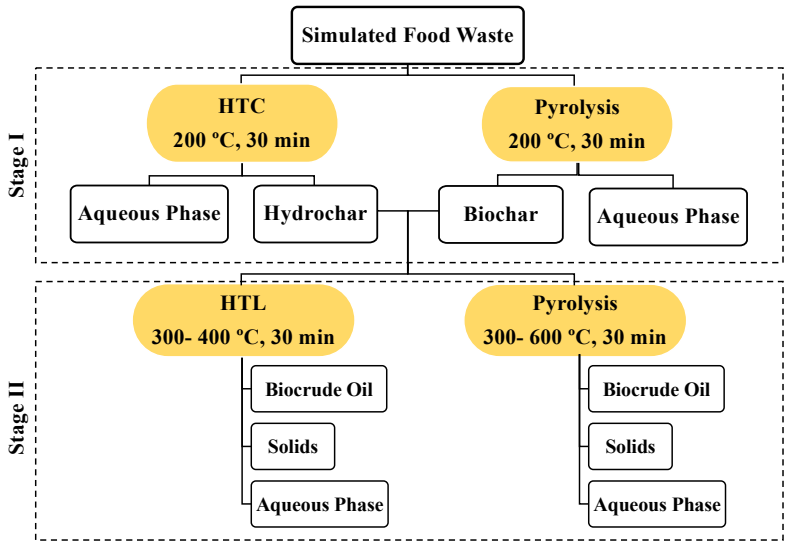

Figure **5-1**: Schematic diagram of the two-step valorization processes.

After the reactors reached room temperature, we opened them and used DI water to recover the products within. We also did a visual inspection of the reactor interior to ensure there were no materials remaining within or adhering to the reactor walls. The products were placed in a centrifuge tube and the solid products were separated from the aqueous-phase products by

centrifugation for 6 min at 6000 rcf. The aqueous phase was then withdrawn using glass Pasteur pipets, transferred into pre-weighed tubes, and placed in an evaporator at 40 °C with flowing N_2 to remove the water. The tubes remained in the evaporator until the mass change was less than 0.5 mg. The centrifuge tubes with the solids were placed in an oven at 60 °C and kept there until their masses changed by less than 0.5 mg. The mass of the dried material in the tubes was then divided by the mass of dried food mixture initially loaded to the reactors to calculate the yields for biochar and aqueous-phase products from Stage 1. We quantified results from three individual runs, and the yields reported herein are the mean values. The standard deviations are also given for each treatment as a measure of run-to-run variability. Production runs in addition to these replicates were conducted to generate enough biochar for the second stage treatment runs.

The dried biochars from HTC or pyrolysis of simulated food waste were treated by either pyrolysis or HTL as Stage II. For the pyrolysis runs, we loaded 0.1174 g of the dried biochar into a reactor. For the HTL runs, we loaded the same amount (0.1174 g) of dried biochar but with an additional 2.355 g DI water. We then sealed the reactors, placed them in a preheated fluidized sand bath, removed them after 30 min, and cooled them to room temperature. We examined HTC and pyrolysis at 300, 350 and 400 °C and extended the work on pyrolysis to higher temperatures (450, 525, 600 °C) as well.

After allowing the reactors to cool and their contents to equilibrate, we opened the reactors and removed the solids and liquids from within. Any gases within the reactors were released. We then added sequentially 3 ml of DI water to recover water-soluble products and 3 ml of DCM to recover less polar organic products. The solutions passed through pre-weighed glass fiber syringe filters to collect any entrained solids. The filtered liquid was collected in a centrifuge tube. This process was repeated until the DCM and DI water aliquots from the reactor returned clear, indicating that all the reactor contents were recovered.

The centrifuge tubes containing the liquid phases were then centrifuged at 6000 rcf for 6 min to separate the aqueous and organic layers. Pasteur pipets were used to remove each phase and transfer them into separate pre-weighed glass tubes. A stream of nitrogen was introduced to the glass tubes containing the DCM phase at 40 °C, using a Labconco RapidEvap Vertex Evaporator, to evaporate dichloromethane and obtain the biocrude oil. The tubes with water-soluble products and the glass fiber syringe filters with solid products were dried in an oven at 40 and 65 °C, respectively. They remained in the oven until their masses changed by less than 0.5 mg.

The dried filters and glass tubes were then weighed, and the masses of each product were calculated by subtracting the mass of the empty tube or filter. The Stage II yields of each product fraction were calculated by dividing the mass of each product by the mass of biochar initially loaded into the reactors. All the runs were conducted in triplicate. The values reported herein are the means, and uncertainties are given as the standard deviations.

Product Analysis

The elemental compositions (C,H,N,S) of the simulated food waste, Stage I biochars, and Stage II biocrude oils were determined by Atlantic Microlab. The oxygen content was calculated by difference. The higher heating values (HHVs) were estimated using their elemental composition (wt %) and the Dulong-Berthelot equation, below.

$$HHV\ (MJ/kg) = 0.3414\ C + 1.4445\ (H-(N+O-1)/8)+ 0.093\ S$$

The energy recoveries were calculated as below.

$$\text{Energy Recovery (\%)} = ((\text{HHV of Biocrude/Biochar}) \times (\text{Yield of Biocrude/Biochar}))/\text{HHV of Simulated Food Waste}$$

Stage II biocrude oil samples were analyzed using a Shimadzu gas chromatograph - mass spectrometer (GC-MS) equipped with a 0.2 mm inner diameter Agilent HP-5MS nonpolar capillary column (50 m length, 0.33 μm film thickness). The column temperature was initially held at 40 °C for 3 min, and then heated to 300 °C at 5 °C min^{-1}. There was also a 5 min hold at the final temperature of 300 °C. The molecular species in each sample were tentatively identified by comparing the mass spectrum of each individual peak with spectra in the NIST library. A relative peak area of ≥ 0.1 % and a similarity index > 85% were required for a tentative identification.

The nitrogen and carbon contents of the water-soluble products from both first and second step treatments were measured using dry combustion analysis (Dumas method).

Results and Discussion

This section first provides product yields from Stage I, HTC or pyrolysis of simulated food waste at 200 °C, and then it provides the yields from Stage II, HTL or pyrolysis of the Stage I biochars. This section also gives the elemental and chemical composition of the Stage I biochars and Stage II biocrudes. It then concludes by providing the N and C recoveries from simulated food waste in the biochars, biocrudes, and water-soluble products.

Stage 1: Product Fraction Yields from Carbonization of Simulated Food Waste

HTC and pyrolysis were conducted at 200 °C for 30 min with the dried simulated food waste. Figure **5-2** shows the Stage I biochar and aqueous-phase yields from each approach. About 57 wt % biochar was produced when pyrolysis was conducted. When water was present in the reactors (HTC), the biochar yield dropped to ~ 46 wt %. The conversion of biomass into biochars

is higher from pyrolysis than HTC. A different study conducted both pyrolysis and HTC on wheat straw, pine bark, and macauba palm at 220 °C for 1 hr[176] with HTC giving the higher biochar yields for all three feedstocks. This difference in outcomes may be due to the different types of biomass being processed. The biomass in the present work is > 40% protein and lipids whereas these components were essentially absent in the lignocellulosic biomass used in the prior study. The composition of the feedstock appears to be a factor in determining the effectiveness of the type of carbonization used to generate biochar.

Figure **5-2** shows that HTC gave a much higher yield of water-soluble products than did pyrolysis. This outcome indicates that the presence of water in the reactor provides an environment where water-soluble compounds have a greater likelihood of being formed and/or surviving during the carbonization process. The low yield of water-soluble products from pyrolysis is consistent with other studies.[177–179] The sum of the yields of biochar and water-soluble products is nearly 100% from HTC and about 65% from pyrolysis. Presumably, the additional mass from pyrolysis was lost as gaseous products.

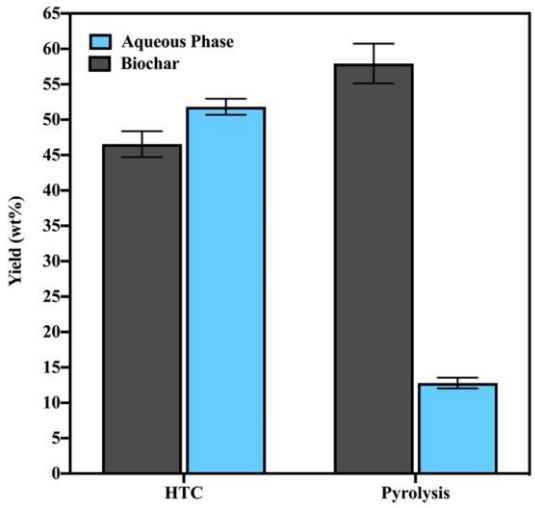

Figure **5-2**: Product Fraction yields from the HTC and pyrolysis of simulated food waste at 200 °C and 30 min.

Stage II: Product Fraction Yields from HTL and Pyrolysis of Biochar

The biochars obtained from Stage I were thermally and hydrothermally treated at 300, 350, and 400 °C for 30 min. Additionally, the biochars from HTC of simulated food waste were subjected to pyrolysis at 450, 525, and 600 °C. The product yields are calculated with respect to the amount of Stage I biochar that was loaded into the reactors.

Figure **5-3** compares product fraction yields from HTL of Stage I biochars that were produced hydrothermally. The yield of biocrude oil was about 45 wt% regardless of the HTL temperature employed, but there was a 9 wt% increase in oil going from 300 to 350 °C. The yields of solids and aqueous-phase products each decreased modestly with the increased HTL temperatures. These results combine to suggest there was some unreacted biochar at 300 °C and increasing temperature to 350 °C converted these components into biocrude oil. An additional increase in the HTL temperature to 400 °C appears to have caused the formation of more gaseous products.

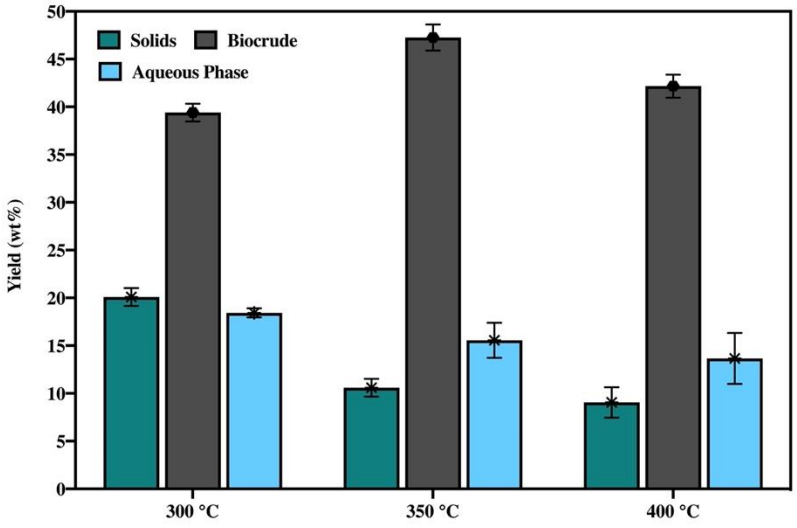

Figure **5-3**: Product fraction yields from the HTL (300, 350, and 400 °C, 30 min) of Stage I biochars from HTC of simulated food waste at 200 °C and 30 min. The yields are calculated with respect to amount of Stage I biochar loaded into the reactors.

A two-step hydrothermal treatment similar that used herein was reported earlier with algae as the feedstock.[52, 162] The yields of biocrude relative to the initial mass of algae were ~ 25 wt% [52] and 13 – 21 wt% [162]. The relevant metric for comparison of these overall biocrude yields with the present work would be the product of the yield of biochar from HTC (Fig. 2) and the yield of biocrude in Fig. 3. These overall biocrude yields range from 19 – 22 wt% in the present work with food waste, in good agreement with the yields observed previously in work with microalgae.

The biochars from HTC in Stage I were also subjected to pyrolysis as an alternative Stage II treatment. Figure **5-4** shows the yields of the different product fractions from pyrolysis at temperatures between 300 and 600 °C. For all runs in this set of experiments, the aqueous-phase samples were clear, and the yields of water-soluble products were nearly zero. The highest yield was just 0.5 ± 0.3 wt %, so we omit aqueous-phase yields from Figure **5-4**.

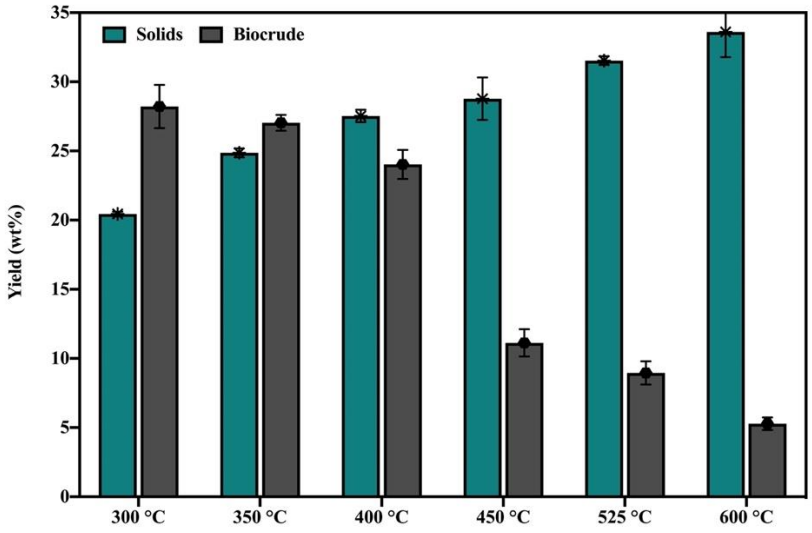

Figure **5-4**: Product fraction yields from pyrolysis (300, 350, 400, 450, 525, and 600 °C, 30 min) of Stage I biochars from HTC of simulated food waste at 200 °C and 30 min. The yields are calculated with respect to amount of Stage I biochar loaded into the reactors.

The biocrude yields from pyrolysis of the HTC biochar decreased from 27 wt % to less than 5 wt % as the temperature increased from 300 to 600 °C. The opposite trend was observed for the solids fraction, where increasing temperature led to formation of an additional 15 wt % of solid products. In a similar two-stage study on microalgae, the solids yield also increased as the temperature increased.[180] The higher temperatures promote the formation of bio-oil into carbonized coke-like material, and therefore larger amounts of solid residue remain in the reactor.[181]

The total amount of solids and biocrude oils was about 50 wt % for treatments at 300, 350, and 400 °C, and it decreased to about 40 wt % for treatments at 450, 525, and 600 °C. Considering that negligible amounts of aqueous phase products were recovered, we infer that about 50 – 60 wt % of the initial biochar was converted into gaseous products.

The next two groups of experiments focused on treatment of biochar from pyrolysis as Stage I. Figure **5-5** shows the product fraction yields from HTL (300, 350 and 400 °C) of the biochars. Similar to the results from HTL of the biochars from hydrothermal carbonization (Figure **5-3)**, HTL of these biochars at 350 °C gave the highest amount of biocrude oil, and both solids and aqueous-phase product fractions decreased as temperature increased. A portion of the solids and/or water-soluble compounds might have converted into biocrude oil when the temperature increased from 300 to 350 °C.

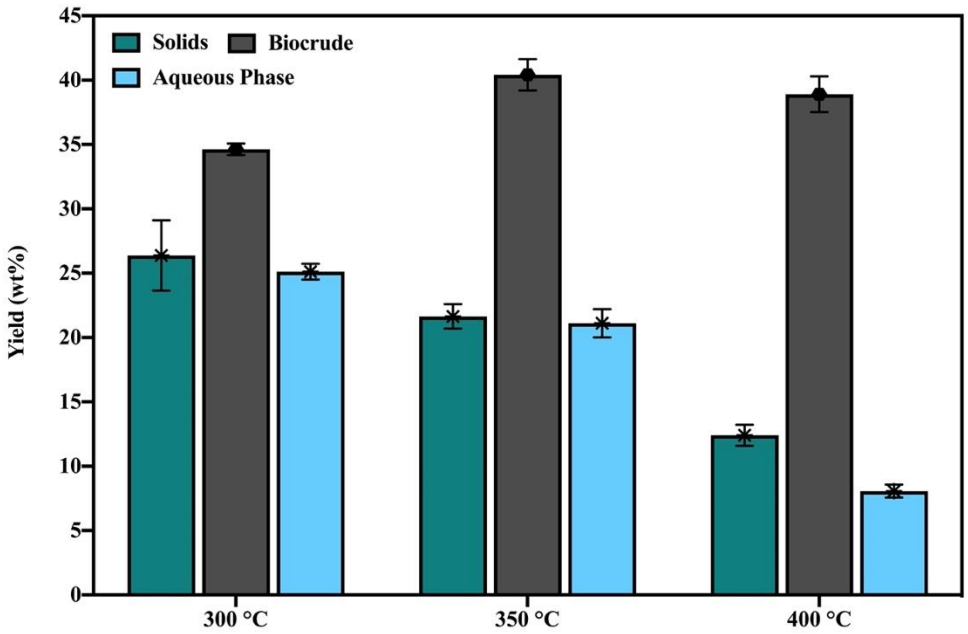

Figure **5-5**: Product fraction yields from HTL (300, 350, 400 °C, 30 min) of Stage I biochars from pyrolysis of simulated food waste at 200 °C and 30 min. The yields are calculated with respect to amount of Stage I biochar loaded into the reactors.

Figure **5-6** provides the results for Stage I biochars from pyrolysis being subjected to a second pyrolysis treatment at 300, 350 and 400 °C. Since even higher pyrolysis temperatures gave lower and lower biocrude yields in Figure **5-4**, we did not examine these high temperatures again with this set of biocrudes. Unlike all other sets of results, increasing temperature here did not have any impact on the product yields. Biocrude yields were always around 23 wt % and solid yields were around 40 wt %. Zhang et al. also conducted two-step pyrolysis, but of soybean stalk, and they also reported little influence of the temperature of the second step on solid product yields.[171] As was the case in Figure **5-4** for pyrolysis of the hydrochar as the Stage II treatment, aqueous-phase products were scarce (highest yield was 0.4 ± 0.2 wt %). Their (very low) yields are not shown in Figure **5-6**.

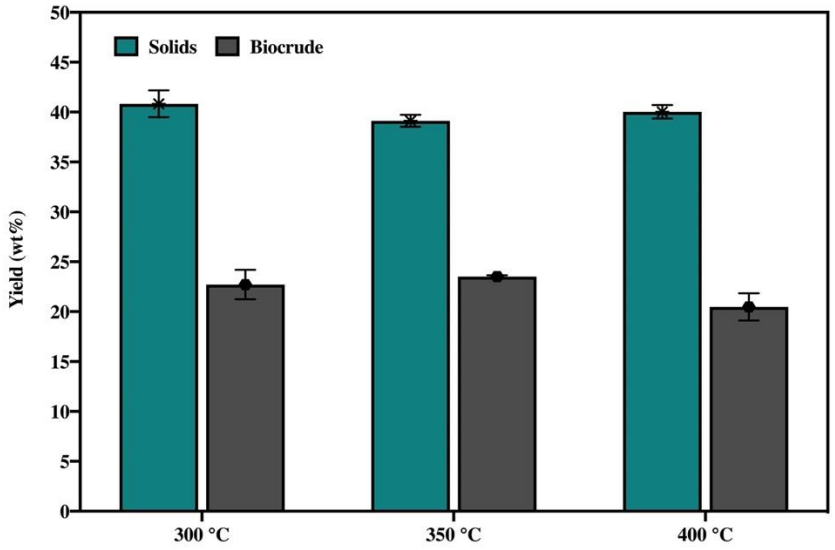

Figure **5-6**: Product fraction yields from the pyrolysis (300, 350, 400 °C, 30 min) of Stage I biochars from pyrolysis of simulated food waste at 200 °C and 30 min. The yields are calculated with respect to amount of Stage I biochar loaded into the reactors.

Elemental Composition of Stage I Biochars and Stage II Biocrude oils

The elemental compositions of simulated food waste, biochars, and biocrudes from all the runs are given in Table **5-1**. The C and H contents of the hydrothermally produced biochars were 60.6 and 7.43 wt %, respectively, which were slightly higher than the values of the pyrolytically generated biochars. This higher C and H content also led to the estimated HHV values of biochars from HTC exceeding those from pyrolysis. These results are consistent with prior studies reporting H and C content in biochars produced hydrothermally being higher than in those produced pyrolytically.[182–184] The N content in the biochar was not affected by the type of treatment and it was about 6.7 wt % for both HTC and pyrolysis. Overall, both treatments improved the HHV by ~ 10 MJ/kg.

Table **5-1**: Elemental composition (wt %) of Simulated food waste, Stage I biochars, and Stage II biocrude oils under different treatment temperatures.

		C	H	N	S	O	HHV (MJ/kg)	Energy Recovery* (%)
Simulated Food Waste		47.4	5.05	4.83	0.24	42.0	15.2	-
Biochar from HTC at 200 °C		60.6	7.43	6.66	0.37	24.9	25.9	80.5
Biochar from Pyrolysis at 200 °C		59.1	6.93	6.68	0.29	27.0	24.3	93.2
Biocrudes								
Biochar from Pyrolysis at 200 °C	HTL- 300 °C	73.1	10.61	3.34	0.17	12.8	37.5	50.2
	HTL- 350 °C	73.9	9.51	4.17	0.27	12.1	36.2	56.6
	HTL- 400 °C	75.2	9.26	4.08	0.30	11.2	36.5	54.8
	Pyrolysis- 300 °C	72.5	10.86	3.34	0.14	13.1	37.7	33.0
	Pyrolysis- 350 °C	74.3	10.71	5.20	0.10	9.70	38.3	34.8
	Pyrolysis- 400 °C	73.9	10.71	5.36	0.07	10.0	38.1	30.1
Biochar from HTC at 200 °C	HTL- 300 °C	73.1	9.95	4.27	0.34	12.3	36.5	44.7
	HTL- 350 °C	74.4	9.62	4.49	0.28	11.3	36.6	53.7
	HTL- 400 °C	75.5	9.64	3.35	0.36	11.1	37.3	48.8
	Pyrolysis- 300 °C	72.3	11.24	2.72	0.11	13.7	38.1	33.4
	Pyrolysis- 350 °C	73.9	10.46	5.44	0.13	10.1	37.7	31.6
	Pyrolysis- 400 °C	76.3	10.72	5.83	0.09	7.10	39.4	29.4
	Pyrolysis- 450 °C	74.6	9.74	6.44	0.11	9.07	36.9	12.8
	Pyrolysis- 525 °C	78.8	8.68	5.55	0.10	6.84	37.4	10.4
	Pyrolysis- 600 °C	76.4	7.15	4.49	0.15	11.8	33.7	5.51

* with respect to the food waste feedstock loaded in Stage I

The first group of biocrudes in Table **5-1** is those produced by liquefaction of Stage I pyrolytic biochars. The biocrudes from runs at 300 °C had similar elemental composition and HHV (~38 MJ/kg) regardless of whether from pyrolysis or HTL. For the higher temperatures of 350 and 400 °C, the H and N contents were lower in biocrudes from HTL than from pyrolysis. Conversely, HTL led to higher amounts of S and O in the biocrudes than did pyrolysis. This then resulted in greater HHVs for the pyrolytically produced biocrudes.

The second group of biocrudes in Table **5-1** is those produced from HTL and pyrolysis of Stage I HTC biochars. The greatest HHV of 39.4 MJ/kg was obtained from pyrolysis at 400 °C.

The biocrude oil with the lowest N content (2.72 wt %) had the second highest HHV (38.1 MJ/kg).

For both types of biochars, increasing temperature for HTL runs in Stage II led to higher C and lower O and H, and it did not cause any specific trend for N and S. There was no clear trend with temperature for the elemental composition or HHV of the biocrude from pyrolysis runs.

The HHV of biocrude from single-step HTL of this simulated food waste at 300 °C and 30 min batch holding time was ~ 33 MJ/kg.[53] Table **5-1** shows the HHVs for the biocrudes from the two stage hydrothermal treatment were about 36.5 MJ/kg with Stage II temperatures of 300 and 350 °C. Thus, the two-stage treatment produced biocrude with a greater heating value than did single-stage HTL at comparable conditions.

The present two-step treatment of simulated food waste afforded energy recovery in the biocrude oil exceeding 50% for several runs. These energy recoveries are essentially the same as those obtained for single-step HTL of this same food waste under many of the conditions explored, but lower than the energy recoveries of ~ 60% obtained in a few runs.[53]

N and C recoveries in aqueous-phase products, biochars, and biocrude oils

The ideal outcome from each type of food-waste valorization examined herein would be to partition as much N as possible into the aqueous-phase products (for its recovery and recycling) and as much carbon (and heating value) as possible into the biochars or biocrude oils. Table **5-2** gives the C and N recoveries in the biochars and water-soluble products from both HTC and pyrolysis of simulated food waste. HTC partitioned 39 % of the biomass N into aqueous-phase products and 56 % into the biochar. Pyrolysis did not perform as well, as it transferred only 12 % of the biomass N into water-soluble products and retained 77 % of it in the biochar. Table **5-2** also

shows more C was distributed to the biochars by pyrolysis than by HTC, which is a favorable outcome. Neither HTC nor pyrolysis distributed the food waste C and N into the product fractions entirely as one would desire.

Table **5-2**: Fraction of nitrogen and carbon in simulated food waste recovered in the Stage I biochar and aqueous phase products from HTC/Pyrolysis at 200 °C, 30 min.

	Stage I Biochar		**Stage I Aqueous Phase**	
	N	**C**	**N**	**C**
HTC	0.56	0.57	0.39	0.31
Pyrolysis	0.77	0.71	0.12	0.10

Table **5-3** gives the recovery of the food waste C and N in the Stage II aqueous phase and biocrudes. The C recovery in the Stage II biocrude oil from HTL was always about 30%. This value is lower than the ~ 40% carbon recoveries obtained from direct, single-step HTL of this simulated food waste feedstock at 300 – 400 °C.[53] The condition in Table **5-3** that gave the highest C recovery in biocrude oils also gave the highest N recovery of 19 %. Even so, these low N recoveries in the oil indicate that the large majority of the feedstock N went elsewhere.

The N recovery in the aqueous-phase products was as high as 55 % (for Stage II HTL at 300 or 350 °C on biochar from pyrolysis). The C recovery in the water-soluble products was just 9% for the run at 300 °C, so it seems this condition had the desirable performance of keeping the carbon recovery low and the nitrogen recovery high in the aqueous-phase products.

Table **5-3** also gives the total recovery of C and N in the combined aqueous-phase product streams from both stages. This metric is the sum of the recoveries in the Stage II aqueous phase with respect to feedstock and recoveries in the Stage I aqueous-phase samples. About 75 % of the N in the simulated food waste was transferred into the aqueous-phase products by conducting both stages hydrothermally with Stage II at 350 °C. One-step HTL of simulated food waste at 350 °C transferred only 10% of the feedstock N into the aqueous phase products.[53]

Costanzo et al. also reported greater recovery of N in the aqueous-phase products by conducting two-step hydrothermal treatment of algal biomass rather than a single-step approach.[157]

Table **5-3**: Fraction of N and C in the simulated food waste transferred into the Stage II biocrude oils and aqueous phase products.

		Recovery in Stage II Biocrude Oil		**Recovery in Stage II aqueous phase**		**Recovery in Stage I+ Stage II Aqueous Phase**	
		N	**C**	**N**	**C**	**N**	**C**
Biochar from Pyrolysis	**HTL- 300** °C	0.13	0.29	0.55	0.09	0.66	0.19
	HTL- 350 °C	0.19	0.35	0.55	0.13	0.67	0.23
	HTL- 400 °C	0.18	0.34	0.42	0.07	0.54	0.17
	Pyrolysis- 300 °C	0.09	0.19	--	--	0.12	0.10
	Pyrolysis - 350 °C	0.14	0.20	--	--	0.12	0.10
	Pyrolysis - 400 °C	0.13	0.18	--	--	0.12	0.10
Biochar from HTC	**HTL- 300** °C	0.14	0.27	0.34	0.12	0.73	0.43
	HTL- 350 °C	0.18	0.33	0.36	0.09	0.75	0.4
	HTL- 400 °C	0.12	0.30	0.26	0.08	0.65	0.39
	Pyrolysis- 300 °C	0.06	0.19	--	--	0.39	0.31
	Pyrolysis - 350 °C	0.12	0.19	--	--	0.39	0.31
	Pyrolysis - 400 °C	0.12	0.17	--	--	0.39	0.31
	Pyrolysis- 450 °C	0.06	0.08	--	--	0.39	0.31
	Pyrolysis - 525 °C	0.04	0.07	--	--	0.39	0.31
	Pyrolysis - 600 °C	0.02	0.04	--	--	0.39	0.31

Inspecting the results for energy recovery in Table **5-2** and for N recovery in the combined aqueous phases in Table **5-3** shows that the run with highest energy recovery provided an overall nitrogen recovery of 67% in the aqueous phase streams. The run with the highest N recovery (75%) provided a 54% energy recovery in the biocrude. Single-step HTL also provided about 55% energy recovery in the biocrude, but it provided less than 10% recovery of the biomass N in the aqueous-phase products. The two-step treatments can partition much more N

into the aqueous-phase products while largely preserving the biocrude energy recoveries available from single-stage HTL.

Molecular characterization of stage II biocrude oils

GC-MS analysis provided information about the types and abundances of GC-eultable molecules in the various biocrude oils. The molecular components that were tentatively identified account for more than 80 % of the area in the total ion chromatograms (TIC). The components were then categorized into different classes of compounds. Table **5-4** gives the TIC area % of each class for the different bio-oils. If a compound contained more than one of the functional groups, the following order was followed for compound assignment: fatty acids (FA) > esters > amides > phenols > nitriles > amines > ketones > alcohols > ethers.

Generally, when HTL was conducted as the Stage II treatment, regardless of whether the biocrude was produced hydrothermally or pyrolytically, the fatty acids fraction in the light biocrude oils was always at least 50 % and reached as high as 76%. With pyrolysis as the Stage II treatment, on the other hand, 37.1% was the highest fatty acids fraction. HTL was more favorable than pyrolysis for generating bio-oils rich in fatty acids, which are desirable molecules for fuel purposes. Consistent with this result, when one-step HTL was conducted on this simulated food waste, fatty acids accounted for more than 80% of the total area.[53] Regardless of the first or second-stage treatment, increasing temperature in the Stage II treatment consistently led to a lower abundance (using area % as a proxy) of fatty acids in the biocrude. This outcome is consistent with the fatty acids being more prone to decomposition reactions as the conditions became more severe. We also note that increasing temperature led to higher area % for hydrocarbons, which is a desirable outcome.

Table **5-4**: Relative peak area % in total ion chromatogram for different groups of compounds in Stage II biocrude oils. (FA: Fatty Acids, HC: Hydrocarbons)

		FA	HC	Alcohols	Amides	Amines	Nitrile	Ketone	Esters	Phenols + Ethers
Biochar from Pyrolysis at 200 °C	**HTL- 300 °C**	68.8	6.89	6.74	8.77	1.40	0.00	5.56	0.29	1.49
	HTL-350 °C	73.8	3.40	2.87	9.64	5.54	0.00	1.41	0.49	2.84
	HTL- 400 °C	50.7	11.4	22.6	1.08	7.79	0.17	1.93	3.75	0.63
	Pyrolysis- 300 °C	37.1	4.30	2.58	32.9	10.3	4.13	0.78	4.88	2.00
	Pyrolysis- 350 °C	15.9	8.87	15.5	7.70	4.51	42.1	0.81	4.45	0.12
	Pyrolysis- 400 °C	11.4	23.0	6.26	10.8	7.13	33.9	1.39	2.53	3.60
Biochar from HTC at 200 °C	**HTL- 300 °C**	75.8	1.79	0.11	17.0	2.82	0.00	0.74	1.76	0.00
	HTL- 350 °C	70.9	3.21	0.30	13.4	5.67	0.00	1.44	1.98	2.99
	HTL- 400 °C	61.9	8.91	15.5	4.31	2.67	1.41	0.55	4.57	0.00
	Pyrolysis- 300 °C	27.0	10.9	8.12	26.1	12.9	1.15	1.95	8.04	3.24
	Pyrolysis- 350 °C	14.5	12.7	5.92	20.9	3.85	30.8	1.98	9.06	0.29
	Pyrolysis- 400 °C	12.9	22.9	5.73	11.6	4.52	38.2	0.81	1.16	1.68
	Pyrolysis- 450 °C	0.77	46.8	18.8	1.12	0.03	20.5	2.00	3.17	4.08
	Pyrolysis- 525 °C	3.00	49.1	6.52	3.37	10.2	4.69	6.00	15.0	0.68
	Pyrolysis- 600 °C	0.15	59.3	1.83	3.42	23.8	3.02	3.11	5.00	0.43

When the Stage II treatment was done pyrolytically, the most abundant products were N-containing molecules. The fraction of amides was as high as 32.9 % and their area % decreased with increasing pyrolysis temperature. Amines and nitriles were as high as 23.8 % and 42.1%, respectively. The abundance of these groups never exceeded a few percent when HTL was used as Stage II to produce biocrude. The greatest nitrile abundances were from Stage II pyrolysis around 350 – 400 °C.

To summarize, HTL as the Stage II treatment gave oils rich in fatty acids. Pyrolysis as the Stage II treatment led to a greater representation of nitrogen-containing compounds in the biocrude. The predominance of N-containing compounds in the biocrude from pyrolysis is consistent with these bio-oils generally having a larger N wt% than the oils from HTL (see Table **5-1**). The lower pyrolysis temperature (300 °C) favors the presence of amides, whereas temperatures around 350 – 400 °C favor the presence of nitriles in the GC-elutable portion of the biocrude oils. HTL in stage II seems to be a better choice for producing biocrudes with fewer N-containing compounds.

Conclusions

Valorizing food waste via a two-step carbonization – hydrothermal liquefaction process provides a crude bio-oil with over 50% of the chemical energy in the biomass and aqueous-phase products with about 70% of the biomass N. This two-step approach is nearly as good as single-step HTL for energy recovery but much better for N recovery. This process shows promise for valorizing food waste, producing a renewable bio-oil, and recovering N, an important component in fertilizer needed to grow more food.

Carbonization of the food waste at 200 °C for 30 min gave biochars with yields of 57 and 46 wt %, respectively, for pyrolysis and HTC. The aqueous-phase yield for the HTC run was 52 wt %, which was 40 wt % higher than that from the pyrolysis run.

The highest overall yields of biocrude oil (based on the initial mass of food waste) were about 22 wt%, and pathways to this yield existed for either pyrolysis or hydrothermal treatment for both the first and second stages. Aqueous phase yields were nearly zero for the runs with pyrolysis as the Stage II treatment. This low yield of water-soluble products from pyrolysis of the biochar limited the N recovery to that available in the initial carbonization step (39% for HTC, 12% for

pyrolysis). There was more N partitioning into the aqueous-phase products when Stage II was conducted hydrothermally.

Chapter 6

Implications and Recommendations

Summary and Conclusions

This dissertation explored the hydrothermal valorization of food waste. The research studies provide advances on optimizing process variables to promote yields and qualities of biocrude oil, identifying abundance of molecular products in the biocrudes, coupling treatments to recover nutrients in aqueous streams, and recovering fatty acids from food waste.

In chapter 2, we report the first account for HTL of food waste under the broadest range of reaction conditions. We elucidated the influence of pressure that generally was neglected in previous works. We also explored fast HTL on food waste, with a short batch holding time of 1 min. Comparable yield of 30 wt %, and HHV of 35 MJ/kg to those obtained from HTL of microalgae were achieved by the HTL of simulated food waste. Temperatures near the critical point (374 °C) and pressures high enough to keep water in liquid or supercritical phase were found to give high biocrude yields. Fast HTL produced biocrude oils with the yields ranging from 25 to 30 wt %, within a batch holding time of just 1 min. Energy recovery in the biocrude of up to 65 % was achieved from HTL of simulated food waste. Partitioning more than half of the nutrients in the food waste to the aqueous phase products demonstrated the potential of this method in recovering nutrients for use in fertilizers.

In chapter 3, we screened a number of potential catalysts including supported metals, metal oxides, acid, bases and salts, to enhance biocrude yields and qualities. This is the first to report such a comprehensive investigation on the catalytic HTL of food waste. Pressurizing reactors with 3500 kPa of H_2, increased the HHV of the biocrudes with the presence of supported

metals. However, these materials did not perform well in promoting the yields of biocrudes, and hence, energy recovery from runs with these materials remained low. When salts, acids, and bases were used, the HHV values increased even further than they did with the supported metals, and therefore gave high energy recoveries. Among the additives tested, formic acid and KH_2PO_4 produced biocrudes with energy recoveries exceeding 83%. The last group of potential catalysts tested were metal oxides. They offered the most promising results. The addition of silica added 9 wt % to the biocrude oil yield and led to energy recoveries exceeding 90%. Save for CaO, all the metal oxides successfully reduced the N content in the biocrude oils. Since this group of materials was the only one that enhanced both yields and energy recoveries of biocrude, we believe that they are good catalyst candidates for HTL of food waste.

Conducting HTC on simulated food waste in chapter 4 established the potential of this treatment in recovering nutrients into aqueous phase products, while allowing the extraction of fatty acids from food waste lipid fraction. About 70 % of the fatty acids in the food waste were retained in the biochars. Recovering them with the use of ethanol gave 49 % overall fatty acid recovery. Under milder reaction conditions, higher aqueous phase yields, but lower fatty acids and carbon recoveries in the biochars were achieved.

In chapter 5, we further investigated a treatment procedure to recover nutrients and produce high yields of biocrude oils. We coupled low temperature treatments of HTC and pyrolysis with higher temperature HTL and pyrolysis. We also analyzed all the product fractions quantitively and qualitatively. Pyrolysis at the first step treatment gave biochars with 57 wt % yields, higher than what HTC gave (46 wt %). The biochars were subjected to additional treatments at the second stage. HTL of hydrothermally produced biochars at 350 °C generated biocrudes with the highest yield of 47 wt %. When pyrolysis was conducted at the second step, no aqueous phase products were recovered. 39.4 MJ/kg was the highest HHV achieved by pyrolysis of Stage I hydrothermally produced biochars at 400 °C. GC-MS results showed that biocrudes

produced pyrolytically at stage II contained heavy fraction of N containing compounds, and therefore less N was transferred into water soluble streams. We also calculated the recovery of C and N in the combined streams of aqueous phase from both stage I and II. About 75% of N was partitioned into these streams under the HTL of biochars produced hydrothermally at 350 °C. On the other hand, the lowest amount of C recovered in those streams was from the run where HTL at 400 °C was conducted on Stage I biochar produced pyrolytically.

Recommendations for Future Research

This dissertation stablished that hydrothermal treatment is an effective process for the valorization of food waste. We thoroughly studied the influence of different parameters governing the process, as well as the effect of introducing a broad range of different types of catalysts into this technique. The work conducted throughout this dissertation used a single simulated food waste feedstock with fixed composition. A number of studies have elucidated the influential effect of feedstock composition on the product fractions from HTL and their elemental and chemical compositions.[27,28,30] Therefore, studying food mixtures with varying composition is a potential direction for future work .

We defined the chemical composition of all the acquired biocrude oils using GC-MS analysis. This method although only analyzes the lighter fraction of the oil (volatile compounds). On the other hand, thermogravimetric analysis data indicated that a considerable portion of the biocrude oils does not elute at the GC-MS temperature range, and therefore was not analyzed. Researchers used Fourier Transform Ion Cyclotron Resonance Mass Spectroscopy (FT-ICR MS) to gain insights into the molecular composition of biocrude oils and water soluble products from HTL of microalgae.[185–187] The molecular formula of each compound in the samples can be determined by this technique, as it provides the molecular weight of each compound to within

<0.001 amu. Testing the biocrude oil samples from HTL of food waste using FT-ICR MS can provide information about their molecular composition and be a good complement to current GC-MS findings.

The importance of acquiring knowledge regarding migration of N, P, and C elements and nutrients into the aqueous phase products has been highlighted many times throughout this dissertation. To gain some understanding of this matter, we used data from elemental characterization of product fractions. There have been works that used high performance liquid chromatography (HPLC) to determine the molecular compounds in the aqueous phase and quantify them.[158,164] Therefore, analyzing the aqueous phase products from food waste using HPLC can further complete our understanding about the recovery of nutrients in this fraction of the products. Additionally, the elemental characterization results for the recoveries of N, P, and C elements reported throughout this work, were all calculated based on single runs. It is important to conduct additional tests to determine uncertainties.

Food waste is also composed of other metals and minerals like (Ca, and K). It is crucial to look into the abundance of these elements in the food mixture, and track their migrations into different products under certain operating conditions.

Furthermore, we used Dulong-Berthelot equation and results from elemental analysis on biocrude oils to calculate HHVs of the same throughout this work. These calculated values are all based on estimation, it will be a great addition to measure these values experimentally using bomb calorimetry. This will give us more reliable understanding regarding the quality of the acquired biocrude oils.

Assisted HTL of simulated of food waste was most advantageous for increasing biocrude yields when SiO_2 was used. Biocrude oil qualities were also improved with the use of certain supported metals. Hence, it will be interesting to support the metals, that gave best performance

in improving biocrudes qualities, with SiO_2, and conduct additional runs to evaluate their effect on HTL of simulated food waste.

We compared the performance of different kinds of metal oxides and supported metals on HTL of simulated food waste. Although, the properties of these materials can also have considerable effects on HTL of food waste. Therefore, it will be a possible direction for future work to look into the effect of these materials properties such as porosity, surface area, and adsorption sites, on the HTL of food waste and make a better comparison.

In chapter 2, we tested a kinetics model developed for microalgae,[73] to examine its ability in predicting biocrude yields from HTL of food waste. The model was able to predict the yields for two-thirds of the cases within ± 5 wt %, and for nearly 90% of the case to within ± 10 wt %. This great predictive ability of the current kinetics model showed that biocrude yields from HTL can be predicted from knowledge of the HTL time and temperature and the biochemical composition of the wet biomass feedstock. The model could be improved via additional work that broadens the model by using data from HTL of polysaccharide-rich feedstocks to regress new values for its kinetics parameters.

Hydrothermal carbonization was beneficial in enhancing the recovery of nutrients in the aqueous phase products, as well as extraction of fatty acids from food waste lipid portion. Each reaction condition examined led to both positive and undesired outcomes in terms of the amount of fatty acids and nutrients recovered in different products. Therefore, additional experimental work along with a technoeconomic analysis can be very beneficial for determining the optimum condition.

The technology of HTL has been shown as a robust process for valorization of food waste, but it has not been commercialized yet. There is a need for more extensive process design work and techno-economic analyses to investigate the economic viability of this technology. Of HTL publications in the literature from 1980 to 2018, only 5 % of them are represented by techno-

economics, which demonstrates a detachment between the investigation of this technology at bench scale and its practical application at large scales.[188] This small percentage of studies also only include preliminary techno-economic analysis of HTL with feedstocks such as microalgae and municipal wastewater treatment plant sludge. No technoeconomic analysis has been reported for the HTL of food waste. This analysis gives the information that will be vital in understanding the economics of the process.

Appendix A

Supporting Figures and Tables for Chapter 2

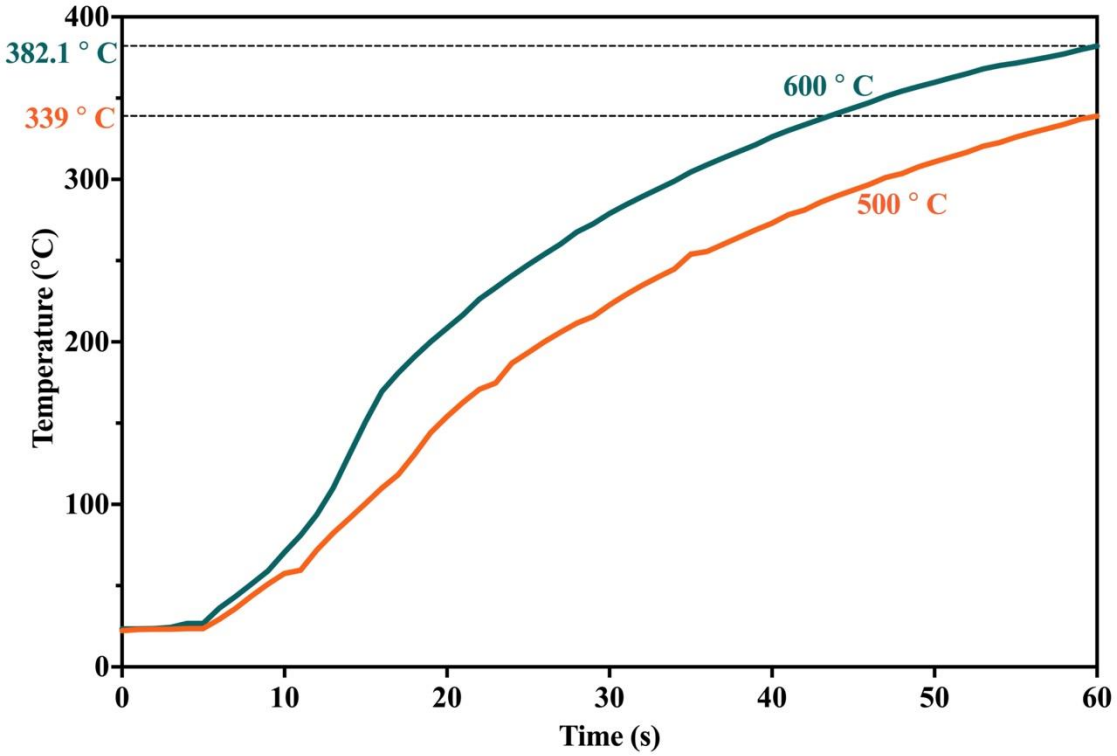

Figure **A-1**: Temperature profile of reactors at sand bath set-point temperature of 500 °C and 600 °C.

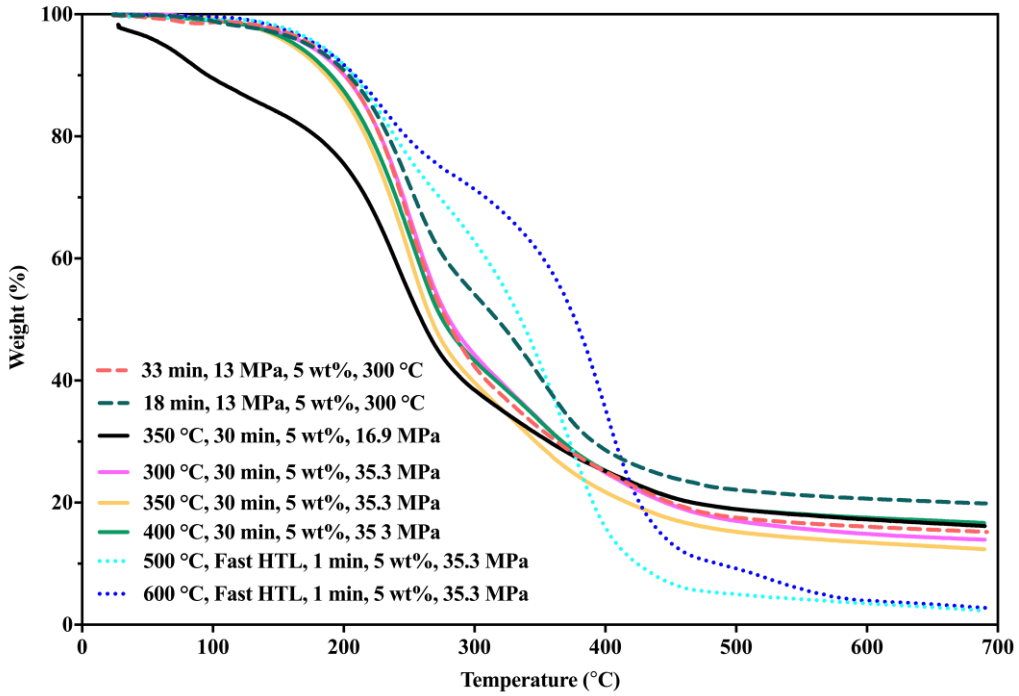

Figure **A-2**: TG curves of biocrudes produced under HTL reaction conditions given in legend.

Table **A-1**: Experimental and model-calculated yields (wt%) of biocrude (X_{BC}) from HTL of mixtures of real food.

Reference	T (°C)	Pressure (MPa)	t (min)	Biomass Loading (wt%)	$x_{BC, exp}$ (wt%)	$x_{BC, model}$ (wt%)
Zastrow et al., 2013	315	-	10	15	40.0	30.8
Zastrow et al., 2013	280	-	10	15	35.5	26.2
Zastrow et al., 2013	250	-	10	15	32.0	22.0
Zastrow et al., 2013	315	-	30	15	34.0	35.5
Zastrow et al., 2013	280	-	30	15	27.5	30.5
Zastrow et al., 2013	250	-	30	15	21.0	26.6
Zastrow et al., 2013	315	-	60	15	26.5	39.0
Zastrow et al., 2013	280	-	60	15	25.5	33.3
Zastrow et al., 2013	250	-	60	15	11.0	28.9
Maag et al., 2018	300	-	60	15	37.5	34.3
Aierzhati et al., 2019	280	-	40	20	38.0	36.8
Aierzhati et al., 2019	300	-	40	20	39.0	39.2
Aierzhati et al., 2019	320	-	40	20	44.0	41.6
Aierzhati et al., 2019	340	-	40	20	46.0	43.7
Aierzhati et al., 2019	360	-	40	20	49.0	45.3
Aierzhati et al., 2019	380	-	40	20	45.0	46.1
Aierzhati et al., 2019	360	-	10	20	26.0	41.6
Aierzhati et al., 2019	360	-	20	20	41.0	43.4
Aierzhati et al., 2019	360	-	60	20	48.0	46.2
Present work	350	25.9	30	5	33.2	38.1
Present work	350	25.9	30	10	35.8	38.1
Present work	350	25.9	30	15	34.3	38.1
Present work	350	25.9	30	20	35.6	38.1
Present work	200	35.3	30	5	11.8	19.2
Present work	300	35.3	30	5	28.8	31.4
Present work	350	35.3	30	5	29.3	38.1
Present work	400	35.3	30	5	30.0	42.3
Present work	300	13	3	5	17.8	22.0
Present work	300	13	8	5	20.8	26.3
Present work	300	13	18	5	29.3	29.4
Present work	300	13	33	5	27.1	31.8
Present work	350	16.9	30	5	36.2	38.1
Present work	350	21.2	30	5	33.7	38.1
Present work	350	30.8	30	5	29.5	38.1
Present work	350	16.9	30	8.7	37.4	38.1

Appendix B

Supporting Figures and Tables for Chapter 5

Table **B-1**: Tentative identities of compounds in the Stage II biocrude oil from the HTL (300, 350, and 400 °C, 30 min) of Stage I biochars from HTC of simulated food waste at 200 °C and 30 min, detected by GC/MS.

300 °C		**350 °C**		**400 °C**	
Name	Area (%)	Name	Area (%)	Name	Area (%)
n-Hexadecanoic acid	22.9	n-Hexadecanoic acid	23.0	n-Hexadecanoic acid	23.4
6-Octadecenoic acid	17.5	Oleic Acid	20.7	1,2-Propanediol, 3-benzyloxy-1,2-diacetyl-	9.91
Octadecanoic acid	8.15	Octadecanoic acid	8.73	Octadecanoic acid	9.53
Tetradecanoic acid	7.15	Tetradecanoic acid	6.29	Oleic Acid	8.51
9-Octadecenoic acid, (E)-	6.01	Benzenemethanamine, N-(phenylmethylene)-	3.28	Tetradecanoic acid	5.91
Hexadecanamide	3.70	Phenol, 4,4'-(1-methylethylidene)bis-	2.50	Hexadecanamide	2.18
2,5-Piperazinedione, 3,6-bis(2-methylpropyl)	2.59	Dodecanamide, N-methyl-	1.81	1-Tetradecanol	1.21
N1-Benzyl-N2(bezylidenyl-benzylamino)-benzamidin	1.72	Hexadecanamide	1.56	1,1':3',1"-Terphenyl, 5'-phenyl-	0.92
Dodecanoic acid	1.66	9-Octadecenamide, (Z)-	1.56	Pentadecane	0.85
n-Decanoic acid	1.09	Dodecanamide, N-isobutyl-	1.29	1-Hexadecanol	0.82
9-Octadecenamide, (Z)-	0.97	Z-11-Hexadecenoic acid	0.87	Heptadecane	0.70
N-Methyldodecanamide	0.92	1-propen-2-amine, 1-(3,3-dimethyl-3H-indol-2-yl	0.87	Undecylcyclohexane	0.68
Pentadecanoic acid	0.90	Dodecanamide, N-ethyl-	0.85	Hexadecane	0.67
3,6-Diisopropylpiperazin-2,5-dione	0.73	Pentadecanoic acid	0.70	3-Heptadecene, (Z)-	0.54
Octadecanamide, N-butyl-	0.67	Palmitoleic acid	0.61	8-Heptadecene	0.54
1,3,6-Cyclooctatriene	0.59	10-Undecenoic acid, propyl ester	0.56	2-Hydroxy-octadeca-9,12,15-trienoic acid, pyrrolidide	0.49

Table **B-2**: Tentative identities of compounds in the Stage II biocrude oil from the pyrolysis (300, 350, 400 °C, 30 min) of Stage I biochars from HTC of simulated food waste at 200 °C and 30 min, detected by GC/MS.

300 °C		**350 °C**		**400 °C**	
Name	Area (%)	Name	Area (%)	Name	Area (%)
n-Hexadecanoic acid	9.67	N1-Benzyl-N2(bezylidenyl-benzylamino)-benzamidin	10.4	Octadecanenitrile	10.7
Hexadecanamide	5.58	Hexadecanenitrile	6.30	Heptadecanenitrile	7.11
9-Octadecenamide, (Z)-	4.96	n-Hexadecanoic acid	6.09	Oleanitrile	5.85
N1-Benzyl-N2(bezylidenyl-benzylamino)-benzamidin	4.49	Myristamide, N-isobutyl-	5.37	Hexadecane	4.64
Oleic Acid	4.17	Oleanitrile	4.76	Tetradecanenitrile	4.52
Octadecanoic acid	4.02	Octadecanenitrile	4.04	n-Hexadecanoic acid	4.17
Dodecanamide, N-isobutyl-	3.77	Octadecanoic acid	2.96	N1-Benzyl-N2(bezylidenyl-benzylamino)-benzamidin	3.37
6-Octadecenoic acid, (Z)-	2.91	Oleic Acid	2.67	Hexadecanamide	2.38
Tetradecanoic acid	2.36	Hexadecanamide	2.55	3-Heptadecene, (Z)-	2.31
3-Cyclohexylpropionamide	1.97	Tetradecanenitrile	2.07	Heptadecane	2.06
Carbonic acid, 2-ethylhexyl nonyl ester	1.54	N-Methyldodecanamide	1.75	Tetradecanoic acid	1.93
N-Methyldodecanamide	1.43	2-(1-Ethoxyethoxy)succinic acid, diethyl ester	1.43	Tetradecanamide	1.63
Tetradecane	1.38	Tetradecane	1.19	Octadecanoic acid	1.59
Phenol, 2,4'-isopropylidenedi-	1.31	Hexadecane	0.99	Oleic Acid	1.50
1-Decanol, 2-hexyl-	1.24	Dodecanamide, N-3-methylbutyl-	0.87	Tetradecane	1.46
Dodecanamide, N-3-methylbutyl-	1.04	4,7-Octadecadiynoic acid, methyl ester	0.8	Undecanenitrile	1.37

Table **B-3**: Tentative identities of compounds in the Stage II biocrude oil from the pyrolysis (450, 525, 600 °C, 30 min) of Stage I biochars from HTC of simulated food waste at 200 °C and 30 min, detected by GC/MS.

450 °C		**525 °C**		**600 °C**	
Name	Area (%)	Name	Area (%)	Name	Area (%)
Heptadecanenitrile	18.0	1,3,5,7-Cyclooctatetraene	17.8	N1-Benzyl-N2(bezylidenyl-benzylamino)-benzamidin	7.83
Hexadecane	15.8	Dimethylmalonic acid, monochloride, tetradecyl ester	1.90	Pyrene	7.77
Heptadecane	6.79	Bis(tridecyl) phthalate	1.70	Benzanthracene	7.55
Tetradecanenitrile	3.97	Phenanthrene	1.44	Phenanthrene, 3-methyl-	2.82
Dodecanenitrile	2.26	Benzene, (3,3-dimethyl-4-pe	1.11	4H-Cyclopenta[def]phenanthrene	1.55
1-Hexadecanol	1.85	2-Cyanosuccinonitrile	1.08	4H-Benzo[def]carbazole	1.35
Tetradecane	1.57	7-Hexyltridecan-1-ol	0.96	1-Azaanthracene	1.16
Cyclohexane, octyl-	0.85	9H-Fluorene, 1-methyl-	0.94	Phenanthrene	1.14
m-Terphenyl, 5'-phenyl-	0.77	Curan-17-oic acid, 19,20-dihydroxy-, methyl ester	0.93	1,4-Ethenoanthracene, 1,4-dihydro-	1.06
Bicyclo[4.2.0]octa-2,4-diene-7-carbonitrile	0.71	Naphthalene, 2-phenyl-	0.82	1,1':3',1"-Terphenyl, 5'-phenyl-	1.05
1-Tetradecene	0.61	4H-Cyclopenta[def]phenanthrene	0.81	Pyrene, 1-methyl-	1
1-Tetradecanol	0.58	6-Phenyltetrahydropyran-2,4-dione	0.71	Benzene, 1,2-(1,8-naphthalenediyl)-	0.99
Tridecane	0.55	Fumaric acid, 2-methylallyl octadecyl ester	0.7	Anthracene, 2-methyl-	0.96
8-Heptadecene	0.53	cis-Bicyclo[2.2.2]oct-5-en-2,3-dicarboxylic acid, anhydride	0.65	Benzene, trinitro-ethyl-	0.86
1,1-Diphenylcyclopropane	0.5	6-Aminohexanoic acid, 2	0.6	Benzene, 1,1'-ethylidenebis-	0.83
n-Nonylcyclohexane	0.46	1,16-Cyclocorynan-17-oic acid, 19,20-didehydro-, methyl ester	0.56	Desoxypipradol	0.75

Table **B-4**: Tentative identities of compounds in the Stage II biocrude oil from the HTL (300, 350, 400 °C, 30 min) of Stage I biochars from pyrolysis of simulated food waste at 200 °C and 30 min, detected by GC/MS.

300 °C		**350 °C**		**400 °C**	
Name	Area (%)	Name	Area (%)	Name	Area (%)
Oleic Acid	22.3	n-Hexadecanoic acid	22.5	n-Hexadecanoic acid	19.2
Tetradecanoic acid	12.7	Tetradecanoic acid	9.21	1,2-Propanediol, 3-benzyloxy-1,2-diacetyl-	12.7
Octadecanoic acid	9.83	Oleic Acid	8.56	Oleic Acid	7.87
Dodecanoic acid	4.04	9-Octadecenoic acid, (E)-	8.19	Octadecanoic acid	6.76
n-Decanoic acid	2.98	Octadecanoic acid	7.54	Tetradecanoic acid	0.84
N1-Benzyl-N2(bezylidenyl-benzylamino)-benzamidin	l.96	Dodecanoic acid	2.64	1,2,5-Oxadiazol-3-amine, 4-[5-(4-pyridinyl)-1,2,4-oxadiazol-3-yl]-	0.8
7-Ethyl-4,6-heptadecandione	1.64	n-Decanoic acid	2.30	1,1':3',1"-Terphenyl, 5'-phenyl-	0.77
9-Octadecenamide, (Z)-	l.54	Hexadecanamide	1.96	Pentadecane	0.74
cis-10-Heptadecenoic acid	1.35	Benzenemethanamine, N-(phenylmethylene)	1.94	Tetradecane	0.7
Palmitoleic acid	1.30	Phenol, 4,4'-(1-methylethylidene)	1.54	1-Tetradecene	0.61
Tetradecane	1.28	(2E)-2-Tridecenoic acid	1.34	1,3,5,7-Cyclooctatetraene	0.6
Pentadecanoic acid	1.13	N-Methyldodecanamide	1.08	l-Alanine, N-(2-thienylacetyl)-, heptyl ester	0.58
Octadecanamide	1.08	2-Pyrrolidinone, 1-butyl-	0.93	3-Nitrophthalic acid, bis-(2-ethyl-hexyl ester	0.57
Pyrrolo[1,2-a]pyrazine-1,4-dione, hexahydro-3-(2-methylpropyl)-	1.08	Tetradecane	0.88	Benzene, 1,3-bis(1,1-dimethylethyl	0.48
11-Methyldodecanol	1.02	Z-11-Tetradecenoic acid	0.86	2-Methoxymyristic acid	0.48
Octadecanamide, N-butyl-	0.83	9-Octadecenamide, (Z)-	0.84	Nonanedioic acid, dioctyl ester	0.45

Table **B-5**: Tentative identities of compounds in the Stage II biocrude oil from the pyrolysis (300, 350, 400 °C, 30 min) of Stage I biochars from pyrolysis of simulated food waste at 200 °C and 30 min, detected by GC/MS.

300 °C		**350 °C**		**400 °C**	
Name	Area (%)	Name	Area (%)	Name	Area (%)
n-Hexadecanoic acid	10.2	Heptadecanenitrile	19.5	Octadecanenitrile	8.68
Hexadecanamide	6.48	1-Tetradecanol	10.1	Heptadecanenitrile	4.67
9-Octadecenamide, (Z)-	4.99	Oleanitrile	8.01	Tetradecanenitrile	3.55
Tetradecanoic acid	4.53	n-Hexadecanoic acid	6.96	Oleanitrile	4.7
Benzenemethanamine, N-hydroxy-N-(phenylmethyl)-	4.42	Tetradecanenitrile	5.24	n-Hexadecanoic acid	3.02
9-Octadecenoic acid, (E)-	3.93	Octadecanoic acid	2.38	Hexadecane	2.82
Octadecanamide	3.75	Tetradecanoic acid	2.09	Hexadecanamide	2.28
Octadecanoic acid	3.71	Myristamide, N-butyl-	1.94	Undecanenitrile	2.16
Tetradecanamide	3.68	Hexadecanamide	1.73	Heptadecane	1.77
Oleic Acid	3.50	Hexadecane	1.61	3-Heptadecene, (Z)-	1.58
Myristamide, N-methyl-	1.40	Myristamide, N-isobutyl-	1.24	1-Tetradecanol	1.51
Hexadecanenitrile	1.32	Hexadecanenitrile	1.18	Tetradecanamide	1.43
Phenol, 4,4'-(1-methylethylidene)bis-	1.26	trans-2,7-Dimethyl-3,6-octadien-2-ol	1.05	Tetradecane	1.26
Dodecanamide, N-3-methylbutyl-	0.92	Tetradecane	0.99	Tetradecanoic acid	1.22
Myristamide, N-ethyl-	0.84	N-Methyldodecanamide	0.99	Octadecanoic acid	1.14
Dodecanoic acid	0.79	Tetradecanenitrile	0.94	Decanenitrile	1.12

References

(1) Pickett, J. *Sustainable Biofuels: Prospects and Challenges*; The Royal Society, 2008

(2) Nakicenovic, N. World Energy Outlook 2007: China and India Insights. IEA/OECD 2007.

(3) Solomon, S.; Manning, M.; Marquis, M.; Qin, D. *Climate Change 2007-the Physical Science Basis: Working Group I Contribution to the Fourth Assessment Report of the IPCC*; Cambridge university press, **2007**; Vol. 4.

(4) Luque, R.; Herrero-Davila, L.; Campelo, J. M.; Clark, J. H.; Hidalgo, J. M.; Luna, D.; Marinas, J. M.; Romero, A. A. Biofuels: A Technological Perspective. *Energy Environ. Sci.* **2008**, *1* (5), 542–564.

(5) Gustavsson, J.; Cederberg, C.; Sonesson, U.; Emanuelsson, A. *The Methodology of the FAO Study : " Global Food Losses and Food Waste - Extent , Causes and Prevention " - FAO , 2011.* **2013**, *SIK report No. 857*.

(6) Flanagan, K.; Lipinski, B.; Goodwin, L. SDG Target 12.3 on Food Loss and Waste: 2019 Progress Report. *An annual update on behalf of Champions*. **2018**, *12*.

(7) Katami, T.; Yasuhara, A.; Shibamoto, T. Formation of Dioxins from Incineration of Foods Found in Domestic Garbage. *Environ. Sci. Technol.* **2004**, *38* (4), 1062–1065. https://doi.org/10.1021/es030606y.

(8) Dou, Z.; Toth, J. D.; Westendorf, M. L. Food Waste for Livestock Feeding: Feasibility, Safety, and Sustainability Implications. *Global Food Security*. **2018**, *17*, 154-161. https://doi.org/10.1016/j.gfs.2017.12.003.

(9) Lin, C. S. K.; Pfaltzgraff, L. A.; Herrero-Davila, L.; Mubofu, E. B.; Abderrahim, S.; Clark, J. H.; Koutinas, A. A.; Kopsahelis, N.; Stamatelatou, K.; Dickson, F.; Thankappan, S.; Mohamed, Z.; Brocklesby, R.; Luque, R. Food Waste as a Valuable Resource for the Production of Chemicals, Materials and Fuels. Current Situation and Global Perspective. *Energy Environ. Sci.* **2013**, *6* (2), 426–464. https://doi.org/10.1039/c2ee23440h.

(10) Pfaltzgraff, L. A.; De Bruyn, M.; Cooper, E. C.; Budarin, V.; Clark, J. H. Food Waste Biomass: A Resource for High-Value Chemicals. *Green Chem.* **2013**, *15* (2), 307–314. https://doi.org/10.1039/c2gc36978h.

(11) Pham, T. P. T.; Kaushik, R.; Parshetti, G. K.; Mahmood, R.; Balasubramanian, R. Food Waste-to-Energy Conversion Technologies: Current Status and Future Directions. *Waste Manag.* **2015**, *38* (1), 399–408. https://doi.org/10.1016/j.wasman.2014.12.004.

(12) Anjum, M.; Mahmood, T.; Arshad, M.; Dawson, L.; Khalid, A. The Anaerobic Digestion of Solid Organic Waste. *Waste Manag.* **2011**, *31* (8), 1737–1744. https://doi.org/10.1016/j.wasman.2011.03.021.

(13) Loizidou, M.; Matsakas, L.; Christakopoulos, P.; Kekos, D. Utilization of Household Food Waste for the Production of Ethanol at High Dry Material Content. *Biotechnol. Biofuels* **2014**, *7:4*, 1–9. https://doi.org/10.1186/1754-6834-7-4.

(14) Déniel, M.; Haarlemmer, G.; Roubaud, A.; Weiss-Hortala, E.; Fages, J. Energy Valorisation of Food Processing Residues and Model Compounds by Hydrothermal Liquefaction. *Renew. Sustain. Energy Rev.* **2016**, *54*, 1632–1652. https://doi.org/10.1016/j.rser.2015.10.017.

(15) Akiya, N.; Savage, P. E. Roles of Water for Chemical Reactions in High-Temperature Water. *Chem. Rev.* **2002**, *102* (8), 2725–2750. https://doi.org/10.1021/cr000668w.

(16) Uematsu, M.; Frank, E. U. Static Dielectric Constant of Water and Steam. *J. Phys. Chem. Ref. Data* **1980**, *4*, 1291-1306. https://doi.org/10.1063/1.555632.

(17) Smith, R. M. Extractions with Superheated Water. *J. Chromatogr. A* **2002**, *975* (1), 31–46. https://doi.org/10.1016/S0021-9673(02)01225-6.

(18) Kruse, A.; Dinjus, E. Hot Compressed Water as Reaction Medium and Reactant. Properties and Synthesis Reactions. *J. Supercrit. Fluids* **2007**, *39* (3), 362–380. https://doi.org/10.1016/j.supflu.2006.03.016.

(19) Brown, T. M.; Duan, P.; Savage, P. E. Hydrothermal Liquefaction and Gasification of Nannochloropsis Sp. *Energy and Fuels*; **2010,** *24* (6), 3639-3646. https://doi.org/10.1021/ef100203u.

(20) Dimitriadis, A.; Bezergianni, S. Hydrothermal Liquefaction of Various Biomass and Waste Feedstocks for Biocrude Production: A State of the Art Review. *Renew. Sustain. Energy Rev.* **2017**, *68*, 113–125. https://doi.org/10.1016/j.rser.2016.09.120.

(21) Garcia Alba, L.; Torri, C.; Fabbri, D.; Kersten, S. R. A.; Wim Brilman, D. W. F. Microalgae Growth on the Aqueous Phase from Hydrothermal Liquefaction of the Same

Microalgae. *Chem. Eng. J.* **2013**, *228*, 214-223. https://doi.org/10.1016/j.cej.2013.04.097.

(22) Biller, P.; Ross, A. B.; Skill, S. C.; Lea-Langton, A.; Balasundaram, B.; Hall, C.; Riley, R.; Llewellyn, C. A. Nutrient Recycling of Aqueous Phase for Microalgae Cultivation from the Hydrothermal Liquefaction Process. *Algal Res.* **2012**, *1* (1), 70-76. https://doi.org/10.1016/j.algal.2012.02.002.

(23) Gollakota, A. R. K.; Kishore, N.; Gu, S. A Review on Hydrothermal Liquefaction of Biomass. *Renew. Sustain. Energy Rev.* **2018**, *81*, 1378–1392. https://doi.org/10.1016/j.rser.2017.05.178.

(24) Peterson, A. A.; Vogel, F.; Lachance, R. P.; Fröling, M.; Antal, M. J.; Tester, J. W. Thermochemical Biofuel Production in Hydrothermal Media: A Review of Sub- and Supercritical Water Technologies. *Energy Environ. Sci.* **2008**, *1* (1), 32–65. https://doi.org/10.1039/b810100k.

(25) Biller, P.; Ross, A. B. Potential Yields and Properties of Oil from the Hydrothermal Liquefaction of Microalgae with Different Biochemical Content. *Bioresour. Technol.* **2011**, *102* (1), 215–225. https://doi.org/10.1016/j.biortech.2010.06.028.

(26) Valdez, P. J.; Nelson, M. C.; Wang, H. Y.; Lin, X. N.; Savage, P. E. Hydrothermal Liquefaction of Nannochloropsis Sp.: Systematic Study of Process Variables and Analysis of the Product Fractions. *Biomass and Bioenergy* **2012**, *46*, 317–331. https://doi.org/10.1016/j.biombioe.2012.08.009.

(27) Posmanik, R.; Cantero, D. A.; Malkani, A.; Sills, D. L.; Tester, J. W. Biomass Conversion to Bio-Oil Using Sub-Critical Water: Study of Model Compounds for Food Processing Waste. *J. Supercrit. Fluids* **2017**, *119*, 26–35. https://doi.org/10.1016/j.supflu.2016.09.004.

(28) Gollakota, A.; Savage, P. E. Hydrothermal Liquefaction of Model Food Waste Biomolecules and Ternary Mixtures under Isothermal and Fast Conditions. *ACS Sustain. Chem. Eng.* **2018**, *6* (7), 9018–9027. https://doi.org/10.1021/acssuschemeng.8b01368.

(29) Robin, T.; Jones, J. M.; Ross, A. B. Catalytic Hydrothermal Processing of Lipids Using Metal Doped Zeolites. *Biomass and Bioenergy* **2017**, *98*, 26–36. https://doi.org/10.1016/j.biombioe.2017.01.012.

(30) Lu, J.; Liu, Z.; Zhang, Y.; Savage, P. E. Synergistic and Antagonistic Interactions during Hydrothermal Liquefaction of Soybean Oil, Soy Protein, Cellulose, Xylose, and Lignin. *ACS Sustain. Chem. Eng.* **2018**, *6* (11), 14501-14509.

https://doi.org/10.1021/acssuschemeng.8b03156.

(31) Teri, G.; Luo, L.; Savage, P. E. Hydrothermal Treatment of Protein, Polysaccharide, and Lipids Alone and in Mixtures. *Energy and Fuels* **2014**, *28* (12), 7501–7509. https://doi.org/10.1021/ef501760d.

(32) Leow, S.; Witter, J. R.; Vardon, D. R.; Sharma, B. K.; Guest, J. S.; Strathmann, T. J. Prediction of Microalgae Hydrothermal Liquefaction Products from Feedstock Biochemical Composition. *Green Chem.* **2015**, *17* (6), 3584–3599. https://doi.org/10.1039/c5gc00574d.

(33) Luo, L.; Sheehan, J. D.; Dai, L.; Savage, P. E. Products and Kinetics for Isothermal Hydrothermal Liquefaction of Soy Protein Concentrate. *ACS Sustain. Chem. Eng.* **2016**, *4* (5), 2725–2733. https://doi.org/10.1021/acssuschemeng.6b00226.

(34) Pavlovič, I.; Knez, Ž.; Škerget, M. Hydrothermal Reactions of Agricultural and Food Processing Wastes in Sub- and Supercritical Water: A Review of Fundamentals, Mechanisms, and State of Research. *J. Agric. Food Chem.* **2013**, *61* (34), 8003–8025. https://doi.org/10.1021/jf401008a.

(35) Déniel, M.; Haarlemmer, G.; Roubaud, A.; Weiss-Hortala, E.; Fages, J. Hydrothermal Liquefaction of Blackcurrant Pomace and Model Molecules: Understanding of Reaction Mechanisms. *Sustain. Energy Fuels* **2017**, *1* (3), 555-582. https://doi.org/10.1039/c6se00065g.

(36) Zastrow, D. J.; Jennings, P. A. Hydrothermal Liquefaction of Food Waste and Model Food. *2013 AIChE Annual Meeting Online Proceedings*. **2013**, 1–9. https://doi.org/Paper No: 336978.

(37) Maag, A. R.; Paulsen, A. D.; Amundsen, T. J.; Yelvington, P. E.; Tompsett, G. A.; Timko, M. T. Catalytic Hydrothermal Liquefaction of Food Waste Using CeZrO X. *Energies* **2018**, 1–14. https://doi.org/10.3390/en11030564.

(38) Sheehan, J. D.; Savage, P. E. Products, Pathways, and Kinetics for the Fast Hydrothermal Liquefaction of Soy Protein Isolate. *ACS Sustain. Chem. Eng.* **2016**, *4* (12), 6931–6939. https://doi.org/10.1021/acssuschemeng.6b01857.

(39) Saber, M.; Golzary, A.; Hosseinpour, M.; Takahashi, F.; Yoshikawa, K. Catalytic Hydrothermal Liquefaction of Microalgae Using Nanocatalyst. *Applied Energy* **2016**, *183*, 566–576.

(40) Luo, L.; Dai, L.; Savage, P. E. Catalytic Hydrothermal Liquefaction of Soy Protein Concentrate. *Energy & Fuels* **2015,** *29* (5), 3208-3214. https://doi.org/10.1021/acs.energyfuels.5b00321.

(41) Duan, P.; Savage, P. E. Hydrothermal Liquefaction of a Microalga with Heterogeneous Catalysts. *Ind. Eng. Chem. Res.* **2011**, *50* (1), 52–61. https://doi.org/10.1021/ie100758s.

(42) Posmanik, R.; Martinez, C. M.; Cantero-Tubilla, B.; Cantero, D. A.; Sills, D. L.; Cocero, M. J.; Tester, J. W. Acid and Alkali Catalyzed Hydrothermal Liquefaction of Dairy Manure Digestate and Food Waste. *ACS Sustain. Chem. Eng.* **2018**, *6* (2), 2724–2732. https://doi.org/10.1021/acssuschemeng.7b04359.

(43) Akarsu, K.; Duman, G.; Yilmazer, A.; Keskin, T.; Azbar, N.; Yanik, J. Sustainable Valorization of Food Wastes into Solid Fuel by Hydrothermal Carbonization. *Bioresour. Technol.* **2019**, *292*, 121959. https://doi.org/10.1016/j.biortech.2019.121959.

(44) McGaughy, K.; Toufiq Reza, M. Hydrothermal Carbonization of Food Waste: Simplified Process Simulation Model Based on Experimental Results. *Biomass Convers. Biorefinery* **2018**, *8* (2), 283–292. https://doi.org/10.1007/s13399-017-0276-4.

(45) Saqib, N. U.; Baroutian, S.; Sarmah, A. K. Physicochemical, Structural and Combustion Characterization of Food Waste Hydrochar Obtained by Hydrothermal Carbonization. *Bioresour. Technol.* **2018**, *266*, 357–363. https://doi.org/10.1016/j.biortech.2018.06.112.

(46) Sharma, H. B.; Panigrahi, S.; Dubey, B. K. Food Waste Hydrothermal Carbonization : Study on the Effects of Reaction Severities , Pelletization and Framework Development Using Approaches of the Circular Economy. *Bioresour. Technol.* **2021**, *333*, 125187.

(47) Tradler, S. B.; Mayr, S.; Himmelsbach, M.; Priewasser, R.; Baumgartner, W.; Stadler, A. T. Hydrothermal Carbonization as an All-Inclusive Process for Food-Waste Conversion. *Bioresour. Technol. Reports* **2018**, *2*, 77–83. https://doi.org/10.1016/j.biteb.2018.04.009.

(48) Lu, Y.; Levine, R. B.; Savage, P. E. Fatty Acids for Nutraceuticals and Biofuels from Hydrothermal Carbonization of Microalgae. *Ind. Eng. Chem. Res.* **2015**, *54* (16), 4066–4071. https://doi.org/10.1021/ie503448u.

(49) Idowu, I.; Li, L.; Flora, J. R. V.; Pellechia, P. J.; Darko, S. A.; Ro, K. S.; Berge, N. D. Hydrothermal Carbonization of Food Waste for Nutrient Recovery and Reuse. *Waste Manag.* **2017**, *69*, 480–491. https://doi.org/10.1016/j.wasman.2017.08.051.

(50) Levine, R. B.; Sierra, C. O. S.; Hockstad, R.; Obeid, W.; Hatcher, P. G.; Savage, P. E. The Use of Hydrothermal Carbonization to Recycle Nutrients in Algal Biofuel Production. *Environ. Prog. Sustain. Energy* **2013**, *32* (4), 962–975.

(51) Aragón-Briceño, C. I.; Pozarlik, A. K.; Bramer, E. A.; Niedzwiecki, L.; Pawlak-Kruczek, H.; Brem, G. Hydrothermal Carbonization of Wet Biomass from Nitrogen and Phosphorus Approach: A Review. *Renew. Energy* **2021**, *171*, 401–415. https://doi.org/https://doi.org/10.1016/j.renene.2021.02.109.

(52) Jazrawi, C.; Biller, P.; He, Y.; Montoya, A.; Ross, A. B.; Maschmeyer, T.; Haynes, B. S. Two-Stage Hydrothermal Liquefaction of a High-Protein Microalga. *Algal Res.* **2015**, *8*, 15–22. https://doi.org/10.1016/j.algal.2014.12.010.

(53) Motavaf, B.; Savage, P. E. Effect of Process Variables on Food Waste Valorization via Hydrothermal Liquefaction. *ACS ES&T Eng.* **2021**, *1* (3), 363–374.

(54) Aierzhati, A.; Stablein, M. J.; Wu, N. E.; Kuo, C.-T.; Si, B.; Kang, X.; Zhang, Y. Experimental and Model Enhancement of Food Waste Hydrothermal Liquefaction with Combined Effects of Biochemical Composition and Reaction Conditions. *Bioresour. Technol.* **2019**, *284*, 139-147.

(55) Chen, W. H.; Lin, Y. Y.; Liu, H. C.; Chen, T. C.; Hung, H. C.; Chen, C. H. Analysis of Physicochemical Properties of Liquefaction Bio-Oil from Food Waste. *Energy Procedia* **2019**, *158*, 61–66. https://doi.org/10.1016/j.egypro.2019.01.036.

(56) Bayat, H.; Cheng, F.; Dehghanizadeh, M.; Soliz, N.; Brewer, C. E.; Jena, U. Hydrothermal Liquefaction of Food Waste : Bio-Crude Oil Characterization , Mass and Energy Balance Written for Presentation at the 2019 ASABE Annual International Meeting Sponsored by ASABE. **2019**, 2–8.

(57) Maddi, B.; Panisko, E.; Wietsma, T.; Lemmon, T.; Swita, M.; Albrecht, K.; Howe, D. Quantitative Characterization of Aqueous Byproducts from Hydrothermal Liquefaction of Municipal Wastes, Food Industry Wastes, and Biomass Grown on Waste. *ACS Sustain. Chem. Eng.* **2017**, *5* (3), 2205-2214. https://doi.org/10.1021/acssuschemeng.6b02367.

(58) Déniel, M.; Haarlemmer, G.; Roubaud, A.; Weiss-Hortala, E.; Fages, J. Bio-Oil Production from Food Processing Residues: Improving the Bio-Oil Yield and Quality by Aqueous Phase Recycle in Hydrothermal Liquefaction of Blackcurrant (Ribes Nigrum L.) Pomace. *Energy and Fuels* **2016**, *30* (6), 4895-4904. https://doi.org/10.1021/acs.energyfuels.6b00441.

(59) Kimbrough, D. E.; Wakakuwa, J. R. Acid Digestion for Sediments, Sludges, Soils, and Solid Wastes. A Proposed Alternative to EPA SW 846 Method 3050. *Environ. Sci. Technol.* **1989**, *23* (7), 898-900. https://doi.org/10.1021/es00065a021.

(60) Brenner, I. J. Inductively Coupled Plasma Mass Spectrometry Applications. In *Encyclopedia of Spectroscopy and Spectrometry*; 2017. https://doi.org/10.1016/B978-0-12-803224-4.00057-1.

(61) Marshall, W. L.; Franck, E. U. Ion Product of Water Substance, 0-1000 °C, 1-10,000 Bars New International Formulation and Its Background. *J. Phys. Chem. Ref. Data* **1983**, *10* (2), 295–304. https://doi.org/10.1063/1.555643.

(62) Gollakota, A.; Savage, P. E. Fast and Isothermal Hydrothermal Liquefaction of Polysaccharide Feedstocks. *Sustainable Chemistry & Engineering* **2020**, *8* (9), 3762-3772. https://doi.org/10.1021/acssuschemeng.9b06873.

(63) Faeth, J. L.; Valdez, P. J.; Savage, P. E. Fast Hydrothermal Liquefaction of Nannochloropsis Sp. to Produce Biocrude. *Energy and Fuels* **2013**, *27* (3), 1391–1398. https://doi.org/10.1021/ef301925d.

(64) U.S. Energy Information Administration (EIA. Crude oil distillation and the definition of refinery capacity. *U.S. Energy Information Administration (EIA* (2012))). Available at: https://www.eia.gov/todayinenergy/detail.php?id=6970#.

(65) Gollakota, A.; Savage, P. E. Biocrude Production from Fast and Isothermal Hydrothermal Liquefaction of Chitin. *Energy and Fuels* **2019**, *33*, 11328–11338. https://doi.org/10.1021/acs.energyfuels.9b03209.

(66) Gai, C.; Zhang, Y.; Chen, W. T.; Zhang, P.; Dong, Y. Energy and Nutrient Recovery Efficiencies in Biocrude Oil Produced via Hydrothermal Liquefaction of Chlorella Pyrenoidosa. *RSC Adv.* **2014**, *4* (33), 16958–16967. https://doi.org/10.1039/c3ra46607h.

(67) Huang, H. J.; Yuan, X. Z.; Li, B. T.; Xiao, Y. D.; Zeng, G. M. Thermochemical Liquefaction Characteristics of Sewage Sludge in Different Organic Solvents. *J. Anal. Appl. Pyrolysis* **2014**, *109*, 176–184. https://doi.org/10.1016/j.jaap.2014.06.015.

(68) Sheehan, J. D.; Savage, P. E. Molecular and Lumped Products from Hydrothermal Liquefaction of Bovine Serum Albumin. *ACS Sustain. Chem. Eng.* **2017**, *5* (11), 10967-10975. https://doi.org/10.1021/acssuschemeng.7b02854.

(69) Yang, W.; Li, X.; Li, Z.; Tong, C.; Feng, L. Understanding Low-Lipid Algae Hydrothermal Liquefaction Characteristics and Pathways through Hydrothermal Liquefaction of Algal Major Components: Crude Polysaccharides, Crude Proteins and Their Binary Mixtures. *Bioresour. Technol.* **2015**, *196*, 99-108. https://doi.org/10.1016/j.biortech.2015.07.020.

(70) Biller, P.; Riley, R.; Ross, A. B. Catalytic Hydrothermal Processing of Microalgae: Decomposition and Upgrading of Lipids. *Bioresour. Technol.* **2011**, *102* (7), 4841–4848. https://doi.org/10.1016/j.biortech.2010.12.113.

(71) Ekpo, U.; Ross, A. B.; Camargo-Valero, M. A.; Williams, P. T. A Comparison of Product Yields and Inorganic Content in Process Streams Following Thermal Hydrolysis and Hydrothermal Processing of Microalgae, Manure and Digestate. *Bioresour. Technol.* **2016**, *200*, 951–960. https://doi.org/10.1016/j.biortech.2015.11.018.

(72) Dai, L.; Tan, F.; Wu, B.; He, M.; Wang, W.; Tang, X.; Hu, Q.; Zhang, M. Immobilization of Phosphorus in Cow Manure during Hydrothermal Carbonization. *J. Environ. Manage.* **2015**, *157*, 49–53. https://doi.org/10.1016/j.jenvman.2015.04.009.

(73) Sheehan, J. D.; Savage, P. E. Modeling the Effects of Microalga Biochemical Content on the Kinetics and Biocrude Yields from Hydrothermal Liquefaction. *Bioresour. Technol.* **2017**, *239*, 144-150. https://doi.org/10.1016/j.biortech.2017.05.013.

(74) Valdez, P. J.; Tocco, V. J.; Savage, P. E. A General Kinetic Model for the Hydrothermal Liquefaction of Microalgae. *Bioresour. Technol.* **2014**, *163*, 123–127. https://doi.org/10.1016/j.biortech.2014.04.013.

(75) Vo, T. K.; Lee, O. K.; Lee, E. Y.; Kim, C. H.; Seo, J. W.; Kim, J.; Kim, S. S. Kinetics Study of the Hydrothermal Liquefaction of the Microalga Aurantiochytrium Sp. KRS101. *Chem. Eng. J.* **2016**, *306*, 763–771. https://doi.org/10.1016/j.cej.2016.07.104.

(76) Motavaf, B.; Capece, S. H.; Savage, P. E. Screening Potential Catalysts for the Hydrothermal Liquefaction of Food Waste. *Energy and Fuels* **2021**, *35* (11), 9437–9449. https://doi.org/10.1021/acs.energyfuels.1c00672.

(77) Biofuels and Bioproducts from Wet and Gaseous Waste Streams: Challenges and Opportunities. *Bioenergy Technologies Office, US Department of Energy, Washington DC, USA*, **2017**.

(78) Shakya, R.; Whelen, J.; Adhikari, S.; Mahadevan, R.; Neupane, S. Effect of Temperature and Na2CO3 Catalyst on Hydrothermal Liquefaction of Algae. *Algal Res.* **2015**, *12*, 80–

90. https://doi.org/10.1016/j.algal.2015.08.006.

(79) Duan, P.; Savage, P. E. Catalytic Treatment of Crude Algal Bio-Oil in Supercritical Water: Optimization Studies. *Energy Environ. Sci.* **2011**, *4* (4), 1447–1456. https://doi.org/10.1039/c0ee00343c.

(80) Xu, D.; Lin, G.; Guo, S.; Wang, S.; Guo, Y.; Jing, Z. Catalytic Hydrothermal Liquefaction of Algae and Upgrading of Biocrude: A Critical Review. *Renew. Sustain. Energy Rev.* **2018**, *97*, 103–118. https://doi.org/10.1016/j.rser.2018.08.042.

(81) Biswas, B.; Kumar, A.; Fernandes, A. C.; Saini, K.; Negi, S.; Muraleedharan, U. D.; Bhaskar, T. Solid Base Catalytic Hydrothermal Liquefaction of Macroalgae: Effects of Process Parameter on Product Yield and Characterization. *Bioresour. Technol.* **2020**, *307*, 123232.

(82) Lu, J.; Wu, J.; Zhang, L.; Liu, Z.; Wu, Y.; Yang, M. Catalytic Hydrothermal Liquefaction of Microalgae over Mesoporous Silica-Based Materials with Site-Separated Acids and Bases. *Fuel* **2020**, *279*, 118529. https://doi.org/10.1016/j.fuel.2020.118529.

(83) Wang, W.; Xu, Y.; Wang, X.; Zhang, B.; Tian, W.; Zhang, J. Hydrothermal Liquefaction of Microalgae over Transition Metal Supported TiO2 Catalyst. *Bioresour. Technol.* **2018**, *250*, 474–480. https://doi.org/10.1016/j.biortech.2017.11.051.

(84) Yu, G.; Zhang, Y.; Guo, B.; Funk, T.; Schideman, L. Nutrient Flows and Quality of Bio-Crude Oil Produced via Catalytic Hydrothermal Liquefaction of Low-Lipid Microalgae. *Bioenergy Res.* **2014**, *7* (4), 1317–1328. https://doi.org/10.1007/s12155-014-9471-3.

(85) Chen, Y.; Mu, R.; Yang, M.; Fang, L.; Wu, Y.; Wu, K.; Liu, Y.; Gong, J. Catalytic Hydrothermal Liquefaction for Bio-Oil Production over CNTs Supported Metal Catalysts. *Chem. Eng. Sci.* **2017**, *161*, 299–307. https://doi.org/10.1016/j.ces.2016.12.010.

(86) Chen, Y.; Wu, Y.; Ding, R.; Zhang, P.; Liu, J.; Yang, M. Catalytic Hydrothermal Liquefaction of D . Tertiolecta for the Production of Bio-Oil over Different Acid / Base Catalysts. **2015**, *61* (4), 1118–1128. https://doi.org/10.1002/aic.

(87) Shi, W.; Li, S.; Jin, H.; Zhao, Y.; Yu, W. The Hydrothermal Liquefaction of Rice Husk to Bio-Crude Using Metallic Oxide Catalysts. *Energy Sources, Part A Recover. Util. Environ. Eff.* **2013**, *35* (22), 2149-2155. https://doi.org/10.1080/15567036.2012.700996.

(88) Yim, S. C.; Quitain, A. T.; Yusup, S.; Sasaki, M.; Uemura, Y.; Kida, T. Metal Oxide-

Catalyzed Hydrothermal Liquefaction of Malaysian Oil Palm Biomass to Bio-Oil under Supercritical Condition. *J. Supercrit. Fluids* **2017**, *120*, 384–394. https://doi.org/10.1016/j.supflu.2016.05.044.

(89) Sánchez-Bayo, A.; Rodríguez, R.; Morales, V.; Nasirian, N.; Bautista, L. F.; Vicente, G. Hydrothermal Liquefaction of Microalga Using Metal Oxide Catalyst. *Processes* **2020**, *8* (1), 15. https://doi.org/10.3390/pr8010015.

(90) Ding, X.; Mahadevan Subramanya, S.; Fang, T.; Guo, Y.; Savage, P. E. Effects of Potassium Phosphates on Hydrothermal Liquefaction of Triglyceride, Protein, and Polysaccharide. *Energy and Fuels* **2020**, *34* (12), 15313-15321. https://doi.org/10.1021/acs.energyfuels.0c01618.

(91) Gollakota, A.; Savage, P. E. Effect of additives on hydrothermal liquefaction of polysaccharides. *Industrial & Engineering Chemistry Research* **2020**, *59* (41), 18480-18488.

(92) Jena, U.; Das, K. C.; Kastner, J. R. Comparison of the Effects of Na2CO3, Ca3(PO4)2, and NiO Catalysts on the Thermochemical Liquefaction of Microalga Spirulina Platensis. *Appl. Energy* **2012**, *98*, 368–375. https://doi.org/10.1016/j.apenergy.2012.03.056.

(93) Ross, A. B.; Biller, P.; Kubacki, M. L.; Li, H.; Lea-Langton, A.; Jones, J. M. Hydrothermal Processing of Microalgae Using Alkali and Organic Acids. *Fuel* **2010**, *89* (9), 2234–2243. https://doi.org/10.1016/j.fuel.2010.01.025.

(94) Yang, Y. F.; Feng, C. P.; Inamori, Y.; Maekawa, T. Analysis of Energy Conversion Characteristics in Liquefaction of Algae. *Resources, Conservation and Recycling* **2004**, *43*, 21–33. https://doi.org/10.1016/j.resconrec.2004.03.003.

(95) Shuping, Z.; Yulong, W.; Mingde, Y.; Kaleem, I.; Chun, L.; Tong, J. Production and Characterization of Bio-Oil from Hydrothermal Liquefaction of Microalgae Dunaliella Tertiolecta Cake. *Energy* **2010**, *35* (12), 5406-5411. https://doi.org/10.1016/j.energy.2010.07.013.

(96) Karagöz, S.; Bhaskar, T.; Muto, A.; Sakata, Y.; Oshiki, T.; Kishimoto, T. Low-Temperature Catalytic Hydrothermal Treatment of Wood Biomass: Analysis of Liquid Products. *Chem. Eng. J.* **2005**, *108* (1–2), 127–137. https://doi.org/10.1016/j.cej.2005.01.007.

(97) Minowa, T.; Murakami, M.; Dote, Y.; Ogi, T.; Yokoyama, S. ya. Oil Production from Garbage by Thermochemical Liquefaction. *Biomass and Bioenergy* **1995**, *8* (2), 117–120.

https://doi.org/10.1016/0961-9534(95)00017-2.

(98) Wang, L.; Chi, Y.; Shu, D.; Weiss-Hortala, E.; Nzihou, A.; Choi, S. Experimental Studies of Hydrothermal Liquefaction of Kitchen Waste with H+, OH− and Fe3+ Additives for Bio-Oil Upgrading. *Waste Manag. Res.* **2021**, *39* (1), 165–173. https://doi.org/10.1177/0734242X20957408.

(99) Cheng, F.; Tompsett, G. A.; Murphy, C. M.; Maag, A. R.; Carabillo, N.; Bailey, M.; Hemingway, J. J.; Romo, C. I.; Paulsen, A. D.; Yelvington, P. E.; Timko, M. T. Synergistic Effects of Inexpensive Mixed Metal Oxides for Catalytic Hydrothermal Liquefaction of Food Wastes. *ACS Sustain. Chem. Eng.* **2020**, *8* (17), 6877-6886. https://doi.org/10.1021/acssuschemeng.0c02059.

(100) Cheng, F.; Tompsett, G. A.; Fraga Alvarez, D. V.; Romo, C. I.; Mckenna, A.; Niles, S. F.; Nelson, R.; Reddy, C. M.; Granados-Focil, S.; Paulsen, A. D.; Zhang, R.; Timko, M. T. Metal Oxide Supported Ni-Impregnated Bifunctional Catalysts for Controlling Char Formation and Maximizing Energy Recovery during Catalytic Hydrothermal Liquefaction of Food Waste. *Sustain. Energy Fuels* **2021**, *5* (4), 941-955. https://doi.org/10.1039/d0se01662d.

(101) Chen, W. H.; Lin, Y. Y.; Liu, H. C.; Baroutian, S. Optimization of Food Waste Hydrothermal Liquefaction by a Two-Step Process in Association with a Double Analysis. *Energy* **2020**, *199*, 117438. https://doi.org/10.1016/j.energy.2020.117438.

(102) Chen, W. H.; Lin, Y. Y.; Liu, H. C.; Chen, T. C.; Hung, C. H.; Chen, C. H.; Ong, H. C. A Comprehensive Analysis of Food Waste Derived Liquefaction Bio-Oil Properties for Industrial Application. *Appl. Energy* **2019**, *237*, 283–291. https://doi.org/10.1016/j.apenergy.2018.12.084.

(103) U.S. EPA. 1993. "Method 350.1: Nitrogen, Ammonia (Colorimetric, Automated Phenate)," Revision 2.0. Cincinnati, OH

(104) Costanzo, W.; Hilten, R.; Jena, U.; Das, K. C.; Kastner, J. R. Effect of Low Temperature Hydrothermal Liquefaction on Catalytic Hydrodenitrogenation of Algae Biocrude and Model Macromolecules. *Algal Res.* **2016**, *13*, 53–68. https://doi.org/10.1016/j.algal.2015.11.009.

(105) Qian, L.; Wang, S.; Savage, P. E. Hydrothermal Liquefaction of Sewage Sludge under Isothermal and Fast Conditions. *Bioresour. Technol.* **2017**, *232*, 27–34. https://doi.org/10.1016/j.biortech.2017.02.017.

(106) Chen, D.; Ma, Q.; Wei, L.; Li, N.; Shen, Q.; Tian, W.; Zhou, J.; Long, J. Catalytic Hydroliquefaction of Rice Straw for Bio-Oil Production Using Ni/CeO2 Catalysts. *J. Anal. Appl. Pyrolysis* **2018**, *130*, 169-180. https://doi.org/10.1016/j.jaap.2018.01.012.

(107) Osada, M.; Hiyoshi, N.; Sato, O.; Arai, K.; Shirai, M. Effect of Sulfur on Catalytic Gasification of Lignin in Supercritical Water. *Energy and Fuels* **2007**, *21* (3), 1400–1405. https://doi.org/10.1021/ef060636x.

(108) Zhang, Y.; Chen, W. T. Hydrothermal Liquefaction of Protein-Containing Feedstocks. In *Direct Thermochemical Liquefaction for Energy Applications*, **2018**, 127-168. https://doi.org/10.1016/B978-0-08-101029-7.00004-7.

(109) Vardon, D. R.; Sharma, B. K.; Jaramillo, H.; Kim, D.; Choe, J. K.; Ciesielski, P. N.; Strathmann, T. J. Hydrothermal Catalytic Processing of Saturated and Unsaturated Fatty Acids to Hydrocarbons with Glycerol for in Situ Hydrogen Production. *Green Chem.* **2014**, *16* (3), 1507–1520. https://doi.org/10.1039/c3gc41798k.

(110) Ding, R.; Wu, Y.; Chen, Y.; Liang, J.; Liu, J.; Yang, M. Effective Hydrodeoxygenation of Palmitic Acid to Diesel-like Hydrocarbons over MoO 2 /CNTs Catalyst. *Chem. Eng. Sci.* **2015**, *135*, 517–525. https://doi.org/10.1016/j.ces.2014.10.024.

(111) Zhang, J.; Huo, X.; Li, Y.; Strathmann, T. J. Catalytic Hydrothermal Decarboxylation and Cracking of Fatty Acids and Lipids over Ru/C. *ACS Sustain. Chem. Eng.* **2019**, *7* (17), 14400–14410. https://doi.org/10.1021/acssuschemeng.9b00215.

(112) Fu, J.; Lu, X.; Savage, P. E. Catalytic Hydrothermal Deoxygenation of Palmitic Acid. *Energy Environ. Sci.* **2010**, *3* (3), 311–317. https://doi.org/10.1039/b923198f.

(113) Zhu, Z.; Toor, S. S.; Rosendahl, L.; Yu, D.; Chen, G. Influence of Alkali Catalyst on Product Yield and Properties via Hydrothermal Liquefaction of Barley Straw. *Energy* **2015**, *80*, 284-292. https://doi.org/10.1016/j.energy.2014.11.071.

(114) Beckers, J.; Rothenberg, G. Sustainable Selective Oxidations Using Ceria-Based Materials. *Green Chem.* **2010**, *12* (6), 939–994. https://doi.org/10.1039/c000191k.

(115) Wang, T.; Zhai, Y.; Zhu, Y.; Peng, C.; Xu, B.; Wang, T.; Li, C.; Zeng, G. Influence of Temperature on Nitrogen Fate during Hydrothermal Carbonization of Food Waste. *Bioresour. Technol.* **2018**, *247*, 182–189. https://doi.org/10.1016/j.biortech.2017.09.076.

(116) Ovsyannikova, E.; Kruse, A.; Becker, G. C. Feedstock-Dependent Phosphate Recovery in

a Pilot-Scale Hydrothermal Liquefaction Bio-Crude Production. *Energies* **2020**, *13* (2), 379.

(117) Motavaf, B.; Dean, R. A.; Nicolas, J.; Savage, P. E. Hydrothermal Carbonization of Simulated Food Waste for Recovery of Fatty Acids and Nutrients. *Bioresour. Technol.* **2021**, *341*, 125872. https://doi.org/10.1016/j.biortech.2021.125872.

(118) Nzihou, A. Toward the Valorization of Waste and Biomass. *Waste and Biomass Valorization* **2010**, *1* (1), 3–7. https://doi.org/10.1007/s12649-010-9014-x.

(119) United States Environmental Protection Agency. Inventory of U.S. Greenhouse Gas Emissions and Sinks: 1990-2019, **2021**.

(120) Carmona-Cabello, M.; Leiva-Candia, D.; Castro-Cantarero, J. L.; Pinzi, S.; Dorado, M. P. Valorization of Food Waste from Restaurants by Transesterification of the Lipid Fraction. *Fuel* **2018**, *215*, 492–498. https://doi.org/10.1016/j.fuel.2017.11.096.

(121) Karmee, S. K.; Linardi, D.; Lee, J.; Lin, C. S. K. Conversion of Lipid from Food Waste to Biodiesel. *Waste Manag.* **2015**, *41*, 169–173. https://doi.org/10.1016/j.wasman.2015.03.025.

(122) Alptekin, E.; Canakci, M.; Sanli, H. Biodiesel Production from Vegetable Oil and Waste Animal Fats in a Pilot Plant. *Waste Manag.* **2014**, *34* (11), 2146–2154. https://doi.org/10.1016/j.wasman.2014.07.019.

(123) Yang, X.; Lee, S. J.; Yoo, H. Y.; Choi, H. S.; Park, C.; Kim, S. W. Biorefinery of Instant Noodle Waste to Biofuels. *Bioresour. Technol.* **2014**, *159*, 17–23. https://doi.org/10.1016/j.biortech.2014.02.068.

(124) Saqib, N. U.; Sharma, H. B.; Baroutian, S.; Dubey, B.; Sarmah, A. K. Valorisation of Food Waste via Hydrothermal Carbonisation and Techno-Economic Feasibility Assessment. *Sci. Total Environ.* **2019**, *690*, 261–276. https://doi.org/10.1016/j.scitotenv.2019.06.484.

(125) Gupta, D.; Mahajani, S. M.; Garg, A. Investigation on Hydrochar and Macromolecules Recovery Opportunities from Food Waste after Hydrothermal Carbonization. *Sci. Total Environ.* **2020**, *749*, 142294. https://doi.org/10.1016/j.scitotenv.2020.142294.

(126) Shen, Y. A Review on Hydrothermal Carbonization of Biomass and Plastic Wastes to Energy Products. *Biomass and Bioenergy* **2020**, *134*, 105479.

https://doi.org/10.1016/j.biombioe.2020.105479.

(127) Gupta, D.; Mahajani, S. M.; Garg, A. Effect of Hydrothermal Carbonization as Pretreatment on Energy Recovery from Food and Paper Wastes. *Bioresour. Technol.* **2019**, *285*, 121329. https://doi.org/10.1016/j.biortech.2019.121329.

(128) Su, H.; Zhou, X.; Zheng, R.; Zhou, Z.; Zhang, Y.; Zhu, G.; Yu, C.; Hantoko, D.; Yan, M. Hydrothermal Carbonization of Food Waste after Oil Extraction Pre-Treatment: Study on Hydrochar Fuel Characteristics, Combustion Behavior, and Removal Behavior of Sodium and Potassium. *Sci. Total Environ.* **2021**, *754*. https://doi.org/10.1016/j.scitotenv.2020.142192.

(129) Heilmann, S. M.; Davis, H. T.; Jader, L. R.; Lefebvre, P. A.; Sadowsky, M. J.; Schendel, F. J.; von Keitz, M. G.; Valentas, K. J. Hydrothermal Carbonization of Microalgae. *Biomass and Bioenergy* **2010**, *34* (6), 875–882. https://doi.org/10.1016/j.biombioe.2010.01.032.

(130) Zhai, Y.; Wang, T.; Zhu, Y.; Peng, C.; Wang, B.; Li, X.; Li, C.; Zeng, G. Production of Fuel Pellets via Hydrothermal Carbonization of Food Waste Using Molasses as a Binder. *Waste Manag.* **2018**, *77*, 185–194.

(131) Li, L.; Diederick, R.; Flora, J. R. V.; Berge, N. D. Hydrothermal Carbonization of Food Waste and Associated Packaging Materials for Energy Source Generation. *Waste Manag.* **2013**, *33* (11), 2478–2492. https://doi.org/10.1016/j.wasman.2013.05.025.

(132) Sharma, H. B.; Dubey, B. K. Co-Hydrothermal Carbonization of Food Waste with Yard Waste for Solid Biofuel Production: Hydrochar Characterization and Its Pelletization. *Waste Manag.* **2020**, *118*, 521–533.

(133) Carmona-Cabello, M.; Sáez-Bastante, J.; Pinzi, S.; Dorado, M. P. Optimization of Solid Food Waste Oil Biodiesel by Ultrasound-Assisted Transesterification. *Fuel* **2019**, *255*, 115817. https://doi.org/10.1016/j.fuel.2019.115817.

(134) Cundiff, D. K.; Raghuvanshi, N. Future Body Mass Index Modelling Based on Macronutrient Profiles and Physical Activity. *Theor. Biol. Med. Model.* **2012**, *9* (1), 1-46. https://doi.org/10.1186/1742-4682-9-43.

(135) Chang, S. Sen; Redondo-Solano, M.; Thippareddi, H. Inactivation of Escherichia Coli O157:H7 and Salmonella Spp. on Alfalfa Seeds by Caprylic Acid and Monocaprylin. *Int. J. Food Microbiol.* **2010**, *144* (1), 141–146. https://doi.org/10.1016/j.ijfoodmicro.2010.09.011.

(136) Nalivaeva, N.; Turner, A. *Lipid Anchors to Proteins*; Springer, Boston,MA., 2009.

(137) Wang, L.; Chang, Y.; Liu, Q. Fate and Distribution of Nutrients and Heavy Metals during Hydrothermal Carbonization of Sewage Sludge with Implication to Land Application. *J. Clean. Prod.* **2019**, *225*, 972–983. https://doi.org/10.1016/j.jclepro.2019.03.347.

(138) Ackman, R. G.; Sipos, J. C. Application of Specific Response Factors in the Gas Chromatographic Analysis of Methyl Esters of Fatty Acids with Flame Ionization Detectors. *J. Am. Oil Chem. Soc.* **1964**, *41* (5), 377–378. https://doi.org/10.1007/BF02654818.

(139) Van Krevelen, D. W. Graphical-Statistical Method for the Study of Structure and Reaction Processes of Coal. *Fuel* **1950**, *29*, 269–284.

(140) Fuertes, A. B.; Arbestain, M. C.; Sevilla, M.; MacIá-Agulló, J. A.; Fiol, S.; López, R.; Smernik, R. J.; Aitkenhead, W. P.; Arce, F.; MacIas, F. Chemical and Structural Properties of Carbonaceous Products Obtained by Pyrolysis and Hydrothermal Carbonisation of Corn Stover. In *Australian Journal of Soil Research* **2010**, *48*, 618–626. https://doi.org/10.1071/SR10010.

(141) Sevilla, M.; Maciá-Agulló, J. A.; Fuertes, A. B. Hydrothermal Carbonization of Biomass as a Route for the Sequestration of CO2: Chemical and Structural Properties of the Carbonized Products. *Biomass and Bioenergy* **2011**, *35* (7), 3152–3159. https://doi.org/10.1016/j.biombioe.2011.04.032.

(142) Huang, R.; Fang, C.; Lu, X.; Jiang, R.; Tang, Y. Transformation of Phosphorus during (Hydro)Thermal Treatments of Solid Biowastes: Reaction Mechanisms and Implications for P Reclamation and Recycling. *Environ. Sci. Technol.* **2017**, *51* (18), 10284–10298. https://doi.org/10.1021/acs.est.7b02011.

(143) Huang, R.; Tang, Y. Speciation Dynamics of Phosphorus during (Hydro)Thermal Treatments of Sewage Sludge. *Environ. Sci. Technol.* **2015**, *49* (24), 14466–14474. https://doi.org/10.1021/acs.est.5b04140.

(144) Holgate, H. R.; Meyer, J. C.; Tester, J. W. Glucose Hydrolysis and Oxidation in Supercritical Water. *AIChE J.* **1995**, *41* (3), 637–648. https://doi.org/10.1002/aic.690410320.

(145) Becker, R.; Dorgerloh, U.; Paulke, E.; Mumme, J.; Nehls, I. Hydrothermal Carbonization of Biomass: Major Organic Components of the Aqueous Phase. *Chem. Eng. Technol.* **2014**, *37* (3), 511–518. https://doi.org/10.1002/ceat.201300401.

(146) Gropper, Sareen S., and Jack. L. Smith. Advanced Nutrition and Human Metabolism. *Cengage Learning*, **2012**.

(147) Huang, W.-C.; Tsai, T.-H.; Chuang, L.-T.; Li, Y.-Y.; Zouboulis, C. C.; Tsai, P.-J. Anti-Bacterial and Anti-Inflammatory Properties of Capric Acid against Propionibacterium Acnes: A Comparative Study with Lauric Acid. *J. Dermatol. Sci.* **2014**, *73* (3), 232–240.

(148) Babayan, V. K. Medium Chain Length Fatty Acid Esters and Their Medical and Nutritional Applications. *J. Am. Oil Chem. Soc.* **1981**, *58*, 49A-51A. https://doi.org/10.1007/bf02540808.

(149) Dayrit, F. M. The Properties of Lauric Acid and Their Significance in Coconut Oil. *J. Am. Oil Chem. Soc.* **2015**, *92* (1), 1–15. https://doi.org/10.1007/s11746-014-2562-7.

(150) Food Wastage Footprint (Project). *Food wastage footprint: impacts on natural resources: summary report*. Food & Agriculture Org, **2013**.

(151) Li, L.; Liu, H.; Jiang, Y.; Hu, Z.; Ma, X.; Guo, P. The Catalytic Pyrolysis of Food Waste by Microwave Heating. *Bioresour. Technol.* **2014**, *166*, 45–50. https://doi.org/10.1016/j.biortech.2014.05.020.

(152) Jo, J. H.; Kim, S. S.; Shim, J. W.; Lee, Y. E.; Yoo, Y. S. Pyrolysis Characteristics and Kinetics of Food Wastes. *Energies* **2017**, *10* (8), 1191. https://doi.org/10.3390/en10081191.

(153) Kim, S.; Lee, Y.; Andrew Lin, K. Y.; Hong, E.; Kwon, E. E.; Lee, J. The Valorization of Food Waste via Pyrolysis. *J. Clean. Prod.* **2020**, *259*, 120816. https://doi.org/10.1016/j.jclepro.2020.120816.

(154) Arvindnarayan, S.; Sivagnana Prabhu, K. K.; Shobana, S.; Kumar, G.; Dharmaraja, J. Upgrading of Micro Algal Derived Bio-Fuels in Thermochemical Liquefaction Path and Its Perspectives: A Review. *Int. Biodeterior. Biodegrad.* **2017**, *119*, 260–272. https://doi.org/10.1016/j.ibiod.2016.08.011.

(155) Elliott, D. C.; Hart, T. R.; Schmidt, A. J.; Neuenschwander, G. G.; Rotness, L. J.; Olarte, M. V.; Zacher, A. H.; Albrecht, K. O.; Hallen, R. T.; Holladay, J. E. Process Development for Hydrothermal Liquefaction of Algae Feedstocks in a Continuous-Flow Reactor. *Algal Res.* **2013**, *2* (4), 445–454. https://doi.org/10.1016/j.algal.2013.08.005.

(156) Galadima, A.; Muraza, O. Hydrothermal Liquefaction of Algae and Bio-Oil Upgrading

into Liquid Fuels: Role of Heterogeneous Catalysts. *Renew. Sustain. Energy Rev.* **2018**, *81*, 1037–1048. https://doi.org/10.1016/j.rser.2017.07.034.

(157) Costanzo, W.; Jena, U.; Hilten, R.; Das, K. C.; Kastner, J. R. Low Temperature Hydrothermal Pretreatment of Algae to Reduce Nitrogen Heteroatoms and Generate Nutrient Recycle Streams. *Algal Res.* **2015**, *12*, 377–387. https://doi.org/10.1016/j.algal.2015.09.019.

(158) Tarhan, S. Z.; Koçer, A. T.; Özçimen, D.; Gökalp, İ. Cultivation of Green Microalgae by Recovering Aqueous Nutrients in Hydrothermal Carbonization Process Water of Biomass Wastes. *J. Water Process Eng.* **2021**, *40*, 101783.

(159) Yu, Y.; Lei, Z.; Yang, X.; Yang, X.; Huang, W.; Shimizu, K.; Zhang, Z. Hydrothermal Carbonization of Anaerobic Granular Sludge: Effect of Process Temperature on Nutrients Availability and Energy Gain from Produced Hydrochar. *Appl. Energy* **2018**, *229*, 88–95. https://doi.org/10.1016/j.apenergy.2018.07.088.

(160) Belete, Y. Z.; Leu, S.; Boussiba, S.; Zorin, B.; Posten, C.; Thomsen, L.; Wang, S.; Gross, A.; Bernstein, R. Characterization and Utilization of Hydrothermal Carbonization Aqueous Phase as Nutrient Source for Microalgal Growth. *Bioresour. Technol.* **2019**, *290*, 121758.

(161) Biller, P.; Friedman, C.; Ross, A. B. Hydrothermal Microwave Processing of Microalgae as a Pre-Treatment and Extraction Technique for Bio-Fuels and Bio-Products. *Bioresour. Technol.* **2013**, *136*, 188–195. https://doi.org/10.1016/j.biortech.2013.02.088.

(162) Huang, Z.; Wufuer, A.; Wang, Y.; Dai, L. Hydrothermal Liquefaction of Pretreated Low-Lipid Microalgae for the Production of Bio-Oil with Low Heteroatom Content. *Process Biochem.* **2018**, *69*, 136–143. https://doi.org/10.1016/j.procbio.2018.03.018.

(163) Prapaiwatcharapan, K.; Sunphorka, S.; Kuchonthara, P.; Kangvansaichol, K.; Hinchiranan, N. Single- and Two-Step Hydrothermal Liquefaction of Microalgae in a Semi-Continuous Reactor: Effect of the Operating Parameters. *Bioresour. Technol.* **2015**, *191*, 426–432. https://doi.org/10.1016/j.biortech.2015.04.027.

(164) Aida, T. M.; Nonaka, T.; Fukuda, S.; Kujiraoka, H.; Kumagai, Y.; Maruta, R.; Ota, M.; Suzuki, I.; Watanabe, M. M.; Inomata, H.; Smith, R. L. Nutrient Recovery from Municipal Sludge for Microalgae Cultivation with Two-Step Hydrothermal Liquefaction. *Algal Res.* **2016**, *18*, 61–68. https://doi.org/10.1016/j.algal.2016.06.009.

(165) Wang, S.; Zhao, S.; Cheng, X.; Qian, L.; Barati, B.; Gong, X.; Cao, B.; Yuan, C. Study on

Two-Step Hydrothermal Liquefaction of Macroalgae for Improving Bio-Oil. *Bioresour. Technol.* **2021**, *319*, 124176.

(166) Chakraborty, M.; Miao, C.; McDonald, A.; Chen, S. Concomitant Extraction of Bio-Oil and Value Added Polysaccharides from Chlorella Sorokiniana Using a Unique Sequential Hydrothermal Extraction Technology. *Fuel* **2012**, *95*, 63–70. https://doi.org/10.1016/j.fuel.2011.10.055.

(167) Miao, C.; Chakraborty, M.; Dong, T.; Yu, X.; Chi, Z.; Chen, S. Sequential Hydrothermal Fractionation of Yeast Cryptococcus Curvatus Biomass. *Bioresour. Technol.* **2014**, *164*, 106–112. https://doi.org/10.1016/j.biortech.2014.04.059.

(168) Mukundan, S.; Sriganesh, G.; Kumar, P. Upgrading Prosopis Juliflora to Biofuels via a Two-Step Pyrolysis – Catalytic Hydrodeoxygenation Approach. *Fuel* **2020**, *267*, 117320. https://doi.org/10.1016/j.fuel.2020.117320.

(169) Zhang, L.; Li, S.; Li, K.; Zhu, X. Two-Step Pyrolysis of Corncob for Value-Added Chemicals and High Quality Bio-Oil: Effects of Pyrolysis Temperature and Residence Time. *Energy Convers. Manag.* **2018**, *166*, 260–267. https://doi.org/10.1016/j.enconman.2018.04.002.

(170) Hammer, N. L.; Garrido, R. A.; Starcevich, J.; Coe, C. G.; Satrio, J. A. Two-Step Pyrolysis Process for Producing High Quality Bio-Oils. *Ind. Eng. Chem. Res.* **2015**, *54* (43), 10629–10637. https://doi.org/10.1021/acs.iecr.5b02365.

(171) Zhang, L.; Li, K.; Zhu, X. Study on Two-Step Pyrolysis of Soybean Stalk by TG-FTIR and Py-GC/MS. *J. Anal. Appl. Pyrolysis* **2017**, *127*, 91–98. https://doi.org/10.1016/j.jaap.2017.08.019.

(172) Stephanidis, S.; Nitsos, C.; Kalogiannis, K.; Iliopoulou, E. F.; Lappas, A. A.; Triantafyllidis, K. S. Catalytic Upgrading of Lignocellulosic Biomass Pyrolysis Vapours: Effect of Hydrothermal Pre-Treatment of Biomass. *Catal. Today* **2011**, *167* (1), 37–45. https://doi.org/10.1016/j.cattod.2010.12.049.

(173) Du, Z.; Mohr, M.; Ma, X.; Cheng, Y.; Lin, X.; Liu, Y.; Zhou, W.; Chen, P.; Ruan, R. Hydrothermal Pretreatment of Microalgae for Production of Pyrolytic Bio-Oil with a Low Nitrogen Content. *Bioresour. Technol.* **2012**, *120*, 13–18. https://doi.org/10.1016/j.biortech.2012.06.007.

(174) Liu, Y.; Zhai, Y.; Li, S.; Liu, X.; Liu, X.; Wang, B.; Qiu, Z.; Li, C. Production of Bio-Oil with Low Oxygen and Nitrogen Contents by Combined Hydrothermal Pretreatment and

Pyrolysis of Sewage Sludge. *Energy* **2020**, *203*, 117829. https://doi.org/10.1016/j.energy.2020.117829.

(175) Chang, S.; Zhao, Z.; Zheng, A.; Li, X.; Wang, X.; Huang, Z.; He, F.; Li, H. Effect of Hydrothermal Pretreatment on Properties of Bio-Oil Produced from Fast Pyrolysis of Eucalyptus Wood in a Fluidized Bed Reactor. *Bioresour. Technol.* **2013**, *138*, 321–328. https://doi.org/10.1016/j.biortech.2013.03.170.

(176) Rodriguez Correa, C.; Hehr, T.; Voglhuber-Slavinsky, A.; Rauscher, Y.; Kruse, A. Pyrolysis vs. Hydrothermal Carbonization: Understanding the Effect of Biomass Structural Components and Inorganic Compounds on the Char Properties. *J. Anal. Appl. Pyrolysis* **2019**, *140*, 137–147. https://doi.org/10.1016/j.jaap.2019.03.007.

(177) Yanik, J.; Kornmayer, C.; Saglam, M.; Yüksel, M. Fast Pyrolysis of Agricultural Wastes: Characterization of Pyrolysis Products. *Fuel Process. Technol.* **2007**, *88* (10), 942–947. https://doi.org/10.1016/j.fuproc.2007.05.002.

(178) Kraiem, T.; Hassen, A. Ben; Belayouni, H.; Jeguirim, M. Production and Characterization of Bio-Oil from the Pyrolysis of Waste Frying Oil. *Environ. Sci. Pollut. Res.* **2017**, *24* (11), 9951–9961. https://doi.org/10.1007/s11356-016-7704-z.

(179) Liang, S.; Han, Y.; Wei, L.; McDonald, A. G. Production and Characterization of Bio-Oil and Bio-Char from Pyrolysis of Potato Peel Wastes. *Biomass Convers. Biorefinery* **2015**, *5* (3), 237–246. https://doi.org/10.1007/s13399-014-0130-x.

(180) Ibrahim, A. F. M.; Dandamudi, K. P. R.; Deng, S.; Lin, Y. S. Pyrolysis of Hydrothermal Liquefaction Algal Biochar for Hydrogen Production in a Membrane Reactor. *Fuel* **2020**, *265*, 116935. https://doi.org/10.1016/j.fuel.2019.116935.

(181) Hu, X.; Zhang, Z.; Gholizadeh, M.; Zhang, S.; Lam, C. H.; Xiong, Z.; Wang, Y. Coke Formation during Thermal Treatment of Bio-Oil. *Energy and Fuels* **2020**, *34* (7), 7863–7914. https://doi.org/10.1021/acs.energyfuels.0c01323.

(182) Liu, Z.; Balasubramanian, R. Upgrading of Waste Biomass by Hydrothermal Carbonization (HTC) and Low Temperature Pyrolysis (LTP): A Comparative Evaluation. *Appl. Energy* **2014**, *114*, 857–864. https://doi.org/10.1016/j.apenergy.2013.06.027.

(183) Wang, Y.; Qiu, L.; Zhu, M.; Sun, G.; Zhang, T.; Kang, K. Comparative Evaluation of Hydrothermal Carbonization and Low Temperature Pyrolysis of Eucommia Ulmoides Oliver for the Production of Solid Biofuel. *Sci. Rep.* **2019**, *9* (1), 1–11. https://doi.org/10.1038/s41598-019-38849-4.

(184) Hognon, C.; Delrue, F.; Texier, J.; Grateau, M.; Thiery, S.; Miller, H.; Roubaud, A. Comparison of Pyrolysis and Hydrothermal Liquefaction of Chlamydomonas Reinhardtii. Growth Studies on the Recovered Hydrothermal Aqueous Phase. *Biomass and Bioenergy* **2015**, *73*, 23–31. https://doi.org/10.1016/j.biombioe.2014.11.025.

(185) Faeth, J. L.; Savage, P. E.; Jarvis, J. M.; McKenna, A. M.; Savage, P. E. Characterization of Products from Fast and Isothermal Hydrothermal Liquefaction of Microalgae. *AIChE J.* **2016**, *62* (3), 815–828. https://doi.org/10.1002/aic.15147.

(186) Sudasinghe, N.; Dungan, B.; Lammers, P.; Albrecht, K.; Elliott, D.; Hallen, R.; Schaub, T. High Resolution FT-ICR Mass Spectral Analysis of Bio-Oil and Residual Water Soluble Organics Produced by Hydrothermal Liquefaction of the Marine Microalga Nannochloropsis Salina. *Fuel* **2014**, *119*, 47–56.

(187) Sudasinghe, N.; Reddy, H.; Csakan, N.; Deng, S.; Lammers, P.; Schaub, T. Temperature-Dependent Lipid Conversion and Nonlipid Composition of Microalgal Hydrothermal Liquefaction Oils Monitored by Fourier Transform Ion Cyclotron Resonance Mass Spectrometry. *BioEnergy Res.* **2015**, *8* (4), 1962–1972.

(188) de Souza Deuber, R.; Fernandes, D. S.; Bressanin, J. M.; Watson, J.; Chagas, M. F.; Bonomi, A.; Fregolente, L. V.; Watanabe, M. D. B. Techno-Economic Assessment of HTL Integration to the Brazilian Sugarcane Industry: An Evaluation of Different Scenarios. *Ind. Crops Prod.* **2021**, *173*, 114139.

Vita

Bita Motavaf

Education

Ph.D. in Chemical Engineering
Pennsylvania State University, University Park, PA August 2016- May 2022
B.Sc. in Chemical Engineering
University of Tehran, Tehran, Iran 2011-2015

Publications

Motavaf, Bita, and Phillip E. Savage. "Effect of process variables on food waste valorization via hydrothermal liquefaction." *ACS ES&T Engineering* 1, no. 3 (2021): 363-374.
Motavaf, Bita, Sofia H. Capece, and Phillip E. Savage. "Screening Potential Catalysts for the Hydrothermal Liquefaction of Food Waste." *Energy & Fuels* (2021).
Motavaf, Bita, Robert A. Dean, Joseph Nicolas, and Phillip E. Savage. "Hydrothermal Carbonization of Simulated Food Waste for Recovery of Fatty Acids and Nutrients." *Bioresource Technology* (2021): 125872.
Recovery of Energy and Nitrogen via Two-Stage Valorization of Food Waste Submitted 2022
Review of kinetics of Hydrothermal Liquefaction of Microalgae *In Preparation*, 2022

Oral Presentations

Motavaf, Bita, Sofia H. Capece, and Phillip E. Savage. "Catalyst Screening for the Hydrothermal Liquefaction of Food Waste." Virtual AICHE annual meeting November 2020
Motavaf, Bita, and Phillip E. Savage. "Effect of Reaction Conditions on Hydrothermal Treatment of Food Waste" Chemical Engineering Graduate Research Symposium, The Pennsylvania State University, University Park, PA September 2019
Motavaf, Bita, and Phillip E. Savage. "Effect of Reaction Conditions on Hydrothermal Treatment of Food Waste" ACS National Meeting, SanDiego, CA August 2019
Invited to Sci-Mix poster session at ACS national meeting as selected most exceptional abstract ACS National Meeting, SanDiego, CA August 2019